

ABSTRACT

Title of Document: POLY (AMIDO AMINE) DENDRIMERS:
TRANSEPITHELIAL TRANSPORT
MECHANISMS AND APPLICATIONS IN
ORAL DRUG DELIVERY

Deborah Sweet Goldberg, Doctor of Philosophy,
2010

Directed By: Professor Hamidreza Ghandehari, Fischell
Department of Bioengineering

Small molecule chemotherapy drugs used in clinical practice are plagued by dose-limiting side effects due to off-target toxicities. In addition, because of their low water solubility and poor bioavailability, they must be administered intravenously, leading to high treatment costs and recurring hospital visits. There is a significant need for therapies that improve the bioavailability of chemotherapy agents and enhance specific drug release in the tumor environment.

Dendrimers, a class of highly-branched, nanoscale polymers, share many characteristics with traditional polymeric carriers, including water solubility, high capacity of drug loading and improved biodistribution. Poly (amido amine) (PAMAM) dendrimers have shown promise as oral drug carriers due to their compact size, high surface charge density and permeation across the intestinal epithelial

barrier. Attachment of chemotherapy drugs to PAMAM dendrimers has the potential to make them orally administrable and reduce off-target toxicities.

In this dissertation we investigate the transport mechanisms of PAMAM dendrimers and their potential in oral drug delivery. We demonstrate that anionic G3.5 dendrimers are endocytosed by dynamin-dependent mechanisms and their transport is governed by clathrin-mediated pathways. We show that dendrimer cellular internalization may be a requisite step for tight junction opening. We also demonstrate that conjugation of small poly (ethylene glycol) chains to anionic dendrimers decreases their transport and tight junction opening due to reduction in surface charge, illustrating that small changes in surface chemistry can significantly impact transepithelial transport. Knowledge of transport mechanisms and the impact of surface chemistry will aid in rational design of dendrimer oral drug delivery systems.

The potential of dendrimers as oral drug delivery carriers is demonstrated by the evaluation of G3.5 PAMAM dendrimer-SN38 conjugates for oral therapy of hepatic colorectal cancer metastases, a pathology present in over 50% of colorectal cancer cases that is responsible for two-thirds of deaths. Conjugation of SN38, a potent chemotherapy drug with poor solubility and low bioavailability, to PAMAM dendrimers via a glycine linker increased intestinal permeability, decreased intestinal toxicity and showed selective release in the presence of liver carboxylesterase, illustrating that PAMAM dendrimers have the potential to improve the oral bioavailability of potent anti-cancer therapeutics.

POLY (AMIDO AMINE) DENDRIMERS: TRANSEPITHELIAL TRANSPORT
MECHANISMS AND APPLICATIONS IN ORAL DRUG DELIVERY

By

Deborah Sweet Goldberg

Dissertation submitted to the Faculty of the Graduate School of the
University of Maryland, College Park, in partial fulfillment
of the requirements for the degree of
Doctor of Philosophy
2010

Advisory Committee:
Professor Hamidreza Ghandehari, Co-Chair
Professor William Bentley, Co-Chair
Professor Robert Briber
Professor Silvia Muro
Professor Peter Swaan

© Copyright by
Deborah Sweet Goldberg
2010

Dedication

To my wonderful husband Hirsh, for his constant, unwavering love and support.

Acknowledgements

I have had the honor of working with many talented individuals during my PhD studies who have helped me reach this milestone in my life. I would first like to thank my advisor **Dr. Hamid Ghandehari** for his enduring commitment to my training as a scientist. Although Dr. Ghandehari moved to the University of Utah shortly after I began my research, he has always strived to maintain constant communication and provide advice on my project. I appreciate his attention to detail in his careful review of my abstracts, posters, presentations, publications and dissertation. Dr. Ghandehari has always inspired me to do my best work, and I know that the impact of his guidance will follow me into my future scientific endeavors.

I would also like to thank **Dr. Peter Swaan** for his contributions to my PhD studies as both my co-advisor and local contact. Dr. Swaan has helped me feel at home at the University of Maryland, Baltimore. I sincerely appreciate the many research discussions that we had during group meetings and individual meetings. I am also thankful for the fresh perspective he offered on my publications and presentations. Dr. Swaan has taught me to think critically and continually question everything, a mindset that will serve me well in the future.

I also wish to thank my committee members, **Dr. Silvia Muro, Dr. Robert Briber** and **Dr. William Bentley** for their helpful suggestions during my research proposal and committee meeting. Their insights have helped shape the trajectory of my project, and I am grateful for their guidance.

In addition to my advisors and my committee members, two other professors have had a significant impact on my PhD studies. I will be forever indebted to **Dr.**

Rohit Kolhatkar for his guidance during the first few years of my PhD studies.

Rohit taught me experimental techniques and advised me on planning experiments, interpreting results and troubleshooting chemical synthesis strategies. After Rohit left to become an assistant professor at the University of Illinois, Chicago I realized that his guidance had taught me everything I needed to think like a scientist and successfully complete the remainder of my studies. I would also like to thank **Dr. Anjan Nan** for graciously allowing me to conduct my research in his laboratory space and use his equipment. Dr. Nan's support of my long distance advisement by Dr. Ghandehari made it possible for me to continue my research on dendrimers.

I wish to acknowledge all of my fellow lab members past and present in the Ghandehari, Swaan and Nan labs who have had an influence on my day-to-day life in the lab. Specifically, I would like to acknowledge **Dr. Mark Borgman** for his endless technical advice on experiments and his wonderful friendship. Even after he graduated, Mark was only a phone call or an email away, and has continued to be a great friend and knowledgeable research consultant. I would also like to thank **Brittany Avaritt, Tatiana Claro da Silva** and **Paul Dowell** for their friendship and support over the years. Finally, I would like to thank **Carl** the janitor who always managed to make me smile on his early morning rounds.

During my PhD experience I was fortunate to complete a summer internship in the Department of Formulation Sciences at MedImmune LLC. Although this internship experience was distinct from my graduate research, it gave me an appreciation of the pharmaceutical industry and taught me new ways of approaching problems, which positively impacted my graduate work after the internship. I would

like to thank my supervisor **Dr. Hasige Sathish** and my formulation sub-group leader **Dr. Ambarish Shah** for their positive contributions to my PhD experience and for providing me with this unique opportunity.

Several fellowships and grants during my graduate studies have helped to fund my research. I would like to thank the **National Science Foundation** for the **Graduate Research Fellowship**, which sponsored my first three years of graduate school. It was an honor to receive this fellowship and it had a positive impact on my graduate school career, providing me with freedom in project selection. I would also like to thank **Dr. Robert Fischell** for generously sponsoring the **Fischell Fellowship in Bioengineering**, which funded my final years in graduate school. Dr. Fischell's commitment to fostering new Bioengineering research is admirable and his enthusiasm is contagious. I also acknowledge **NIH R01 EB007470** for funding supplies for this research.

I would like to recognize my friends and family, whose support and encouragement have been critical for the successful completion of my PhD studies. My parents, **Shari and Rick Sweet**, have always been my biggest cheerleaders, supporting all of my academic and personal pursuits. I truly appreciate their excitement about all of my accomplishments from elementary school until today and their constant encouragement to strive for my dreams. I would also like to thank my mother and father in-law, **Karen and Larry Goldberg** for their interest and support throughout my PhD studies. I would like to acknowledge the wonderful support of my friends **Marie Jeng, Chloe Marin, Rifat Jafreen** and **Kevin Nelson** among many others who have shown interest in my PhD progress over the years and offered

countless words of encouragement. I wish to express my gratitude to the instructors at **Columbia Jazzercise** for providing a fun and exhilarating stress release as well as all of my friends at Jazzercise for their constant interest and encouragement. Finally, I would like to thank my husband **Hirsh** who has been my greatest supporter through all of the ups and the downs of my PhD research. Hirsh has always offered emotional support and encouragement when I was frustrated with unsuccessful experiments and has unselfishly taken over household responsibilities when I had to work late at night or on the weekend to meet a deadline. I know that his love and unwavering support helped me push through the most difficult challenges of my PhD and I could not have done it without him. He truly deserves this degree as much as I do.

Table of Contents

Dedication	ii
Acknowledgements	iii
List of Tables	xi
List of Figures.....	xii
Abbreviations	xv
Chapter 1 : Introduction	1
1.1 Introduction	1
1.1.1 Polymer Therapeutics.....	1
1.1.2 Oral Drug Delivery	2
1.1.3 Poly (amido amine) Dendrimers.....	3
1.1.4 SN38.....	4
1.2 Specific Aims	5
1.3 Scope and Organization	6
Chapter 2 : Background.....	8
2.1 Introduction	8
2.2 Polymeric Drug Delivery	8
2.2.1 Therapeutic Advantages of Polymer-Drug Conjugates in Chemotherapy... 9	
2.2.2 Polymer-Drug Conjugates Currently in Clinical Trials	12
2.3 Administration of Drugs via the Oral Route	13
2.3.1 Physiology of the Gastrointestinal Tract.....	14
2.3.1.1 Compartments and Functions	14
2.3.1.2 Intestinal Epithelial Barrier.....	17
2.3.1.3 Tight Junction Biology: Structure and Function.....	18
2.3.2 Mechanisms of Transport Across the Intestinal Barrier	21
2.3.2.1 Paracellular Transport	21
2.3.2.2 Passive Diffusion	23
2.3.2.3 Carrier-Mediated Transport	24
2.3.2.4 Endocytosis.....	25
2.3.3 Physiochemical Properties that Govern Intestinal Absorption.....	28
2.3.3.1 The Lipinski Rule of 5.....	28
2.3.3.2 The Biopharmaceutics Classification System (BCS).....	28
2.4 Models to Predict Oral Absorption and Oral Bioavailability.....	30
2.4.1 In Silico Models.....	30
2.4.2 Parallel Artificial Membrane Permeability Assay	31
2.4.3 Caco-2 Monolayers.....	33
2.4.4 Fast-Caco-2 Assay	36

2.4.5 Other Types of Cell-Monolayer Systems.....	37
2.4.6 Everted Rat Intestinal Sac	38
2.4.7 Isolated Intestinal Tissue	39
2.4.8 Rat Intestinal Perfusion	40
2.4.9 In Vivo Models	40
2.5 Current Strategies for Oral Drug Delivery.....	41
2.5.1 Prodrugs.....	42
2.5.2 Efflux and Metabolic Inhibitors.....	43
2.5.3 Tight Junction Modulators	44
2.5.4 Macromolecules.....	45
2.6 Dendrimers.....	47
2.6.1 History of Dendrimer Development	47
2.6.2 Dendrimer Synthesis	49
2.6.3 Types of Dendrimers.....	49
2.7 Poly (amido amine) Dendrimers	51
2.7.1 Structure of PAMAM Dendrimers.....	51
2.7.2 Biocompatibility and Biodistribution of PAMAM Dendrimers.....	53
2.7.3 Applications of PAMAM Dendrimers as Drug Carriers.....	55
2.8 PAMAM Dendrimers as Oral Drug Delivery Systems	57
2.8.1 Transepithelial Transport of PAMAM Dendrimers.....	57
2.8.2 Cytotoxicity of PAMAM Dendrimers	60
2.8.3 Surface Modification of PAMAM Dendrimers	61
2.8.4 PAMAM Dendrimer Internalization.....	62
2.8.5 PAMAM Dendrimers as Oral Drug Delivery Systems.....	63
2.8.6 Designing PAMAM Dendrimer-Drug Conjugates for Oral Delivery	64
2.9 Colorectal Cancer	65
2.9.1 Prevalence.....	65
2.9.2 Colorectal Cancer Screening	66
2.9.3 Colorectal Cancer Diagnosis and Staging	67
2.9.4 Colorectal Cancer Metastasis and Treatment	67
2.10 SN38	69
2.10.1 Mechanism of Action of Irinotecan and SN38	70
2.10.2 Current SN38 Drug Delivery Systems.....	72
2.11 Unresolved Issues in Oral Delivery by Dendrimers	73

Chapter 3 : Cellular Entry of G3.5 Poly (amido amine) Dendrimers by Clathrin- and Dynamin-Dependent Endocytosis Promotes Tight Junctional Opening in Intestinal Epithelia

3.1 Introduction	75
3.2 Materials and Methods.....	77
3.2.1 Materials	77
3.2.2 Synthesis of G3.5-OG	77
3.2.3 Caco-2 Cell Culture	78
3.2.4 Cytotoxicity of Endocytosis Inhibitors	79
3.2.5 Cellular Uptake	79

3.2.6 Colocalization and Intracellular Trafficking	80
3.2.7 Transepithelial Transport	82
3.2.8 Caco-2 Monolayer Visualization and Occludin Staining.....	83
3.3 Results.....	85
3.3.1 Cytotoxicity of Endocytosis Inhibitors	85
3.3.2 Cellular Uptake of G3.5-OG Dendrimers in the Presence of Endocytosis Inhibitors	87
3.3.3 Intracellular Trafficking	90
3.3.4 Transepithelial Transport of G3.5-OG Dendrimers in the Presence of Endocytosis Inhibitors	93
3.3.5 Visualization of G3.5-OG Dendrimer Interaction with Caco-2 Cell Monolayers.....	93
3.3.6 Occludin Staining in Presence of Dendrimers with and without Dynasore Treatment	96
3.4 Discussion	99
3.5 Conclusion.....	104

Chapter 4 : G3.5 PAMAM Dendrimers Enhance Transepithelial Transport of SN38 While Minimizing Gastrointestinal Toxicity 105

4.1 Introduction	105
4.2 Materials and Methods.....	106
4.2.1 Materials	106
4.2.2 Synthesis and Characterization of G3.5-Gly-SN38 and G3.5-βAla-SN38 Conjugates.....	107
4.2.3 Stability Studies	109
4.2.4 Cell Culture.....	110
4.2.5 Potential Short-Term Cytotoxicity of G3.5-SN38 Conjugates.....	111
4.2.6 Potential Delayed Cytotoxicity of G3.5-SN38 Conjugates.....	111
4.2.7 Transepithelial Transport	112
4.2.8 Cellular Uptake.....	112
4.2.9 IC ₅₀ in HT-29 Cells	113
4.3 Results.....	114
4.3.1 Stability of G3.5-SN38 Conjugates	114
4.3.2 Short-Term Cytotoxicity	119
4.3.3 Delayed Cytotoxicity	121
4.3.4 Transepithelial Transport	121
4.3.5 Cellular Uptake.....	125
4.3.6 IC ₅₀ in HT-29 Cells.....	127
4.4 Discussion	129
4.5 Conclusion.....	133

Chapter 5 : Transepithelial Transport of PEGylated Anionic Poly (amido amine) Dendrimers: Implications for Oral Drug Delivery..... 135

5.1 Introduction	135
------------------------	-----

5.2 Materials and Methods.....	136
5.2.1 Materials.....	136
5.2.2 Conjugation of mPEG750 to PAMAM Dendrimers.....	137
5.2.3 Characterization of PEGylated G3.5 and G4.5 Dendrimers.....	139
5.2.4 Synthesis of Radiolabeled Dendrimers.....	140
5.2.5 Caco-2 Cell Culture.....	140
5.2.6 Cytotoxicity Assay.....	140
5.2.7 Cellular Uptake Studies.....	140
5.2.8 Transepithelial Permeability Assessment.....	141
5.2.9 Occludin Staining.....	142
5.3 Results.....	144
5.3.1 Synthesis and Characterization of PEGylated Anionic PAMAM Dendrimers.....	144
5.3.2 Short-Term Cytotoxicity.....	146
5.3.3 Cellular Uptake.....	150
5.3.4 Transepithelial Transport.....	150
5.3.5 Tight Junction Opening Monitored by Occludin Staining.....	155
5.4 Discussion.....	155
5.5 Conclusion.....	160
Chapter 6 : Conclusions and Future Directions.....	162
6.1 Conclusions.....	162
6.2 Future Directions.....	165
Appendix 1: Visualization of Intracellular Trafficking of G3.5 Dendrimers and Transferrin in Caco-2 Cells.....	168
Appendix 2: Quantification of SN38 by High Pressure Liquid Chromatography	171
Appendix 3: Quantification of PEG Content of PAMAM G3.5 and G4.5-PEG Conjugates by Proton Nuclear Magnetic Resonance.....	178
Bibliography.....	183

List of Tables

Table 2.1. Physiology of the Gastrointestinal Tract.....	16
Table 2.2. Physical Properties of PAMAM Dendrimers.....	54
Table 3.1. Endocytosis Inhibitor Concentration and % Cell Viability in Caco-2 Cells	86
Table 3.2. Percent Uptake of G3.5-OG Dendrimers and Control Ligands in Caco-2 Cells in the Presence of Endocytosis Inhibitors.	88
Table 5.1. Characteristics of PAMAM Dendrimer-PEG Conjugates	145
Table A2.1. HPLC Gradient Method for SN38 Detection	172
Table A3.1. Quantification of PEG Conjugation to G3.5 and G4.5 Dendrimers by ¹ H NMR	180

List of Figures

Figure 2.1. Design and Optimization of Polymer-Drug Conjugates.....	10
Figure 2.2. Major Proteins Involved in Tight Junctions.....	19
Figure 2.3. Mechanisms of Transport through the Intestinal Barrier.....	22
Figure 2.4. Clathrin- and Caveolin-Mediated Endocytosis and Transcytosis.	27
Figure 2.5. The Biopharmaceutics Classification System.	29
Figure 2.6. Transwell® System used in the Caco-2 Monolayer Permeability Assay..	34
Figure 2.7. Dendrimers as Multifunctional Nanocarriers.....	48
Figure 2.8. Divergent and Convergent Syntheses of Dendrimers.....	50
Figure 2.9. Chemical Structures of Common Dendrimers	52
Figure 2.10. Conversion of Irinotecan to SN38 by Carboxylesterase and Equilibrium of Carboxylate and Lactone forms of SN38 and Irinotecan	71
Figure 3.1. Intracellular Trafficking of G3.5-OG Dendrimers over Time in Caco-2 Cells.	91
Figure 3.2. Intracellular Trafficking of Transferrin-AF488 over Time in Caco-2 Cells	92
Figure 3.3. Percent Transport of G3.5-OG Dendrimers across Caco-2 Monolayers in the Presence of Endocytosis Inhibitors or at 4°C	94
Figure 3.4. Visualization of G3.5-OG Dendrimer Interaction with Caco-2 Monolayers.....	95
Figure 3.5. Occludin Staining in the Presence and Absence of G3.5-OG Dendrimers in Caco-2 Cells Treated with HBSS or Dynasore	97
Figure 3.6. Quantification of Occludin Staining.....	98
Figure 3.7. Mechanisms of Dendrimer Transport Across Caco-2 Cell Monolayers.	103
Figure 4.1. Conjugation of SN38 to G3.5 Dendrimers via Glycine and β -Alanine Linkers	108

Figure 4.2. Stability of G3.5-Gly-SN38 and G3.5-βAla-SN38 Conjugates in Simulated Stomach Conditions for 6 hours	115
Figure 4.3. Stability of G3.5-Gly-SN38 and G3.5-βAla-SN38 Conjugates in Simulated Intestinal Conditions for 24 hours.....	116
Figure 4.4. Stability of G3.5-Gly-SN38 and G3.5-βAla-SN38 Conjugates in Simulated Liver Conditions for 48 hours.....	117
Figure 4.5. Caco-2 Cell Viability after Treatment for 2 hours with G3.5 Dendrimers, G3.5-SN38 Conjugates and SN38.....	120
Figure 4.6. Caco-2 Cell Viability 24 hours after 2-hour Treatment with G3.5, G3.5-SN38 Conjugates and SN38.....	122
Figure 4.7. Equivalent SN38 Flux across Differentiated Caco-2 Monolayers Treated with G3.5-SN38 Conjugates and SN38	123
Figure 4.8. Cellular Uptake of G3.5-SN38 Conjugates and Free SN38 in Differentiated Caco-2 Monolayers after 2-hour Treatment on the Apical Side.	126
Figure 4.9. IC ₅₀ Curves of SN38, G3.5-Gly-SN38 and G3.5-βAla-SN38 in HT-29 Cells	128
Figure 5.1. PEGylation of G3.5 Dendrimer with mPEG750.....	138
Figure 5.2. Zeta Potential of PEGylated G3.5 and G4.5 PAMAM Dendrimers.....	147
Figure 5.3. Caco-2 Cell Viability in the Presence of G3.5 Native and PEGylated Dendrimers after a 2-hour Incubation Time.....	148
Figure 5.4. Caco-2 Cell Viability in the Presence of G4.5 Native and PEGylated Dendrimers after a 2-hour Incubation Time.....	149
Figure 5.5. Uptake of G3.5 Native and Differentially PEGylated Dendrimers.....	151
Figure 5.6. Uptake of G4.5 Native and Differentially PEGylated Dendrimers.....	152
Figure 5.7. Apparent Permeability of G3.5 Native and Differentially PEGylated Dendrimers.....	153
Figure 5.8. Apparent Permeability of G4.5 Native and Differentially PEGylated Dendrimers.....	154

Figure 5.9. Staining of the Tight Junction Protein Occludin in the Presence and Absence of Dendrimers Visualized by Confocal Microscopy	156
Figure 5.10. Quantification of Occludin Staining in the Presence and Absence of Dendrimers.....	157
Figure A1.1. Visualization of G3.5 Dendrimer Trafficking over Time in Caco-2 Cells by Confocal Microscopy.....	169
Figure A1.2. Visualization of Transferrin Trafficking over Time in Caco-2 Cells by Confocal Microscopy.....	170
Figure A2.1. Typical HPLC Elution Profile of SN38	173
Figure A2.2. Standard Curve Elution Profiles.....	175
Figure A2.3. HPLC Standard Curve Comparing SN38 Concentration and Peak Area	176
Figure A2.4. Precision of HPLC Detection	177
Figure A3.1. NMR Spectra of G3.5-PEG Conjugates	181
Figure A3.2. NMR spectra of G4.5-PEG Conjugates	182

Abbreviations

5FU	5 fluorouracil
ABC	ATP binding cassette
Å	Angstrom
AF	Alexa Fluor
ATP	Adenosine triphosphate
AUC	Area under the curve
βAla	Beta-alanine
BCA	Bicinchoninic acid
BCS	Biopharmaceutics classification system
BOP	Benzotriazole-1-yl-oxy-tris-(dimethylamino)- phosphoniumhexafluorophosphate
BSA	Bovine serum albumin
CH	Carbohydrazide
CME	Caveolin-mediated endocytosis
CPT	Camptothecin
CPT-11	Irinotecan
CT	Computed tomography
CYP	Cytochrome P450
D ₂ O	Deuterated water
Da	Dalton
DACH	Diaminocyclohexane

DAPI	4',6-diamidino-2-phenylindole
DDS	Drug delivery system
DI	Deionized
DLS	Dynamic light scattering
DMEM	Dulbecco's modified eagle's medium
DMSO	Dimethyl sulfoxide
DNA	Deoxyribonucleic acid
DPBS	Dulbecco's phosphate buffered saline
DYN	Dynasore
EDC	1-Ethyl-3-(3-dimethylaminopropyl)-carbodiimide
EDTA	Ethyelendiamine tetraacetic acid
EEA-1	Early endosome antigen-1
EGFR	Epidermal growth factor receptor
EPR	Enhanced permeability and retention
FBS	Fetal bovine serum
FDA	Food and Drug Administration
FIL	Filipin
FITC	Fluorescein isothiocyanate
FOBT	Fecal occult blood tests
FOLFIRI	5FU/Leucovorin + Irinotecan chemotherapy regiment
FOLFOX	5FU/Leucovorin + Oxaliplatin chemotherapy regiment
FPLC	Fast protein liquid chromatography

G	Generation
GEN	Genistein
GFLG	Glycine-phenylalanine-leucine-glycine
Gly	Glycine
GTPase	Guanosine triphosphate hydrolytic enzyme
HBSS	Hank's balanced salt solution
HCl	Hydrochloric Acid
HEPES	N-(2-hydroxyethyl)piperazine-N'-179 (2 ethanesulfonic acid) hemisodium salt
HPLC	High pressure liquid chromatography
HPMA	N-(2-hydroxypropyl)methacrylamide
IC ₅₀	Half maximal inhibitory concentration
IgG	Immunoglobulin G
IU	International unit
IV	Intravenous
JAM	Junction adhesion molecule
LAMP-1	Lysosome-associated membrane protein-1
LDH	Lactate dehydrogenase
LY	Lucifer yellow carbohydrazide
MALLS	Multi-angle laser light scattering
MAPK	Mitogen activated protein kinase
M-cells	Microfold cells

MDC	Monodansyl cadaverine
MDR	Multidrug resistant protein
MLCK	Myosin light chain kinase
mPEG	Methoxy poly (ethylene glycol)
MS	Mass spectrometry
MW	Molecular weight
MWCO	Molecular weight cut off
NHS	<i>N</i> -Hydroxysuccinimide
NMR	Nuclear magnetic resonance
OG	Oregon green
PAMAM	Poly (amido amine)
PAMPA	Parallel artificial membrane assay
PAO	Phenylarsine oxide
P_{app}	Apparent permeability
PBS	Phosphate buffered saline
PD10	Protein desalting column
PEG	Poly (ethylene glycol)
PG	Poly (L-glutamic acid)
P-gp	P-glycoprotein
PG-TXL	Poly (L-glutamic acid)- Paclitaxel conjugate
PPI	Poly (propylene imine)
PVDF	Poly vinylidene fluoride

QELS	Quasi-elastic light scattering
QSAR	Quantitative structure activity relationship
QSPR	Quantitative structure property relationship
RI	Refractive index
RME	Receptor-mediated endocytosis
RNA	Ribonucleic acid
RPM	Rotations per minute
SEC	Size exclusion chromatography
SGF	Simulated gastric fluid
SIF	Simulated intestinal fluid
SLC	Solute carrier
SN38	7-Ethyl-10-hydroxy-camptothecin
SNAP	S-nitroso-N-acetyl-DL-penicillamine
TEER	Transepithelial electrical resistance
TEM	Transmission electron microscopy
TJ	Tight junction
TFA	Trifluoroacetic acid
TNM	Tumor-lymph node-metastasis classification system
TSP-d ₄	3-(trimethylsilyl) propionic-2,2,3,3-d ₄ acid
UDPGA	Uridine diphosphoglucuronic acid
UDPGT	Uridine diphosphate glucuronyltransferase
UV	Ultraviolet
VEGF	Vascular endothelial growth factor

WST-1	Water soluble tetrazolium salt
Z-Arg-AMC	Benzyloxycarbonyl-L-arginine-4-methylcoumaryl-7-amide
ZO	Zonulla occludens
Zot	Zona occludins toxin

Chapter 1 : Introduction

1.1 Introduction

1.1.1 Polymer Therapeutics

Carrier-based drug delivery strategies have been used to improve the therapeutic profile of small molecule drugs by enhancing uptake at the site of action and minimizing off-target effects. In particular, water-soluble polymer-based drug delivery systems can improve the efficacy of therapeutically active compounds with intrinsically poor water solubility and high toxicity [1]. In the field of nanomedicine, carriers such as polymeric nanoparticles and liposomes have also shown promise in altering the biodistribution of drugs, improving efficacy and enhancing intracellular accumulation [2]. Importantly, targeting moieties and imaging agents can be conjugated to delivery vehicles, making such carriers ideal for multifunctional drug delivery [3].

Chemotherapy drugs are promising candidates for drug delivery strategies because they are often plagued by poor water solubility and dose-limiting toxicities. Conjugation of chemotherapeutics to linear water-soluble polymers such as poly(ethylene glycol) (PEG) and N-(2-hydroxypropyl)methacrylamide (HPMA) copolymers can improve their therapeutic profile by increasing the drug concentration at the tumor site due to enhanced permeability and retention in the leaky tumor vasculature [4]. In addition, targeting moieties can be conjugated to the polymer backbone to further enhance tumor-specific uptake. Finally, drug linkers can be designed to release the drug from the polymer in the tumor environment in response to pH changes or specific

enzymes [5]. Increased tumor accumulation and selective release improve the overall therapeutic profile compared to the free drug by increasing the concentration of drug at the site of action and reducing side effects caused by drug accumulation in off-target tissues [6].

1.1.2 Oral Drug Delivery

Due to their low water solubility and poor bioavailability, chemotherapy agents are traditionally administered intravenously, requiring recurring hospital visits and significant direct and indirect costs to the patient [7]. While conjugation to water-soluble polymers can improve their solubility, the large size of these macromolecular constructs necessitates intravenous administration. Because of the strong patient preference for oral therapy and the numerous advantages of polymeric drug delivery systems, there is a significant need for development of orally administrable polymer-drug conjugates that can improve the oral bioavailability of the drug as well as target the drug to the tumor site. Advantages of oral chemotherapy include the convenience of at-home administration, reduction of costs associated with hospital procedures and with transportation to and from the treatment center, a more flexible dosing regimen and a decreased burden on hospitals and the healthcare system [8, 9].

Oral delivery is challenging because systems must have appropriate solubility, stability in the gastrointestinal pH and enzymatic environment, and the ability to permeate the epithelial barrier of the gut. The mucosa of the intestinal tract is composed of polarized enterocytes that form a tight barrier to transport, preventing the diffusion of many molecules based on size, shape and charge [10]. In addition, compounds must have

some degree of lipophilicity to be transported via passive diffusion, otherwise, they are relegated to the paracellular pathway which is generally limited to small hydrophilic molecules of 100-200 Da [11]. Therefore, oral delivery of polymer-drug conjugates while convenient and beneficial to the patient is also challenging.

1.1.3 Poly (amido amine) Dendrimers

Dendrimers, a class of highly branched polymers, have been shown to be effective drug delivery vehicles due to their unique physical properties including near monodispersity and nanoscopic size [12, 13]. With each increase in dendrimer generation, the diameter increases linearly while the number of surface groups increases exponentially. This creates a high density of surface groups that can be conjugated to drug molecules, targeting moieties, and imaging agents, making dendrimers a versatile drug delivery platform [14]. Dendrimers are more compact than traditional linear polymers and thus show potential in oral drug delivery. Specifically, poly (amido amine) or PAMAM dendrimers have shown promise as oral drug delivery carriers due to their nanoscale size and high surface charge density.

Originally developed by Tomalia in 1979, PAMAM dendrimers have an ethylene diamine core, an amido amine branching structure and are commercially available as cationic “full” generations (G1, G2, etc.) with amine-terminated branches, and anionic “half” generations (G1.5, G2.5, etc.) with carboxylic acid terminated branches. Previous studies indicate that PAMAM dendrimers in a specified size and charge window can effectively cross the intestinal epithelial barrier, making them suitable as drug delivery carriers for poorly water-soluble chemotherapeutics [15-20]. While it has been firmly

established that generation, charge and surface chemistry influence PAMAM dendrimer transport across the epithelial barrier, more needs to be done to investigate how surface modification and drug conjugation impact the degree and mechanism of dendrimer transport. In addition, chemical linkers that promote stability of the dendrimer-drug conjugate in the gastrointestinal milieu while favoring release of drug in the tumor environment must be developed to achieve a functional delivery system.

1.1.4 SN38

Because of its low water solubility and poor bioavailability, SN38 (7-ethyl-10-hydroxy-camptothecin) is an ideal candidate for polymeric delivery strategies. SN38 is the active metabolite of Irinotecan, a water-soluble camptothecin analogue that is commonly used for treatment of metastatic colorectal cancer [21]. With more than 140,000 new cases of colorectal cancer each year and over 51,000 deaths projected in 2010, there is a significant need for novel, targeted therapies for colorectal cancer [22]. The most common site of colorectal cancer metastasis is the liver, with over 20% of patients presenting liver metastases at the time of diagnosis and 50% in the duration of the disease [23]. These liver metastases are responsible for two-thirds of all colorectal cancer deaths, indicating the grave need for novel treatments of this condition. SN38 works by inhibition of topoisomerase-1, and shows 100-1000 fold greater *in vitro* activity than Irinotecan. However, it has had limited clinical success due to poor water solubility and adverse gastrointestinal effects. Therefore a delivery system that improves SN38 water solubility, decreases gastrointestinal toxicity and targets SN38 to liver metastases

has the potential to significantly improve its therapeutic profile and increase the efficacy of colorectal cancer treatment.

1.2 Specific Aims

This dissertation seeks to investigate the mechanisms of transepithelial transport of anionic PAMAM dendrimers and their conjugates with SN38 and PEG, with the long-term goal of delivering SN38 orally to colorectal cancer metastases in the liver. The global hypothesis of the dissertation is that anionic PAMAM dendrimers can be used to improve the oral bioavailability of SN38 for the treatment of colorectal hepatic metastases and that the degree and mechanism of transepithelial transport of PAMAM dendrimers will be impacted by surface modification and drug loading. This global hypothesis was investigated by the following three Specific Aims:

1. To determine the transepithelial transport mechanisms of anionic G3.5 PAMAM dendrimers across Caco-2 monolayers as a model of the intestinal epithelial barrier.

2. To evaluate the toxicity, transport and uptake of G3.5-SN38 conjugates in Caco-2 cell monolayers and the stability of the conjugates in simulated gastrointestinal and liver environments.

3. To investigate the impact of surface modification of anionic PAMAM dendrimers with PEG on cytotoxicity, uptake, and transepithelial transport in Caco-2 cells.

These Specific Aims are designed to test the following three hypotheses:

1. Transepithelial transport of anionic PAMAM dendrimers occurs via several pathways including transcytosis, governed by specific endocytic mechanisms, and paracellular transport, driven by dendrimer-mediated tight junction opening.

2. Conjugation of SN38 to G3.5 dendrimers via a glycine or β -alanine peptide linker will increase SN38 permeability while reducing intestinal toxicity. The conjugates will be stable in the gastrointestinal environment and will release SN38 in the presence of liver carboxylesterase.

3. Conjugation of PEG to anionic dendrimers will influence uptake and transport across Caco-2 cell monolayers.

1.3 Scope and Organization

Chapter 2 provides background on the benefits and challenges of oral drug delivery as well as the current strategies used to improve oral bioavailability and the laboratory methods used to predict oral absorption. Chapter 2 also offers background on dendrimers, a detailed description of PAMAM dendrimers and a literature review of current knowledge on these polymers in the context of oral drug delivery [24]. In addition, colorectal cancer and current limitations and delivery strategies for SN38 are reviewed in this Chapter. Chapter 3 describes the mechanisms of transport, uptake, intracellular trafficking and tight junction opening of native, anionic G3.5 PAMAM dendrimers in Caco-2 cells [25]. In particular, Chapter 3 explores the role of endocytosis in dendrimer tight junction opening. In Chapter 4, G3.5-SN38 conjugates are evaluated for their potential in oral drug delivery [26]. Specifically, their intestinal toxicity,

stability in simulated gastrointestinal environment and in the presence of liver carboxylesterase as well as their cellular uptake and transport across Caco-2 monolayers and efficacy in HT-29 cells are investigated. Chapter 5 describes the evaluation of PEG surface modification of G3.5 and G4.5 dendrimers in the context of oral drug delivery, specifically examining the impact of PEGylation on dendrimer cytotoxicity, uptake, transport and tight junction modulation in Caco-2 cell monolayers [27]. Finally, Chapter 6 summarizes the major findings of this dissertation and suggests future directions for this research.

Chapter 2 : Background

2.1 Introduction

The objective of drug delivery science is to control the spatial and temporal distribution of a drug molecule in the body in order to improve therapeutic effect and/or reduce toxicity [28]. Drug delivery technologies can alter a drug's solubility, absorption, metabolism, elimination and biodistribution *in vivo*. One of the most common drug delivery strategies is to attach therapeutic compounds to “carriers” by physical and chemical mechanisms, with the overall goal of modifying the drug's biodistribution and controlling release from the carrier. Examples of drug delivery carriers include nanoparticles, micelles, liposomes and water-soluble polymers [29-31]. These advanced “formulation strategies,” can be modified to yield an optimized delivery system for the cargo, which can improve the therapeutic index compared to the free drug. In this dissertation we will explore poly (amido amine) (PAMAM) dendrimers as oral drug delivery vehicles for anti-cancer therapeutics. This chapter will provide the pertinent background on the concepts of polymeric drug delivery, oral drug delivery, dendrimers, colorectal cancer and SN38 as well as a literature review on the current state of knowledge on poly (amido amine) (PAMAM) dendrimers as oral drug delivery carriers.

2.2 Polymeric Drug Delivery

Polymeric systems are among the most widely used drug carriers. Although synthetic polymers were used as early as the 1830's in the field of materials science [32],

water-soluble polymers were not conceptualized for use as targeted drug delivery systems until 1975 when Ringsdorf first wrote of “pharmacologically active polymers” [33]. In this concept, a drug molecule is covalently conjugated to a polymeric carrier through a selectively degradable chemical linker, which releases the drug at the site of action. Targeting moieties are conjugated to the polymer in order to enhance the accumulation of the polymer-drug conjugate at the site of action, maximizing efficacy and minimizing non-specific toxicities. Several properties of the polymer backbone, including chemical composition, molecular weight and architecture, can be tailored for a given drug delivery application. In addition, the number of drug molecules, choice of chemical linker and type of targeting moiety can be modified to create an optimized polymeric drug delivery system [6]. A schematic of polymer-drug conjugate design is shown in Figure 2.1.

2.2.1 Therapeutic Advantages of Polymer-Drug Conjugates in Chemotherapy

One of the most common applications of polymer-drug conjugates is in the delivery of anti-cancer therapeutics. Because chemotherapy drugs have high potency but low selectivity, their use is severely limited by unintended toxic effects to healthy tissues [34]. Conjugation of chemotherapeutics to polymeric carriers has the capacity to improve their therapeutic index by enhanced drug accumulation at the tumor site with fewer off-target effects [35]. One of the most widely studied properties of polymeric drug delivery systems is the enhanced permeability and retention (EPR) effect. The EPR effect, coined by Hiroshi Maeda, describes the propensity of macromolecules to accumulate in solid tumors [36]. Because of the rapid angiogenesis associated with solid

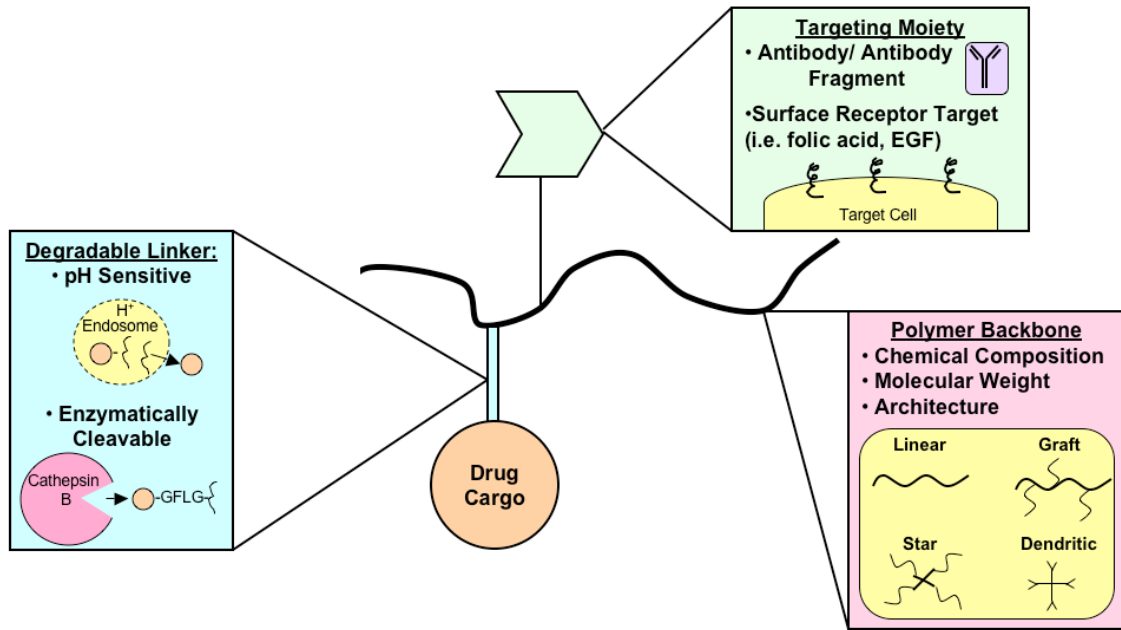


Figure 2.1. Design and Optimization of Polymer-Drug Conjugates. Several parameters can be optimized when designing polymer-drug conjugates including polymer backbone composition, molecular weight and architecture, drug cargo identity and amount, type of chemical linker and nature of targeting moiety.

tumor formation, tumors have dense and leaky vasculature. This leaky tumor vasculature, coupled with the long half-life of macromolecules, leads to higher accumulation of polymer-drug conjugates in the tumor compared to other tissues that have lesser fenestrations in endothelial cell layers. Thus, passive targeting by the EPR effect allows for accumulation of the drug at the tumor site, improving the therapeutic index compared to the free drug. Moreover, conjugation of antibodies and ligands to the polymer backbone that target specific receptors over-expressed on tumor cells can enhance tumor accumulation [37]. The ability of polymers to serve as backbones for the conjugation of drugs, targeting moieties and imaging agents makes them powerful multifunctional delivery systems.

In addition to promoting drug localization at the tumor site, polymer-drug conjugates can also be designed to optimize drug release at the site of action [6]. There are several chemical linkers that are cleaved by select enzymes. For example, the amino acid sequence Gly-Phe-Leu-Gly (GFLG) has been shown to be selectively cleaved by cathepsin B, which is over-expressed in the lysosomes of tumor cells [38]. This linker can be used to optimize drug release in the tumor environment, thus minimizing side effects. A commonly used linker in the context of colonic delivery is the azo spacer [39]. Azo spacers are cleaved by azo-reductase enzymes produced by bacteria in the colon, confining drug release to the colonic environment. Therefore, appropriate drug linker selection allows for specific release in the target site and further enhances the therapeutic effect of polymer-drug conjugates.

2.2.2 Polymer-Drug Conjugates Currently in Clinical Trials

There are several promising polymer-drug conjugates that are currently being evaluated in clinical trials. Two HPMA (N-(2-hydroxypropyl) methacrylamide)-based systems are currently in clinical trials for the delivery of Doxorubicin and Platinite [40]. FCE 28068 contains Doxorubicin conjugated to 30 kDa HPMA copolymer via a GFLG spacer. FCE28068 showed 2-5 fold less toxicity than free Doxorubicin with tumor responses documented in breast, non-small cell lung cancers and hepatocellular carcinoma [41, 42]. AP5346 is also in Phase II clinical trials and contains DACH (diaminocyclohexane) platinum, the active form of the marketed drug Oxaliplatin, conjugated to 25 kDa HPMA copolymer via a pH sensitive linker. AP5346 showed promising pre-clinical activity in 11 different tumor models and has shown both safety and efficacy in ovarian cancer in clinical trials [43]. In addition, poly (ethylene glycol) (PEG) is currently being evaluated in clinical trials for the administration of Camptothecin, SN38, Irinotecan, Docetaxel and Paclitaxel [44].

The most advanced polymer-drug conjugate currently in late stage Phase III clinical trials is PG-TXL, a conjugate of poly (L-glutamic acid) and Paclitaxel [45]. While this polymeric conjugate was originally synthesized to improve the solubility of Paclitaxel, preclinical studies showed enhanced tumor accumulation of PG-TXL compared to free Paclitaxel, contributing to its improved efficacy [46]. In addition, cathepsin B, which is over expressed in tumor cells, was found to proteolytically degrade the PG backbone, allowing for targeted release of Paclitaxel at the tumor site. Clinical trials in several different tumor types demonstrated that PG-TXL was as effective as Paclitaxel, but it did not demonstrate superior efficacy as has been shown in the preclinical studies.

However, PG-TXL had several advantages over Paclitaxel, namely a reduction in the incidence of hair loss, nausea and hypersensitivity reactions, which are often limiting factors for chemotherapy. These trials demonstrate the promise for the clinical application of polymer-drug conjugates, as well as challenges they face in translation to the clinic.

2.3 Administration of Drugs via the Oral Route

Administration of drugs via the oral route is preferred by patients owing to its convenience and comfort, generally leading to higher patient compliance compared to parenteral treatments and self-administration routes such as transdermal and inhalation. In addition, oral drug administration provides a more flexible dosing regimen and a lower burden on hospitals and the healthcare system [8, 9]. Finally, in diseases such as cancer, oral therapy minimizes treatment costs due to hospital procedures as well as indirect costs associated with lost time at work, transportation to and from the treatment center and additional childcare [7].

Oral delivery of therapeutics is challenging because drugs must have appropriate solubility, stability in the gastrointestinal pH and enzyme environment, and the ability to permeate the epithelial barrier of the gut [47]. Unfortunately, many current chemotherapy drugs are poorly water soluble with low oral bioavailability, necessitating administration by the intravenous route, which requires recurring hospital visits and significant direct and indirect costs to the patient. Because of the strong patient preference for oral therapy, much research is being done to find alternative orally administrable chemotherapy drugs that are as effective as traditional intravenous

therapies and preferably with lower off-target toxicities [48]. This section will provide the necessary background on oral drug administration.

2.3.1 Physiology of the Gastrointestinal Tract

2.3.1.1 Compartments and Functions

The gastrointestinal tract is composed of several unique sections which each have a distinct pH, residence time, absorptive area and group of enzymes which must be considered for oral drug delivery [49]. The gastrointestinal tract begins with the oral cavity where the drug comes in contact with saliva. With the exception of specially designed sublingual and buccal formulations, negligible drug absorption occurs in the oral cavity. After passage down the esophagus, the drug encounters the stomach. The stomach is lined with approximately 3.5 million gastric pits, which contain cells that secrete mucus and gastric juice. This gastric juice contains hydrochloric acid, which maintains the acidic pH of the stomach, as well as pepsin. Thus, any drug that enters the stomach must be resistant to acidic conditions and proteolysis by pepsin to prevent premature degradation. The contents of the stomach are emptied at regular intervals, which are dependent on the fasted or fed state of the individual, amongst other factors including disease state or drug treatment. After these pulsatile waves, the entire content of the stomach is propelled into the small intestine [49].

The small intestine serves as the major absorptive site in digestion and contains three distinct sections: the duodenum, jejunum and ileum. Absorption is favored by a large surface area due to mucosal folds and villous formation thereby maximizing the number of intestinal absorptive cells that come into contact with the luminal contents. In

addition, the large blood flow to the small intestine serves to maintain the concentration gradient across the intestinal barrier, again, enhancing absorption of nutrients and drug molecules. Biliary secretion from the gallbladder into the duodenum enhances absorption of lipids by formation of mixed micelles, and lipid digestion is promoted by lipase enzymes secreted by the pancreas. In addition, Brunner's glands, located in the duodenum, secrete bicarbonate and neutralize the acidic stomach contents. This neutral pH promotes enzymatic activity in the small intestine and influences the charged state of drug molecules, which can enhance absorption. Food can also influence the absorption of drugs by binding to the drugs or competing for intestinal transporters. Another potential barrier to absorption is the thick mucus layer that lines the intestinal epithelium, which creates a formidable barrier to drug diffusion. In order to successfully penetrate through mucus, drugs must be small enough to avoid encumbrance by the dense mucin fiber mesh and avoid adhesion to the fibers [50]. Post-epithelial structures include the intraepithelial lymphocytes, basement membrane and lamina propria mononuclear cells. These specialized elements of the gut-associated lymphoid tissue contribute to the mucosal immune response and present antigens to the lymphatic system, but do not present a significant barrier to transport [51]. Once drugs and nutrients are absorbed in the small intestine, they are transported through the hepatic portal vein and undergo first-pass metabolism in the liver before entering systemic circulation [49].

Materials that are not absorbed in the small intestine are transferred to the large intestine for further processing. The large intestine is populated by a wide range of bacteria that produce enzymes to further break down foods and drugs. Finally, the material is cleared from the large intestine and is transferred to the colon. Table 2.1

Table 2.1. Physiology of the Gastrointestinal Tract

Compartment	Absorptive Area (m²)	Residence time	Fasted pH	Enzymes
Oral cavity	-	-	7.0	Amylase
Esophagus	0.02	3.5 s	6.0-7.0	-
Stomach	0.1	2-8 h	1.3-2.1	Pepsin, lipase
Small Intestine:	200			Peptidases,
-Duodenum		5 min	5.5-6.5	lipases,
-Jejunum		1-2 h	6.1-7.1	amylase
-Ileum		2-3 h	7.0-8.0	
Large Intestine	0.3	15-48 h	-	Diverse bacterial enzymes
Colon	0.25	-	8.0	-
Rectum	-	-	7.0	-

(Adapted from [49])

summarizes the major compartments of the gastrointestinal tract as well as the absorptive area, residence time, pH and enzymatic activity in each compartment [49].

2.3.1.2 Intestinal Epithelial Barrier

The intestinal epithelial barrier is the main site of intestinal absorption of drugs and nutrients. This barrier forms a boundary between the “external environment” and the “internal environment” and is designed to allow for the absorption of nutrients while preventing transport of “undesirable” components such as bacteria or toxins. While epithelial barriers like the skin are designed to be virtually impermeable, the intestinal epithelial barrier must be selectively permeable to permit fluid exchange and nutrient absorption, and is therefore relatively leaky in comparison [52]. The intestinal epithelium contains a monolayer of columnar absorptive cells, or enterocytes, that are oriented with the “apical membrane” facing the intestinal lumen and the “basolateral membrane” facing the serosal side. The apical membrane contains a brush border of microvilli that, together with mucosal and villous folds, are responsible for the large absorptive surface area of the small intestine [53]. In addition to the absorptive cells, the intestinal barrier also contains specialized M-cells (microfold cells) located in Peyer’s patches of the gut-associated lymphoid tissue. These cells continuously sample antigens in the intestine and present them to the mucosal lymphoid tissue for initiation of the immune response [54]. M-cells have been popular targets for viral drug delivery vectors as well as nanoparticles. Finally, the intestinal epithelium is covered by a mucus layer, which is secreted by the intestinal goblet cells, and prevents large particles from approaching the epithelial barrier and especially, protects the sensitive intestinal crypt region. In addition, the mucus

serves as an unstirred layer, slowing the absorption of nutrients by limiting diffusion to the intestinal cells. The mucus layer can also enhance absorption of compounds produced by brush border enzymes by preventing diffusion of these molecules back into the intestinal lumen [53].

The integrity of the intestinal epithelial barrier is maintained by three types of cell-to-cell contacts: tight junctions, adherens junctions and desmosomes [53].

Desmosomes and adherens junctions form the cell-to-cell contacts that maintain the integrity of the barrier and allow for communication between the intestinal cells. Tight junctions are formed at the apical side of the epithelial barrier and serve to regulate the passage of hydrophilic molecules between the intestinal cells. The structure of the tight junctions as well as the mechanism by which they regulate paracellular permeability is discussed in detail in Section 2.3.1.3. A schematic showing the major proteins involved in cell-to-cell junctions is shown in Figure 2.2. Genetic mutations that compromise intestinal barrier function are responsible for the pathology of several intestinal diseases including Crohn's disease, ulcerative colitis and Celiac disease [52]. These conditions illustrate the importance of preserving the integrity of the gastrointestinal barrier to maintain healthy function.

2.3.1.3 Tight Junction Biology: Structure and Function

Tight junctions regulate the openings between the epithelial cells, allowing for paracellular transport. Although the function of tight junctions has been known for decades, the precise protein composition and function of tight junctions was not discovered until the 1990's [55]. Occludin, a 65 kDa transmembrane protein, was the

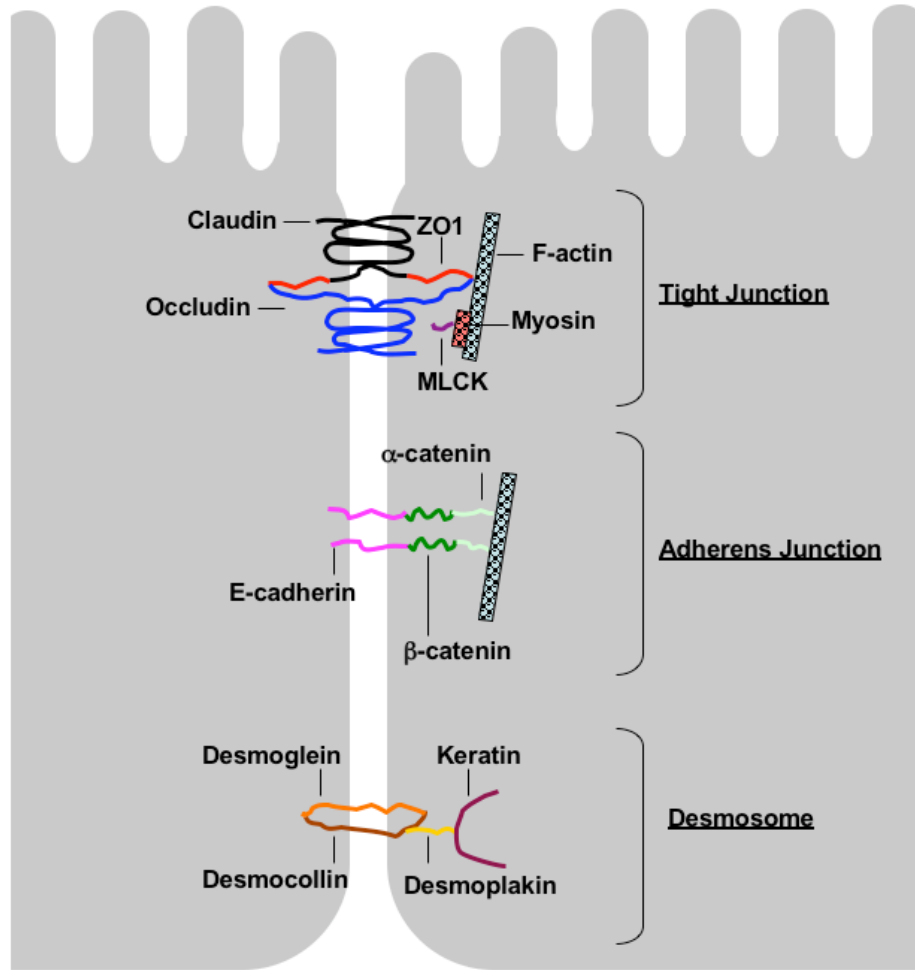


Figure 2.2. Major Proteins Involved in Tight Junctions, Adherens Junctions and Desmosomes between the Intestinal Epithelial Cells. In the tight junctions MLCK is myosin light chain kinase and ZO-1 is zonula occludens 1. (Adapted from [53].)

first tight junction protein to be isolated, and was reported by Furuse and colleagues in 1993 [56]. The cytosolic face of occludin is thought to interact with several zonula occludens (ZO) as well as actin [57]. Subsequently, the same group reported the involvement of claudins in tight junctions in 1998 [58, 59]. There have been 18 different claudins reported with specific claudins being expressed in certain cell and tissue types [57]. Like occludin, claudins also interact with ZO proteins. Both occludin and claudin were examined in knockout studies and were found to be critical for tight junction function. Junction adhesion molecule (JAM) has also been implicated in tight junctions [60]. Finally, tricellulin, a 64 kDa polypeptide discovered in 2005, is a necessary component of tight junctions in areas where three cells come into contact [61]. In addition to these tight junctional components, actin and myosin form a perijunctional actomyosin ring that plays a role in the contraction of tight junctional proteins upon stimulation [53].

Tight junction modulation is regulated by several complex signaling pathways including those controlled by protein kinases, rho kinases, myosin light chain kinase (MLCK) and mitogen activated protein kinase (MAPK) [62]. These pathways can be activated in normal physiological conditions and exploited by tight junction modulating drugs. One of the most common instances of tight junction opening occurs during nutrient absorption. Apical co-transport of Na^+ and glucose activates an MLCK-dependent signaling pathway that causes condensation of the perijunctional actomyosin ring, leading to opening of the tight junctions [63]. This allows for enhanced water and nutrient transport through the paracellular route. This example illustrates the interconnectedness of transcellular and paracellular fluxes. Extracellular calcium ions

(Ca²⁺) are also critical for tight junction function. Ma and co-workers [64] demonstrated that the removal of extracellular calcium caused an increase in the paracellular permeability and a drop in transepithelial electrical resistance (TEER) of Caco-2 monolayers. In addition, they observed a rapid contraction of actin and myosin filaments and movement of ZO-1 and occludin away from the membrane, which was initiated by MLCK activation. Addition of Ca²⁺ was found to quickly reverse these effects, illustrating the critical role of extracellular calcium in the maintenance of tight junction integrity.

2.3.2 Mechanisms of Transport Across the Intestinal Barrier

There are two major pathways of transport across the intestinal barrier: paracellular transport, which occurs between cells, and transcellular transport, which occurs across cells. The following four sections discuss paracellular transport and transcellular transport, which can occur by passive diffusion, carrier-mediated transport and endocytosis. Importantly, molecules may follow one or more transport pathways and these pathways may be interconnected. Figure 2.3 illustrates potential mechanisms of transport through the intestinal barrier.

2.3.2.1 Paracellular Transport

Paracellular transport occurs when molecules pass between epithelial cells in the intestinal barrier. This mechanism of transport is driven by the concentration gradient and is thus both energy-independent and unsaturable. Because molecules permeate through the restricted tight junctions, they must be water-soluble and small (i.e. MW<200

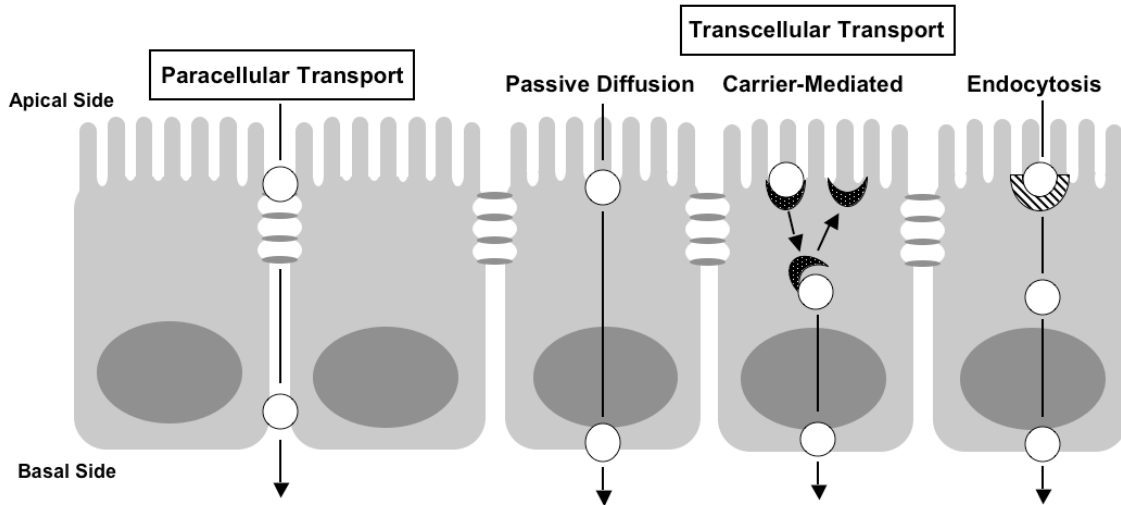


Figure 2.3. Mechanisms of Transport through the Intestinal Barrier. Transport may be either paracellular or transcellular. Transcellular transport includes passive diffusion, carrier-mediated transport, which may be energy-independent (facilitated diffusion) or energy-dependent (active transport) or endocytosis, which can be fluid phase, adsorptive or receptor-mediated.

Da). Studies of permeability of hydrophilic compounds across Caco-2 monolayers suggested a tight junction pore size of approximately 4.5-4.8 Å [65, 66]. Molecules such as mannitol, a small sugar alcohol, and lucifer yellow carbohydrazide, a fluorescent dye, are known to permeate across the intestinal barrier strictly by the paracellular route and thus can be used to monitor changes in paracellular flux [67, 68]. In general, the paracellular route is impermeable to macromolecules because they are too large to pass through the tight junction pores [69].

2.3.2.2 *Passive Diffusion*

Passive diffusion is the simplest mode of transcellular transport and occurs when membrane-permeable molecules are transported across the intestinal barrier from a region of high concentration on the apical side to a region of lower concentration on the basolateral side of the membrane. This mechanism of transport is energy-independent and unsaturable. Passive diffusion across the intestinal barrier is governed by Fick's Law of Diffusion, which states that flux (J) is directly proportional to the concentration gradient (dC/dx), the lipid-water partition coefficient (K), the diffusion coefficient (D) and the area of transport (A):

$$J = -DAK \frac{dC}{dx} \quad (\text{Eq. 2.1})$$

The partition coefficient, a ratio of the compound's lipid solubility to water solubility, is a critical component in determining the overall flux since compounds must be able to diffuse into the lipid-rich cell membrane in order to be transported via the transcellular route. Thus, more lipophilic molecules have higher rates of passive diffusion across the intestinal barrier. However, there is an upper limit: highly lipophilic drugs tend to be

insoluble thus preventing their absorption. Since uncharged molecules are always more lipid-soluble than charged molecules, the ionization state of a compound at pH of the intestine is a critical determinant of its passive permeability. Many orally administered drug compounds are lipophilic, allowing for passive diffusion across the intestinal barrier.

2.3.2.3 Carrier-Mediated Transport

Carrier-mediated transport plays an important role in intestinal transport of compounds such as peptides, nucleic acids, monosaccharides, organic cations and monocarboxylic acids that cannot be transported via the paracellular pathway or passive diffusion [70]. In carrier-mediated transport, transmembrane proteins move cargo across the cell membrane. After the cargo has been released, the transporters resume their initial configuration and are available to transport additional cargo. Importantly, because there are a limited number of transporters, carrier-mediated transport is a saturable process. Carrier-mediated transport can occur by facilitated diffusion, which is energy-independent and occurs down the concentration gradient or by active transport, which occurs against the concentration gradient and requires an energy source. Active transport can either be driven directly by ATP (ATP binding cassette [ABC] transporters), or coupled to transport of ions such as H^+ or Na^+ (solute carrier [SLC] transporters). Examples of types of membrane transport proteins include monocarboxylic acid transporters, human peptide transporters, nucleoside transporters and organic cation transporters [70].

In addition to influx transporters, efflux transporters can also influence intestinal transport. P-glycoprotein (P-gp), a member of the ABC superfamily and the multidrug resistance subfamily, is one of the most well characterized efflux transporters [70]. Although it is intended to protect the body from harmful toxins, it also causes efflux of many drugs. Orally administered P-gp substrates often have poor intestinal permeability because of this efflux and must be co-administered with P-gp inhibitors to overcome this challenge. Therefore it is important to consider if a drug may be a P-gp substrate when examining its intestinal permeability [70].

2.3.2.4 Endocytosis

Endocytosis is a generalized term that refers to the active internalization of specific substrates into the cell by membrane engulfment. Endocytosis is often used to transport macromolecules that are too large for paracellular transport or carrier-mediated mechanisms [71]. In the context of the intestinal epithelial barrier, endocytosis contributes to overall transport when the cargo endocytosed at the apical membrane is trafficked to the basolateral membrane and exits the cell. Endocytosis can be divided into phagocytosis, which occurs in particle uptake by macrophages, and pinocytosis, in which the cell membrane invaginates to enclose extracellular fluid and any molecules bound to the cell surface. Pinocytosis can be further classified to receptor-mediated endocytosis (RME), which is either clathrin or non-clathrin-mediated, as well as adsorptive and fluid-phase endocytosis [71]. Adsorptive and fluid-phase endocytosis are non-specific mechanisms in which molecules are either physically adsorbed to the cell surface or engulfed with the extracellular fluid and brought into the cytosol. Because these

mechanisms are non-specific, they are typically unsaturable and show low substrate affinity. In contrast, receptor-mediated endocytosis is highly specific, saturable and shows high affinity for the substrate, making it a much more efficient transport method.

Receptor-mediated endocytosis occurs when ligands bind to specific cell surface receptors and are internalized into the cell for further trafficking [72]. RME can be divided into classical clathrin-dependent RME and non-clathrin RME, such as caveolin-mediated endocytosis (CME). Clathrin-dependent endocytosis occurs when a ligand binds its receptor and concentrates in a clathrin coated-pit on the plasma membrane presenting specific adaptor proteins. After ligand binding, the membrane closes around the ligand-receptor complex and dynamin, a small GTPase, pinches off the vesicle from the membrane. Upon internalization, hydrogen pumps are recruited to the vesicle, thereby lowering its pH. Consequently, the vesicle sheds its clathrin coat and matures into an early endosome. From that point, the vesicle can be recycled to the apical surface, continue for degradation in the lysosomes or be transcytosed to the basolateral side of the cell. Transferrin is a classical ligand for clathrin-mediated endocytosis and is often used as a control to monitor endocytosis and trafficking [71]. Caveolin-mediated endocytosis occurs by a similar process except instead of trafficking to early endosomes, the cargo is trafficked to caveosomes and then to the endoplasmic reticulum, thus eliminating the pH lowering step central to clathrin RME [73]. Avoidance of low pH and lysosomal enzymes makes the caveolar pathway more suitable for uptake of degradation-sensitive bioactive agents than clathrin-mediated endocytosis. Cholera Toxin B is a classical caveolin endocytosis ligand and can be used as a control to monitor caveolin RME. These two mechanisms of RME are illustrated in Figure 2.4.

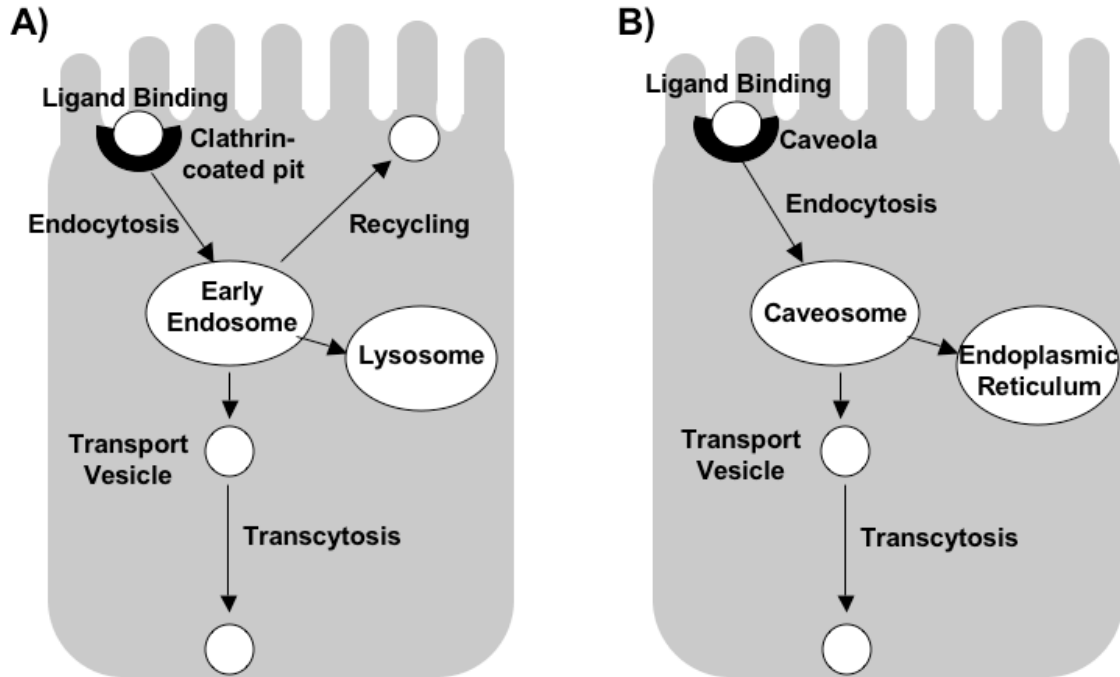


Figure 2.4. Clathrin- and Caveolin-Mediated Endocytosis and Transcytosis. A) In clathrin-mediated endocytosis, ligands are transported to the early endosomes where they can either be recycled to the apical side, transcytosed to the basolateral side or sent to the lysosomes for degradation. B) In caveolin-mediated endocytosis, ligands can either be transcytosed or sent to the endoplasmic reticulum from the caveosomes.

2.3.3 *Physicochemical Properties that Govern Intestinal Absorption*

2.3.3.1 *The Lipinski Rule of 5*

Due to the restricted pathways of intestinal permeation, there are several key physicochemical properties that govern oral absorption. The “Lipinski Rule of 5”, derived from a large dataset of compounds with favorable or unfavorable permeation properties, states that compounds likely to have poor intestinal absorption have at least one of the following: 1) a molecular weight greater than 500 Da, 2) log P greater than 5, 3) more than 5 hydrogen-bond donors, and 4) more than 10 hydrogen-bond acceptors [74]. These parameters are derived from the requirement for small size and a minimum amount of lipophilicity for passive diffusion across the intestinal barrier. However, compounds must also have sufficient aqueous solubility to dissolve in the aqueous intestinal environment, creating a delicate balance between solubility and lipophilicity [75]. Importantly, the Lipinski Rule of 5 does not apply to substrates of intestinal transporters such as antibiotics or vitamins.

2.3.3.2 *The Biopharmaceutics Classification System (BCS)*

The Biopharmaceutics Classification System was developed in 1995 to characterize factors that determine the rate and extent of drug absorption in the gastrointestinal tract. Solubility and permeability were found to be the key parameters that govern intestinal absorption [76] and compounds are designated as Class I- Class IV based on these factors (Figure 2.5). The BCS is used by the Food and Drug Administration and the World Health Organization to set bioavailability and bioequivalence standards for oral drug approval [77]. These classes are used to predict *in*

<i>Permeability:</i> Human intestinal absorption	<i>Class I</i> High Solubility High Permeability	<i>Class II</i> Low Solubility High Permeability
	<i>Class III</i> High Solubility Low Permeability	<i>Class IV</i> Low Solubility Low Permeability
	<i>Solubility:</i> Volume of water required to dissolve the highest dose strength across the physiological pH range	

Figure 2.5. The Biopharmaceutics Classification System. Compounds are classified as BCS Class I-Class IV based on their solubility and permeability. (Adapted from [77])

vitro/ in vivo correlations of oral drug absorption as well as the rate-limiting step in absorption. For Class I compounds, since the solubility and permeability are both high, the rate-limiting step in absorption is defined by gastric emptying. In contrast, for Class II compounds, dissolution is a rate-limiting step while for Class III compounds, membrane absorption is rate-limiting. Finally, the gastrointestinal absorption of Class IV drugs is classified as highly unpredictable, thus these drugs present significant problems for oral delivery and are often administered intravenously [76].

2.4 Models to Predict Oral Absorption and Oral Bioavailability

There are several experimental models used to predict oral absorption in the human gastrointestinal tract. This section will describe a series of *in silico*, *in vitro*, *in vivo*, *ex vivo* and *in situ* models as well as discuss the merits and drawbacks of each.

2.4.1 In Silico Models

In silico models are often used to predict the gastrointestinal absorption and oral bioavailability of compounds in early drug development. Because drug molecules often fail in later stages of development due to poor oral absorption, creation of efficient and predictive *in silico* models is critical for pharmaceutical development. One of the most commonly used techniques is QSAR/QSPR, or Quantitative Structure Activity/ Property Relationship, in which datasets of compounds with known absorption properties are combined with a series of molecular descriptors to predict properties of novel drug molecules. Molecular descriptors such as molecular weight, number of hydrogen bond donors, number of hydrogen bond acceptors, octanol-water partitioning coefficient

(logP), apparent partition coefficient (logD), and intrinsic solubility have all been used to predict passive absorption [78]. These types of models are highly dependent on the size and quality of the dataset. While many pharmaceutical companies have large in-house datasets, this information is often not available to the general public. Recently, Hou and colleagues published one of the largest intestinal absorption datasets with 647 drugs and drug like compounds [79], and a corresponding data set for oral bioavailability with 768 compounds [80]. These robust datasets have the capability to dramatically improve the predictive quality of *in situ* models. Many analysis algorithms have been developed including multiple linear regression, partial least squares, recursive partitioning and finally support vector machines, which have shown the highest predictive ability when used on training and test sets [78].

These *in silico* methodologies can aid in the prediction of absorptive behavior of novel compounds. They are efficient as well as economical in early drug screening since they can be completed prior to compound synthesis. However, as mentioned earlier, they are severely limited by the training dataset. In addition, while they can reliably predict gastrointestinal absorption via passive diffusion, they do not account for active transport, which can be a significant pathway of intestinal transport for certain molecules [78]. Finally, they are very poor at predicting overall bioavailability since first pass metabolism can have a large impact on bioavailability and is difficult to model [80].

2.4.2 Parallel Artificial Membrane Permeability Assay

PAMPA, or the parallel artificial membrane permeability assay, was first introduced in 1998 by Kansy and co-workers as a rapid permeability assessment tool

[81]. This cell-free system uses artificial membranes to measure the permeability of compounds in a 96 well microplate format. There have been several different variations of PAMPA that differ by the type of membrane, pore size, nature and percentage of lipids as well as the incubation time of the assay, which can range from 2-15 hours [82]. The most commonly used membrane material is a hydrophobic poly (vinylidene fluoride) (PVDF) membrane with 125 μm pore size. Traditionally, detection was achieved by a UV plate reader, but more recently enhanced detection is accomplished by HPLC-UV and HPLC-MS/MS techniques.

There are several advantages of PAMPA, which have lead to its widespread use. It is a direct measure of passive permeability and mimics the membrane nature of the gastrointestinal barrier. In addition, it is amenable to a 96 well plate format, making it a high-throughput method, which is critical for early pharmaceutical development. It is simple to manipulate the membrane characteristics to design a system that is suited for a given application. Finally, the effect of excipients on compound permeability can be easily studied [82]. Unfortunately, because PAMPA is a cell-free system, it can only measure passive permeability via the transcellular route and does not account for active transport or paracellular permeability, which can have significant contributions to the transport of certain types of compounds [82]. Therefore, while PAMPA is an excellent screening tool, it does not provide mechanistic insight and only measures one type of transport.

2.4.3 Caco-2 Monolayers

The Caco-2 monolayer model, first introduced by Hidalgo and colleagues in 1989 [83], has become one of the most widely used absorption screening technologies in both academic and industrial laboratories [84, 85]. In this technique, Caco-2 cells grown on semi-permeable supports are used to mimic the intestinal barrier. Caco-2 cells are derived from human colonic adenocarcinoma, and spontaneously differentiate into intestinal enterocytes when grown to confluence on semi-permeable membrane supports. After differentiation, the Caco-2 cells are polarized, display apical microvilli, form tight junctions and have apical enzymes and transport systems similar to absorptive enterocytes [86].

Caco-2 cells are grown on semi-permeable membranes in a Transwell[®] system, containing an apical chamber, corresponding to the intestinal lumen, and a basolateral chamber, corresponding to the blood stream (Figure 2.6). Caco-2 cells are seeded on the membrane and grown for 21-28 days to produce confluent, differentiated monolayers. Compounds can be added in either the basolateral or apical chamber to study directional transport. Apical to basolateral transport corresponds to intestinal absorption while basolateral to apical transport corresponds to intestinal efflux [87]. Transwell[®] systems are available in microplate format from 6 to 96 wells, and can be adapted to work in a robotic system, allowing for simultaneous screening of many different compounds. The apparent permeability (P_{app}) of compounds in the apical to basolateral direction has been shown to correlate with human intestinal absorption, making the Caco-2 monolayer system an excellent high throughput technique to predict absorption properties of novel compounds [88].

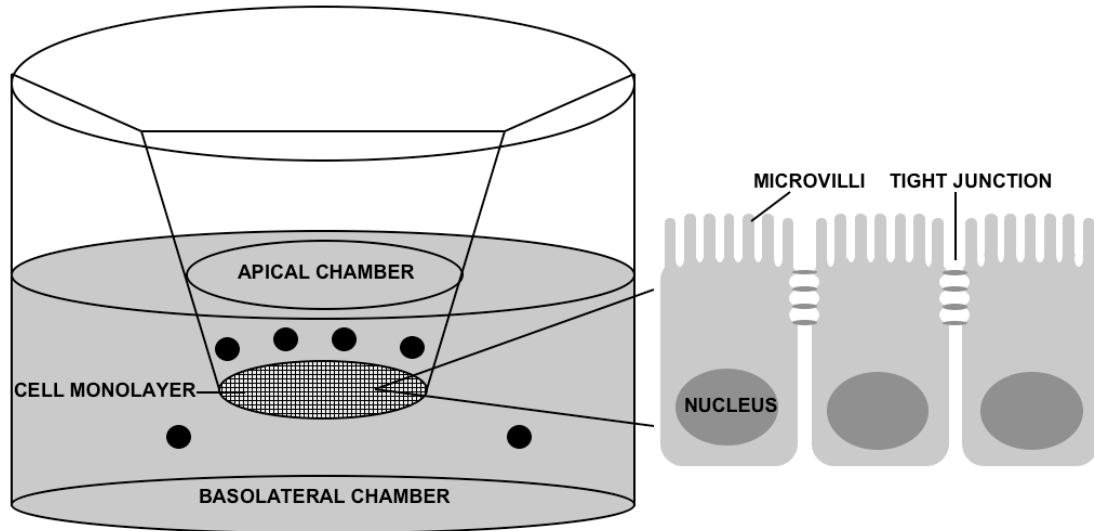


Figure 2.6. Transwell[®] System used in the Caco-2 Monolayer Permeability Assay.

Caco-2 cells are seeded on the membrane insert and allowed to grow for 21-28 days to produce confluent, differentiated monolayers. Compound flux from the apical to basolateral chamber is used to measure permeability.

Because differentiated Caco-2 cells have well-defined tight junctions as well as developed active transport systems, the Caco-2 cell monolayer system can be used to study not only passive diffusion, but also active transport, paracellular transport and potential drug efflux. Therefore, the Caco-2 monolayer system can be used as a tool to study both the amount of transport, which is predictive of human intestinal absorption, as well as the mechanism of transport of novel compounds [87].

In order to form differentiated monolayers, Caco-2 cells must be grown on permeable supports for 21-28 days. During this time, the cells achieve confluence and differentiate, forming tighter junctions and expressing proteins similar to absorptive enterocytes rather than colonic cells. This transformation can be monitored by transepithelial electrical resistance (TEER), which quantifies the tightness of the monolayer. TEER increases over time, and ultimately plateaus between 21 and 28 days when the cells can be used for experiments [87]. Typical TEER values of competent differentiated monolayers range from 600-800 ohm-cm². Measurement of TEER serves as a control for monolayer integrity before and during a transport assay. Transport of paracellular markers such as mannitol and lucifer yellow, which should have P_{app} less than 1×10^{-6} cm/s, can also serve as controls for monolayer integrity [87].

There are several advantages to using the Caco-2 monolayer system to predict intestinal absorption of novel compounds in humans. The system can be performed in multiwell format, allowing for parallel testing of different compounds using minimal compound, reagents and assay time. In addition, because Caco-2 cells mimic intestinal enterocytes, many aspects of intestinal absorption including passive transport, active transport, paracellular transport and drug efflux can be studied in one assay.

Unfortunately, there are also several disadvantages to the Caco-2 monolayer system. Because the cells must be cultured for 21 days, this assay is labor intensive and requires a significant amount of serum-enriched media, increasing the cost of the assay. In addition, studies using the monolayer system to measure permeability of compounds in different laboratories have shown that there is a high degree of variability in the assay, mostly due to the intrinsic variability in Caco-2 cells [86]. Caco-2 cells contain several different sub-populations, which can be inadvertently selected for depending on the culture conditions, causing shifts in the population over time. These shifts can significantly affect the monolayer formation including the tightness of the tight junctions as well as protein expression [89]. Many experimental conditions can also affect the ultimate performance of the monolayers including cell passage number, seeding density, filter type and pore size, cell culture media, transport buffer and monolayer age. Therefore it is critical to control these parameters within a given laboratory so that experiments are comparable. In addition, it is important to run standards of known permeability as well as measure the TEER to ensure monolayer consistency. Despite these challenges, the Caco-2 monolayer system continues to be a powerful tool for studying the extent and mechanism of intestinal absorption.

2.4.4 Fast-Caco-2 Assay

Because the 21-day growth period is both labor-intensive and expensive, alternative differentiation systems have been developed for faster Caco-2 assays. Beckton Dickenson (BD) markets the BD Biocoat Caco-2 HTS Assay system, which can create differentiated Caco-2 monolayers in 3 days instead of 21 days. In this system,

Caco-2 cells are seeded at high density onto Transwell® filters coated with fibrillar collagen. After the cells attach to the Transwells on the first day, differentiation medium containing butyric acid is added for the next two days, causing rapid differentiation of the cells into intestinal enterocytes [90]. The resulting monolayers are slightly leakier than traditional Caco-2 monolayers and show poor expression of transporters, but they can still provide rank order measurements for permeability. Adding fetal bovine serum to the seeding medium reduces these problems as it facilitates cell attachment, making this assay system more closely mimic 21-day standard [90]. Therefore, although the monolayers are not exactly the same as the traditional 21-day Caco-2 monolayer system, the fast-Caco-2 assay can effectively determine rank order of permeability and provides significant time and labor savings.

2.4.5 Other Types of Cell-Monolayer Systems

In addition to Caco-2 cells, several other cell types have been used to mimic the intestinal barrier in the Transwell® system. MDCK cells, derived from the canine kidney, are useful alternatives to Caco-2 cells as they form differentiated monolayers in 3 days instead of 21 days. They have looser tight junctions than Caco-2 cells and do not mimic the protein expression of human enterocytes as well as Caco-2 cells, but they are still useful as a rapid screening tool for passive permeability and paracellular transport [87, 91]. In addition, MDCK cells can be stably or transiently transfected, which allows researchers to study the impact of selected transporters, which is not possible in Caco-2 cells. Recently, TC-7 cells, a subclone of Caco-2 cells, have been used to study intestinal transport [92]. TC-7 cells have higher expression of CYP enzymes, which have very low

expression in Caco-2 cells. This allows for the simultaneous study of both transport and metabolism, which is important for compounds that are metabolized in the intestinal barrier. Finally, co-cultures of mucus secreting HT-29 and MTX cells have been used [93]. While these show lower active transport than Caco-2 cells, they show higher paracellular transport and may more accurately predict the paracellular passage of hydrophilic molecules. Importantly, all of these cell culture monolayer systems are able to isolate different elements of the intestinal transport process and are useful for studying a variety of compounds in a high throughput system that mimics the *in vivo* environment.

2.4.6 Everted Rat Intestinal Sac

Often, it is desirable to use a tissue-based system rather than a cell-based system to more closely mimic gastrointestinal absorption. The everted rat intestinal sac model, introduced by Wilson and co-workers in 1954, has been used to study intestinal absorption in an *ex vivo* environment [94]. In this method, the intestine is removed from a sacrificed rat, everted over a glass rod so that the mucosal side is facing outward and then sectioned into 2-4 cm sacs and filled with oxygenated cell culture medium. The sacs are then placed in media containing the drug of interest and the amount of drug transported into the sac (mucosal to serosal direction) is quantified [87]. The assay time is limited by the viability of the intestinal tissues, which is usually 2 hours. There are several advantages to the everted rat intestinal sac model compared to cell-based models, including the presence of a mucosal layer and the ability to study different sections of the intestine. In addition, transport can be studied in conjunction with intestinal metabolism. This method is fast and relatively inexpensive compared to other animal studies [87].

However, the drug must cross the muscle layer in addition to the intestinal barrier, which can potentially underestimate permeability, and the method is low-throughput compared to cell-based assays. Despite these drawbacks, the everted rat intestinal sac method is an effective way to measure intestinal permeability in an *ex vivo* environment.

2.4.7 Isolated Intestinal Tissue

First conceptualized by Hans Ussing in 1949 [95] and later miniaturized by Grass and Sweetana in 1988 [96], the Ussing Chamber method uses isolated intestinal tissue to study transport of compounds across the gastrointestinal barrier. Sections of intestinal tissue are placed between two chambers and exposed to Krebs Ringer Bicarbonate buffer gassed with 95:5 CO₂:O₂. The gassing is used to maintain tissue viability and promote flow in the chambers. Importantly, similar to the everted sac model, intestinal metabolism can be studied at the same time as absorption and transport. This system allows for studying transport across different sections of the intestine as well as in different species, which can assist in choosing a relevant *in vivo* model [87]. In addition, the muscle layer can be removed from the tissue, allowing the study of the epithelial barrier in isolation. While this method is very useful, there are several disadvantages, most notably the difficulty of preparation of the intestinal sheets, especially removing the muscle layer. The viability of the tissue sheet during the experiment is also a significant concern and can vary dramatically. Finally, this system is significantly lower throughput than *in vitro* cell-based models, but can provide more information and is closer to the *in vivo* environment [87].

2.4.8 Rat Intestinal Perfusion

In situ perfusion of the rat intestine most closely mimics *in vivo* environment without using the whole animal. In this technique, compounds are added to the lumen of sections of the intestine in anesthetized rats and the disappearance of the compound is monitored over time. This system allows the study of the gastrointestinal transport in isolation without confounding factors such as first pass metabolism, biliary excretion or enterohepatic circulation [87]. Importantly, most *in situ* perfusion experiments assume that disappearance of the compound from the lumen indicates transport across the intestinal barrier. If there is significant metabolism of the compound or absorption in the intestinal barrier, this method can significantly overestimate transport. Therefore, the assay can be amended to sample blood from the mesenteric vein to measure transport, although this becomes much more technically challenging. *In situ* perfusion serves as a bridge between tissue-based models and *in vivo* models and combines the advantages of each into a powerful experimental technique.

2.4.9 In Vivo Models

In vivo administration of compounds by the oral route in laboratory animals is a commonly used method to predict oral bioavailability in humans. Because the epithelial barrier composition between mouse, rat and human are similar, gastrointestinal transport should be similar between species. However, differences in gastrointestinal transit time, expression of transporters and even pH can differ between species, so direct comparison is often not possible [87]. In oral bioavailability studies, dosing by the oral or intraduodenal route is compared to intravenous dosing. Plasma samples are taken over

time and the area under the curve (AUC) of the oral administration methods are compared to the intravenous route to get the fraction of the dose absorbed which is represented as the overall percent bioavailability. Administration of the compound intraduodenally instead of orally eliminates confounding factors from the stomach such as residence time and gastric absorption. Importantly, measuring bioavailability by plasma concentration includes the effects of both gastrointestinal absorption as well as first pass metabolism. Sampling from the portal vein before the liver instead of from the circulation allows for isolation of intestinal transport and can be useful in determining the impact of absorption and metabolism on overall bioavailability [87]. Because *in vivo* studies have all of the complexity of the human absorption system, they can often provide the closest estimate to oral absorption in humans. However, there are several disadvantages of *in vivo* studies including the use of whole animals, difficult and tedious plasma sampling and analysis as well as the aforementioned interspecies differences. Despite these challenges, *in vivo* studies in laboratory animals are still the closest approximation to human intestinal absorption and are a good follow up experiment to evaluate promising candidates from high-throughput techniques.

2.5 Current Strategies for Oral Drug Delivery

Unfortunately, many newly discovered drugs have low solubility and poor intestinal permeability, which would categorize them as problematic BCS Class IV compounds. In fact, the bioavailability of novel chemotherapy drugs is often so low that these drugs must be administered intravenously. There are several current strategies to improve the bioavailability of poorly water-soluble and poorly permeable therapeutics

including 1) prodrug approaches, 2) efflux and metabolic inhibitors, 3) tight junction modulators and 4) novel macromolecules. Each of these approaches will be discussed in further detail below.

2.5.1 Prodrugs

A prodrug is defined as a drug molecule chemically conjugated to a promoiety that is used to improve the drug's physicochemical properties and is cleaved to release the pharmacologically active, free drug [97]. Common drug delivery obstacles overcome by prodrug strategies include poor aqueous solubility, low permeability, fast elimination, off-target effects and premature metabolism [97]. In the context of oral drug delivery, prodrugs can be used to improve the aqueous solubility of a drug and permeability across the intestinal barrier. Promoieties are subsequently cleaved by enzymatic mechanisms or by hydrolysis to yield the free, active drug.

Poor aqueous solubility is becoming an increasingly common problem with 40% of new chemical entities discovered by pharmaceutical companies in combinatorial screening now identified as poorly water soluble [98]. In addition, traditional formulation techniques to improve water solubility such as use of different salt and crystalline forms or reducing particle size are not always successful, necessitating the use of new strategies. Examples of prodrug modifications to improve aqueous solubility include addition of phosphate groups via an ester bond, addition of amino acids via ester bonds or conjugation to PEG [98]. For example, phosphate prodrugs of Buparvaquone, used to treat leishmaniasis, increase the aqueous solubility from 0.03 $\mu\text{g/ml}$ to greater than 4 mg/ml [99]. The prodrug releases free buparvaquone upon metabolism by

cytochrome P450. Unfortunately, these methods can also potentially decrease membrane permeability due to the addition of charged groups in the case of phosphates or amino acids or increased size, in the case of PEG. Therefore, solubility-enhancing prodrug modifications must be used in delicate balance with maintaining sufficient membrane permeability [100].

Prodrugs have also been used to overcome permeability limitations in oral drug administration [101]. Conjugation of lipophilic constituents to polar functional groups on the parent drug serves to increase the overall lipophilicity of the drug and improve passive permeability through the intestinal barrier [101]. This is especially important when the polar groups are ionizable in the pH of the small intestine, as charge can severely limit intestinal permeability. These groups can be designed to be cleaved during first-pass metabolism in the liver so that the free drug is liberated prior to reaching the general circulation. Finally, if passive diffusion across the intestinal barrier is not possible, prodrugs can be designed to be substrates of gastrointestinal transporters, taking advantage of carrier-mediated transport pathways [101].

2.5.2 Efflux and Metabolic Inhibitors

In addition to poor solubility and poor passive permeability, drugs can have poor intestinal absorption due to efflux or metabolism in the intestinal barrier. These problems are especially prevalent with anti-cancer drugs which are often effluxed by P-glycoprotein (P-gp) or multidrug resistance proteins (MDR), or metabolized by Cytochrome P-450 (CYP) enzymes [102]. To address this issue, these drugs are often co-administered with inhibitors of drug efflux and drug metabolism to decrease these effects.

For example, Paclitaxel, a taxane anti-cancer drug, shows *in vivo* bioavailability of only 10%, mostly due to efflux by P-gp. Co-administration of P-gp inhibitors SDZ PSC833, a cyclosporine D analogue or GF120918, a non-immunosuppressive P-gp blocker, showed significant improvements in oral Paclitaxel bioavailability [103]. In the case of Docetaxel, which is a P-gp substrate and metabolized by CYP3A4, co-administration of Ritonavir, a CYP3A4 inhibitor, led to significant gains in oral bioavailability [103]. Similar improvements in oral bioavailability have been observed by co-administration of CYP3A4 inhibitors with Irinotecan [104] and HIV-protease inhibitors [105]. These examples illustrate the potential of co-administration of metabolic and efflux inhibitors to improve oral bioavailability.

2.5.3 Tight Junction Modulators

For hydrophilic molecules that cannot permeate the intestinal barrier by passive diffusion, but are too large for the paracellular route, tight junction opening serves as a novel mechanism to enhance intestinal permeability. Several molecules have been developed to transiently open the tight junctions in the intestinal barrier. Medium chain fatty acids such as sodium caprate have been shown to open the tight junctions, as indicated by increased paracellular flux of markers such as mannitol. These fatty acids are thought to activate phospholipase C on the plasma membrane, which then causes an increase in intracellular calcium concentration [106]. This elevated calcium concentration causes contraction of calmodulin-dependent actin filaments, which subsequently opens the tight junctions. *In vivo* studies of sodium caprate have been completed in several animal models and in humans. Modest increases in oral bioavailability of a variety of

drugs were seen with minimal damage to the intestinal barrier, suggesting the potential of sodium caprate as a safe absorption enhancer [107].

Similar to sodium caprate, medium chain mono- and di-glycerides and medium- and long-chain fatty acid esters of carnitine and choline can also open tight junctions, as evidenced by reduced TEER and increased permeation of low molecular weight paracellular markers [108]. Nitric oxide donors such as S-nitroso-N-acetyl-DL-penicillamine (SNAP), have been shown to increase permeability of 4 kDa FITC-dextran and influence the expression and localization of tight junction proteins, suggesting their potential as absorption enhancers [62]. While SNAP showed promising results in rabbits and rats, the mechanism of tight junction modulation is still unknown. Finally, zonula occludens toxin (Zot), a protein derived from *Vibrio cholerae*, has demonstrated tight junction modulation. Fasano and colleagues report that Zot selectively opens tight junctions in the small intestine in a dose-dependent and reversible manner [109]. Studies in rats showed a significant increase in insulin and immunoglobulin bioavailability in rats treated with Zot. Tight junction modulators can improve delivery of large, water-soluble drugs via the paracellular route.

2.5.4 Macromolecules

In addition to the above-mentioned permeation enhancers there are several macromolecular permeation enhancers that are currently being investigated. Polyacrylates, or synthetic high molecular weight polymers of acrylic acid, have been shown to be mucoadhesive and to modulate tight junction integrity [110]. It is hypothesized that polyacrylates achieve permeation enhancement by binding calcium

ions that are required for tight junction maintenance. Importantly, studies in rats showed that long term oral administration of polyacrylates did not cause any significant toxicities *in vivo*, suggesting the safety of this strategy [111].

Chitosan and chitosan derivatives have also been shown to modulate tight junction integrity [107]. Studies on Caco-2 cells showed that treatment with chitosan and chitosan derivatives caused enhanced paracellular flux of small molecules such as mannitol and large markers such as FITC-dextran. The precise structure of chitosan can vary both in molecular weight and in the amount of deacetylation, as well as the addition of methyl groups for enhanced solubility in basic pH conditions. All of these changes alter the degree to which chitosan can enhance paracellular transport. It has been shown that chitosan binds to the intestinal cells, causing redistribution of cytoskeletal F-actin and ZO-1 tight junctional proteins [112]. The toxicity of chitosan is directly related to its degree of deacetylation and there exists an optimum amount of deacetylation that causes tight junction opening with minimal toxicity.

Recently, poly (amido amine) (PAMAM) dendrimers have been identified as potent tight junction modulators. Treatment of Caco-2 cells with PAMAM dendrimers of different sizes and surface functionalities has been shown to increase the paracellular flux of mannitol, reduce TEER and increase accessibility of actin and occludin proteins [15, 16]. PAMAM dendrimers are transported across the intestinal barrier, making them both permeation enhancers and potential oral drug delivery carriers [113]. The following three sections will describe a detailed background on dendrimers, applications of PAMAM dendrimers in drug delivery and the current knowledge of these constructs as oral drug delivery carriers.

2.6 Dendrimers

2.6.1 History of Dendrimer Development

Dendrimers are unique polymeric structures that are highly-branched, nanoscale in size and have a wide range of applications in the field of nanobiotechnology. The term dendrimer is derived from the greek “dendra” meaning tree and “meros” meaning part [114]. Dendrimers were first conceived of in the late 1970’s by the groups of Vogtle, Denkwalter, Tomalia and Newkome and were first presented to the public by Tomalia in 1983 [14]. Since then, the number of dendrimer-related publications and technologies has increased rapidly, illustrating the utility of this nanoscale structure [115]. Several commercial applications of dendrimers have shown promise in the past decade.

VivagelTM, a vaginal topical microbicide for the prevention of HIV transmission, was granted fast track status for clinical trials in 2006 [116]. SuperFect[®], developed by Qiagen, uses dendrimer technology to improve transfection in a wide range of cell lines [117]. Finally, Stratus CS[®] Acute Care Diagnostic System, uses dendrimers to rapidly detect myoglobin, a sensitive marker for acute coronary diseases [118].

One of the most promising areas of application of dendrimers is in the field of nanomedicine. Dendrimers have many unique physical properties including near monodispersity and nanoscopic size [12, 13]. With each increase in dendrimer generation, the diameter increases linearly while the number of surface groups increases exponentially. This creates high density surface groups that can be conjugated to drug molecules [20, 119-124], targeting moieties [125-128], and imaging agents [129-131], or complexed with DNA [132, 133], making dendrimers versatile drug delivery platforms [14]. Figure 2.7 illustrates the multifunctional nature of dendrimers [24].

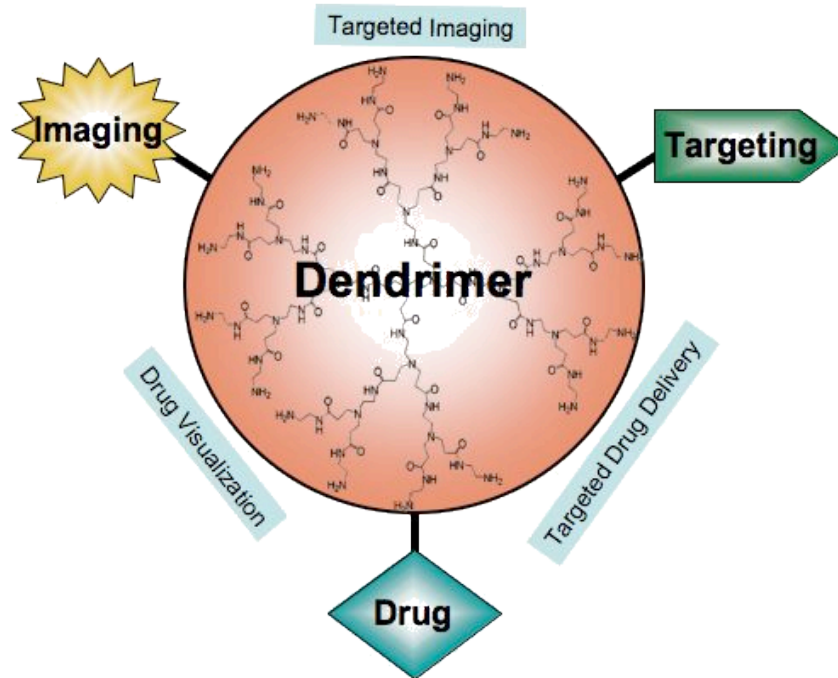


Figure 2.7. Dendrimers as Multifunctional Nanocarriers. Targeting moieties can be attached to the dendrimer surface groups while drugs and imaging agents can be conjugated to the surface, encapsulated in the dendrimer core or complexed (such as therapeutic DNA) with the dendrimer structure. (From [24]).

2.6.2 Dendrimer Synthesis

In the early stages of development, dendrimers were synthesized by the divergent method, wherein repeating units were progressively added to an initiator core, increasing the generation number with each reaction step (Figure 2.8) [115]. While straightforward, this synthetic strategy is somewhat tedious, requires purification after each step and is difficult to scale-up. Subsequently, dendrimers were produced by convergent synthesis methods where reactive dendrons are synthesized and then attached to a multifunctional initiator core to generate the final product (Figure 2.8) [134]. Convergent synthetic strategies are useful for larger dendrimers as they contain fewer steps than divergent approaches.

Recent innovations in dendrimer synthesis have facilitated commercial production of dendrimers, focusing on producing high yields of intermediates and minimizing toxic byproducts. “Lego chemistry” uses branched monomers, which facilitates production of dendrimers by minimizing the number of reaction and purification steps. In addition “click chemistry” has been developed to produce dendrimers with specific surface chemistries using a copper catalyst. These innovations have allowed several families of dendrimers to be produced commercially, which has had a significant impact on the use of dendrimers in biomedical research [13].

2.6.3 Types of Dendrimers

More than 100 different types of dendrimers with more than 1,000 different surface modifications have been developed to date [13]. These dendrimers differ in the identity of the initiator core, branching units and surface groups, all of which can have a

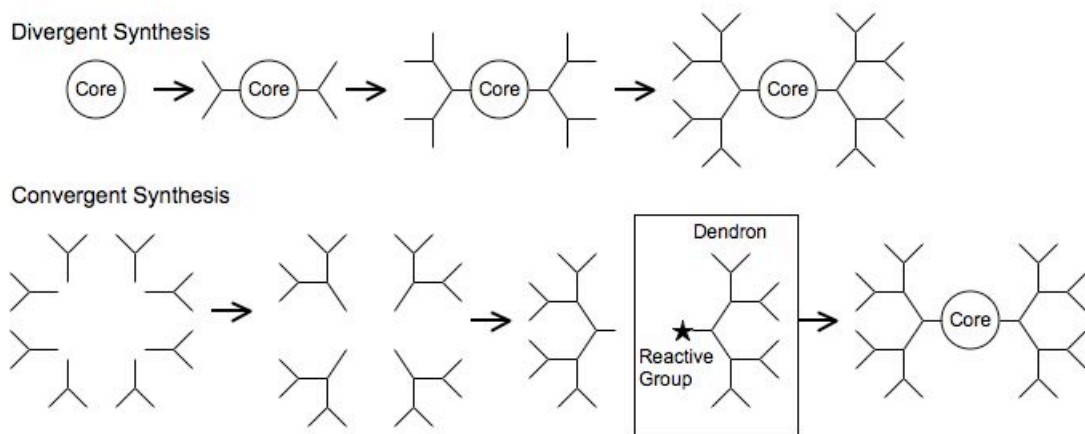


Figure 2.8. Divergent and Convergent Syntheses of Dendrimers. In divergent synthesis, monomeric branches are repeatedly added to the initiator core, increasing the dendrimer generation with each addition. In convergent synthesis, reactive dendrons are added to a multifunctional core. (From [24]).

profound impact on their biological properties. In addition, the synthetic strategy used to produce each type of dendrimer is often different. Some of the most common types of dendrimers, including poly (propylene amine) (PPI), polyether and poly (amido amine) (PAMAM) dendrimers, are illustrated in Figure 2.9. PPI dendrimers were first produced by Vogtle and are synthesized by the divergent method (Figure 2.9 A) [135]. They are commercially available and can be amine or nitrile terminated, which significantly impacts their biological properties [115]. Polyether dendrimers or “Frechet-type” dendrimers are synthesized by the convergent method (Figure 2.9 B) and have been used in applications such as light harvesting and catalysis [115]. PAMAM dendrimers, commercially available as Starburst[®] PAMAM dendrimers, have an ethylene diamine core and amido amine branching units with carboxyl or amine terminal groups (Figure 2.9 C,D). They are described in detail in the following section.

2.7 Poly (amido amine) Dendrimers

2.7.1 Structure of PAMAM Dendrimers

Poly (amido amine) (PAMAM) dendrimers were originally developed by Tomalia at Dow Laboratories in 1979. PAMAM dendrimers have numerous applications in nanobiotechnology and are some of the most commonly used since they are both fully characterized and commercially available [136-138]. Starburst[®] PAMAM dendrimers have an ethylene diamine core, an amido amine repeat branching structure and are available in generations 0.5 through 10. As generation number is increased, the number of active terminal groups doubles, while the diameter increases by approximately 1 nm, giving PAMAM dendrimers a diameter range of 1.5 to 14.5 nm [136]. In PAMAM

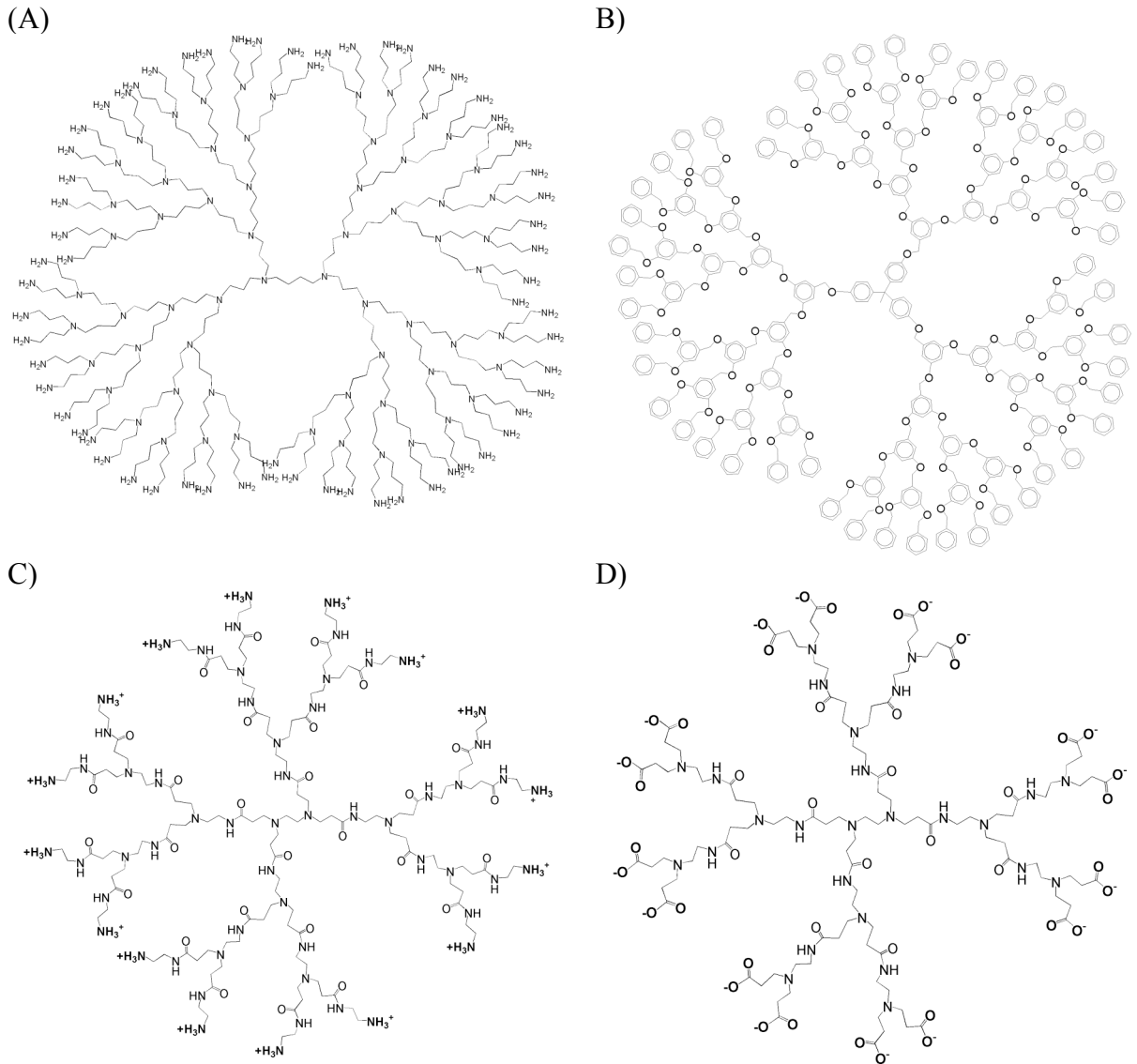


Figure 2.9. Chemical Structures of Common Dendrimers. A) G4 PPI dendrimer with a 1,4-diaminobutane core, B) G4 polyether dendrimer, C) G2 PAMAM dendrimer with amine terminal groups and an ethylenediamine core and D) G1.5 PAMAM dendrimer with carboxylic acid terminal groups and an ethylenediamine core. (From [24]).

dendrimers “full” generations (G1, G2, G3, etc.) have amine-terminated branches whereas “half” generations (G1.5, G2.5, G3.5, etc.) have carboxylic acid terminated branches (Figure 2.9 C,D). They can also be modified with terminal hydroxyl groups to neutralize the surface charge. The surface charge and chemistry of PAMAM dendrimers have a significant impact on their biological properties including toxicity and biodistribution. Table 2.2 summarizes the physical properties of G0-G5 dendrimers commercially available from Dendritech.

2.7.2 Biocompatibility and Biodistribution of PAMAM Dendrimers

In order to be suitable for clinical use, polymeric carriers must be non-toxic and non-immunogenic [139]. In addition, polymeric carriers must display biodistribution properties that allow for uptake in the target tissue with minimal off-site accumulation [139]. One of the first tests for biocompatibility is performance in *in vitro* toxicity screens against different cell lines. *In vitro* toxicology studies have shown that dendrimer cytotoxicity is primarily governed by surface chemistry, although the core identity can play a role. In general, cationic PAMAM dendrimers show increasing toxicity with increases in concentration and generation, while anionic dendrimers have been found to be non-toxic against a large variety of cell lines [139]. This charge-dependent effect is consistent with PAMAM dendrimer impact on red blood cells. Cationic dendrimers have been shown to cause changes in red blood cell morphology at lower concentrations and significant hemolysis at higher concentrations. In contrast, anionic PAMAM dendrimers of generations 3.5 through 9.5 have been found to show no toxicity against red blood cells up to 2 mg/ml concentration [139]. These *in vitro* studies illustrate the significant

Table 2.2. Physical Properties of PAMAM Dendrimers

Generation	Surface Functionality	Number of Surface Groups	Molecular Weight	Measured Diameter (Å)
-0.5	-COOH	4	436	-
0	-NH ₂	4	517	15
0.5	-COOH	8	1,269	-
1	-NH ₂	8	1,430	22
1.5	-COOH	16	2,935	-
2	-NH ₂	16	3,256	29
2.5	-COOH	32	6,267	-
3	-NH ₂	32	6,909	36
3.5	-COOH	64	12,931	-
4	-NH ₂	64	14,215	45
4.5	-COOH	128	26,258	-
5	-NH ₂	128	28,826	54

Reported by Dendritech, Inc. Midland, MI

impact of dendrimer surface chemistry on the toxicological properties of these novel carriers.

Malik and co-workers investigated the biodistribution of ^{125}I -labeled anionic (generations 2.5, 3.5, 5.5) and cationic (generations 3,4) PAMAM dendrimers in Wistar rats after intravenous administration [140]. Cationic dendrimers were cleared rapidly from the circulation, while anionic dendrimers showed longer retention times in the blood stream. In addition, both cationic and anionic dendrimers were found to have significant accumulation in the liver. Passive accumulation of polymeric carriers at the tumor site due to the enhanced permeability and retention effect is critical for the applicability of dendrimers as anti-cancer drug delivery carriers. In a separate work, Malik et al. showed that G3.5 PAMAM dendrimer-Cisplatin conjugates showed significant tumor accumulation at a 50-fold increase relative to IV administered free drug at the maximum tolerated dose, suggesting the potential of G3.5 PAMAM dendrimers for tumor delivery of anti-cancer agents [141]. While there are still many *in vivo* studies necessary to characterize the toxicity and biological fate of PAMAM dendrimers, it is clear that surface charge significantly influences both toxicity and biodistribution.

2.7.3 Applications of PAMAM Dendrimers as Drug Carriers

Because of their high water solubility and large number of ionizable surface groups, dendrimers can be used to encapsulate drugs with poor aqueous solubility. It has been well established that dendrimers have a core-shell architecture, allowing for encapsulation of drug molecules in the voids of the dendrimer core [13]. Encapsulation of drug cargo in dendrimers allows for improved water solubility and thus preferential

presentation of the drug to the biological membrane and subsequent internalization. In addition, the dendrimer can also protect the encapsulated drug cargo from degradation. Kannan et al. improved solubility of ibuprofen by encapsulation in G3 dendrimers [142]. Ibuprofen encapsulated in dendrimers showed a much higher rate of cellular internalization in A549 lung cells compared to free ibuprofen. Drug loading was approximately 50% for the G3-ibuprofen complexes, indicating the high capacity of PAMAM dendrimers for incorporation of small molecular weight bioactive agents.

Despite their ease of synthesis, PAMAM dendrimer-drug complexes are plagued by non-specific drug release, which can lead to unwanted toxicity *in vivo*, especially in the case of anti-cancer drugs. Therefore, there has been much research done on PAMAM dendrimer-drug conjugates where drugs are covalently attached to dendrimer periphery groups by chemical linkers. These linkers can be designed to maximize drug release at the site of action. Wiwattanapatapee and colleagues studied PAMAM dendrimer-5-aminosalicylic acid conjugates for targeted colonic delivery [122]. The conjugates had two different azo spacers, which are susceptible to degradation by azoreductase, an enzyme that is abundant in the colonic environment. The conjugates showed free drug release in the presence of rat cecal contents, but not in the gastric fluid, indicating the specificity of the release mechanism. This study illustrates that the choice of the spacer can have a profound impact on the ability of the dendrimer-drug conjugate to release the drug in the appropriate environment and time after administration.

Finally, targeting and imaging agents can be attached to dendrimer-drug conjugates for multifunctional delivery strategies. Majoros and co-workers conjugated folic acid, a targeting moiety that binds to over-expressed folate receptors on cancer cells,

Paclitaxel, a chemotherapeutic agent, and FITC, a fluorescent ligand, to G5 PAMAM dendrimers, creating a tri-functional therapeutic agent [143]. The cytotoxicity and cellular uptake of this dendrimer system was evaluated in KB cells. The folate-labeled dendrimers were found to selectively internalize in folate-receptor-expressing KB cells and those containing Paclitaxel caused cytotoxicity similar to the free drug. In contrast, folate receptor- negative cells did not internalize the dendrimers, indicating the strong targeting ability. This work illustrates the potential of using dendrimers as multifunctional nanodevices for drug delivery.

2.8 PAMAM Dendrimers as Oral Drug Delivery Systems

2.8.1 Transepithelial Transport of PAMAM Dendrimers

The potential of PAMAM dendrimers as oral drug delivery carriers was first reported in 2000 by Wiwattanapatapee et al [144]. In this study, the tissue uptake and serosal transfer rates of anionic (G2.5, G3.5 and G5.5) and cationic (G3, G4) PAMAM dendrimers were measured in *in vitro* everted rat intestinal sacs. Anionic dendrimers were found to have high serosal transport rates and minimal tissue uptake, while cationic dendrimers had lower serosal transport rates and more tissue uptake, most likely due to nonspecific binding. Importantly, the dendrimer transport rates were higher than what is typically seen for large macromolecules, suggesting the unique potential of PAMAM dendrimers as polymeric drug carriers.

This report of dendrimer transepithelial transport was followed by a comprehensive investigation of the influence of dendrimer size, charge and incubation time on dendrimer transport across Caco-2 cell monolayers as well as the mechanism of

dendrimer transport. As described in Section 2.4.3, Caco-2 cell monolayers serve as a model of the intestinal barrier and can be used to elucidate the degree and mechanisms of intestinal permeability without the confounding factors associated with *in vitro* intestinal sac models. El-Sayed et al. first explored transepithelial transport of cationic dendrimers across Caco-2 cell monolayers in 2002 [145]. In this study, PAMAM dendrimer generations G0-G4 were investigated for their potential in oral delivery. Permeability of the dendrimers was found to increase with concentration and incubation time. G0-G2 dendrimers were found to be non-toxic with appreciable permeability, suggesting the potential of these constructs as oral drug carriers. Kitchens et al. studied the transepithelial transport of cationic (amine-terminated), anionic (carboxylic acid-terminated) and surface neutral (hydroxyl-terminated) dendrimers across Caco-2 cell monolayers [15]. When comparing dendrimers of the same size, cationic dendrimers showed the highest permeability, followed by anionic dendrimers and neutral dendrimers. Increasing the generation of anionic dendrimers caused an increase in permeability while increasing the generation of cationic dendrimers lead to decreased permeability and increased toxicity. These studies indicate that within a specified size, charge and concentration window, dendrimers can enhance transepithelial transport.

In addition to determining the transport rates of PAMAM dendrimers across Caco-2 cells, several studies have been performed to elucidate the mechanism of transport. Studies have shown that dendrimers are transported by a combination of transcellular and paracellular mechanisms. Tight junction opening can be monitored by several different methods including a reduction in transepithelial electrical resistance (TEER), an increase in flux of paracellular markers such as [¹⁴C]-mannitol or Lucifer

yellow and an increase in exposure of tight junction proteins such as occludin [15]. El-Sayed et al. reported that G2.5 and G3.5 dendrimers reduced TEER and increased [¹⁴C]-mannitol flux up to 6 fold compared to the control [146]. In contrast, OH-terminated dendrimers did not cause a significant change in TEER or mannitol permeability. Kitchens et al. reported that cationic dendrimers increased [¹⁴C]-mannitol flux and reduced TEER to a greater extent than anionic dendrimers, indicating a strong charge dependence of dendrimer tight junction opening ability [16]. In addition, higher generation dendrimers of both cationic and anionic dendrimers opened the tight junctions to a greater degree than lower generations. Finally, increasing incubation time from 90 to 210 minutes increased tight junction opening for all dendrimer generations. In a parallel study, both cationic and anionic dendrimers were found to interact with tight junction proteins, increasing occludin and actin staining, thus further establishing the ability of dendrimers to open tight junctions [15]. These studies illustrate that the size and charge of PAMAM dendrimers have a significant impact on their interaction with differentiated enterocytes. In addition, there may be an optimal window of size, charge and incubation time that will lead to the best dendrimer system for a specific oral drug delivery application.

In addition to opening the tight junctions, dendrimers are also transported across the intestinal barrier by the transcellular route. In 2003 El-Sayed et al. reported energy-dependent transport of G2 dendrimers, suggesting the involvement of transcytosis in addition to transport via the paracellular route [147]. Jevprasephant et al. further confirmed this phenomenon by investigating internalization of G3 dendrimers into Caco-2 cells by visualizing the interaction between Caco-2 cells and FITC labeled G3

dendrimers using flow cytometry and confocal microscopy and gold-labeled G3 dendrimer by transmission electron microscopy (TEM) [19]. These studies showed a significant amount of dendrimer cellular internalization with minimal non-specific binding on the cell surface, suggesting transport of G3 dendrimers by the transcellular route. In addition, Kitchens and colleagues examined the impact of endocytosis inhibitors on cellular internalization and transepithelial transport of G4 dendrimers in Caco-2 cells [148]. Inhibitors including brefeldin A, colchicine, filipin, and sucrose all decreased the uptake and transport of the dendrimers, indicating the involvement of endocytosis mechanisms in the transport of G4 dendrimers.

2.8.2 Cytotoxicity of PAMAM Dendrimers

In order to be useful as oral drug delivery carriers, it is crucial that dendrimers do not cause toxicity to intestinal cells during transport. Toxicity of PAMAM dendrimers to Caco-2 cells has been investigated using cell viability assays. El-Sayed et al. established cationic dendrimers are significantly more toxic than anionic dendrimers and this toxicity increases with dendrimer generation and incubation time [146]. In contrast, anionic dendrimers are much less toxic and only displayed slight increases in LDH release when cells were treated with 10 mM concentrations of G3.5 and G4.5 dendrimers for a 90 minute incubation time [146]. Since anionic dendrimers are much less toxic they can be used at higher concentrations and longer incubation times without causing damage to the intestinal cells.

In addition to cell viability assays, Kitchens et al. investigated the impact of dendrimer treatment on the morphology of differentiated intestinal cells, specifically

examining the effect on the microvilli by TEM [18]. G2 cationic dendrimers, with 16 amine terminal groups, did not cause appreciable damage to the cell monolayer, even up to 1 mM concentration. In contrast, G4 dendrimers, which have 64 amine terminal groups, showed significant toxicity at 1 mM. When the concentration of G4 dendrimers was reduced to 0.01 mM, they were non-toxic, illustrating that G4 dendrimers can be used safely at lower concentrations. Finally, even high generation G3.5 anionic dendrimers, which have 64 terminal carboxylic acid groups, did not cause a change in cell morphology up to 1 mM, indicating the low intrinsic toxicity of anionic dendrimers. Thus, in choosing a dendrimer carrier for oral drug delivery, one must choose a generation and concentration that maximizes transport, while minimizing toxicity. In addition, it is critical to first assess the toxicity of the dendrimers before assessing permeability since a toxic treatment could compromise the integrity of the monolayer, causing artificially high permeability measurements.

2.8.3 Surface Modification of PAMAM Dendrimers

Because of their large number of terminal groups, PAMAM dendrimers have been modified with different ligands in order to alter their biological properties including cytotoxicity and permeability. Jevprasesphant and co-workers conjugated lauroyl chloride chains to cationic dendrimers and measured their toxicity towards Caco-2 cells and their permeability across Caco-2 cell monolayers [17]. Modification with lauroyl chains decreased the cytotoxicity of cationic dendrimers and increased their permeability as well as their tight junction opening ability. It was hypothesized that the significant reduction in cytotoxicity was observed because the lauroyl chains were able to shield

some of the positive charges. In a similar study, Kolhatkar et al. investigated the impact of modifying G2 and G4 dendrimers with acetyl groups, effectively neutralizing half or all of the surface charges [149]. Acetylation of G2 and G4 dendrimers significantly reduced their cytotoxicity towards Caco-2 cells, with full acetylation causing the greatest decrease in cytotoxicity. In addition, the partially acetylated dendrimers showed comparable permeability to unmodified dendrimers, indicating that acetylation can reduce cytotoxicity without compromising permeability. These studies illustrate that surface modification of PAMAM dendrimers can be a powerful tool to modulate both cytotoxicity and transepithelial transport to create an optimized oral drug delivery system.

2.8.4 PAMAM Dendrimer Internalization

Because dendrimers are thought to cross the epithelial barrier by transcellular and paracellular routes, the mechanisms of dendrimer internalization in Caco-2 cells and subsequent trafficking have been studied. After El-Sayed et al. established the energy dependent cellular internalization mechanism of G2 dendrimers [147], Kitchens and colleagues further evaluated the cellular internalization of G1.5 and G2 dendrimers in Caco-2 cells and monitored their colocalization with markers for clathrin, early endosomes and lysosomes [18]. Both G1.5 and G2 dendrimers were internalized after 20 minutes and showed colocalization with all three markers, indicating that they are likely internalized by clathrin-mediated endocytosis. Interestingly, G1.5 and G2 dendrimers showed slightly different trafficking patterns, with G1.5 dendrimers showing greater colocalization with the lysosomes at earlier time points, illustrating the importance of surface charge on dendrimer trafficking. Importantly, since dendrimers colocalize with

early endosomes and lysosomes, these studies suggest that these organelles could potentially be targeted for drug release.

2.8.5 PAMAM Dendrimers as Oral Drug Delivery Systems

While there has been significant progress on studying the transport characteristics of PAMAM dendrimers, there have been comparatively few studies using dendrimers to improve the oral bioavailability of therapeutics. D'Emanuele et al. investigated G3 dendrimers to improve the oral bioavailability of Propranolol, which has low water-solubility and is a P-gp efflux transporter substrate [113]. By conjugating Propranolol to the G3 dendrimers, the apical to basolateral flux of Propranolol increased while the basolateral to apical transport decreased, indicating that G3 dendrimers were able to prevent Propranolol efflux by P-gp. This study illustrates that PAMAM dendrimers can be used to both improve drug solubility and avoid efflux, thus improving overall bioavailability.

One of the most promising areas for drug delivery is directing chemotherapy to the site of action. Chemotherapeutics often have poor bioavailability due to low water solubility and can also cause intestinal toxicity. In 2008, Kolhatkar et al. reported the complexation of PAMAM G4 with SN38, which enhanced the solubility, transepithelial transport and cellular uptake of SN38 relative to free drug, suggesting its potential as an oral drug delivery system [150]. Ke and co-workers examined the ability of G3 dendrimers to improve the oral bioavailability of Doxorubicin, an anthracycline antibiotic used to treat a wide range of cancers [151]. The dendrimer-drug complexes were found to enhance Doxorubicin cellular uptake and transport across rat intestinal tissue compared to

free drug. In addition, oral bioavailability of Doxorubicin in rats was increased 200-fold relative to free drug. These studies illustrate the utility of dendrimers to improve the oral bioavailability of chemotherapeutics.

2.8.6 Designing PAMAM Dendrimer-Drug Conjugates for Oral Delivery

Combining our knowledge of PAMAM dendrimer transepithelial transport with the challenges associated with the oral delivery of chemotherapeutics, we can begin to envision the requirements for an optimized dendrimer-drug oral delivery system. Several elements of the system will affect the ultimate performance of the DDS including the choice of dendrimer generation, drug and drug linker. As described in Section 2.8.1 there have been many studies examining the impact of size and charge on dendrimer transport. While cationic dendrimers show enhanced transport, their cytotoxicity restricts their use to lower concentrations. Therefore, anionic dendrimers, which have very low intrinsic toxicity and have shown promising *in vitro* results in everted rat intestinal sacs as well as Caco-2 cell monolayers, may be a better choice for the carrier.

The choice of drug cargo is also critical for having a successful dendrimer drug delivery system. In addition to having low solubility and poor bioavailability, the drug must have functional groups such as amines, acids or alcohols available for conjugation to the dendrimer. The drug must be highly potent, ensuring that even if only a fraction of the administered dose is transported across the intestinal barrier that the ultimate concentration in the bloodstream is still within the therapeutic window of the drug.

The final element of a successful dendrimer drug delivery system is the drug linker. This linker must be designed such that it is stable in the gastrointestinal tract, but

is released at the site of action in the tumor environment. In order to stay intact through the gastrointestinal environment, the linker must be stable under low pH in the stomach (pH 1-2) as well as the elevated pH in the small intestine (7.5-8). In addition, the linker must be resistant to the peptidases in the gastric environment and in the brush border of the intestinal mucosa. However, in order for the drug to be active, the free drug must be released at the site of action. Finally, the linker chemistry can be adjusted by the use of a spacer. A spacer can allow for increased access of enzymes to the bond of interest, allowing for release in the tumor environment. Selection of the proper dendrimer, drug, linker and spacer has the potential to create a smart dendrimer drug delivery system, which can enhance the oral bioavailability of chemotherapeutics, thus improving patient lives and treatment.

2.9 Colorectal Cancer

2.9.1 Prevalence

According to the American Cancer Society Facts and Figures 2010, there are more than 140,000 new cases of colorectal cancer each year and over 51,000 deaths projected in 2010 [152]. Colorectal cancer is the third most diagnosed cancer in men and women and the third leading cause of cancer death in the United States [153]. Although development of colorectal cancer is usually sporadic, risk factors include increasing age, male gender, diseases such as diabetes and inflammatory bowel syndrome and environmental factors including high fat / low fiber diets, excessive alcohol consumption, smoking, obesity and a sedentary lifestyle. In addition, approximately 6% of colorectal cancer cases are thought to be genetically inherited [154]. Colorectal cancer places a

significant burden on the healthcare system, comprising approximately 12% of cancer-related healthcare costs in the United States with total costs estimated between \$4.5 and \$9.6 billion dollars per year [153]. Reduction in treatment costs by novel therapies could improve the quality of life of patients and dramatically reduce the burden on the healthcare system.

2.9.2 Colorectal Cancer Screening

Current colorectal cancer screening guidelines recommend testing for men and women over the age of 50. Colorectal cancer screening tests include fecal occult blood tests (FOBT), sigmoidoscopies and colonoscopies, which are recommended for every one, five and ten years, respectively [154]. An FOBT detects blood in a stool sample, which may be an indication of colorectal cancer. It is the simplest and lowest cost test, but positive results can indicate other pathologies such as hemorrhoids, anal fissures, polyps, inflammatory bowel disease or Crohn's disease. For this reason, a positive FOBT result is followed up with a more extensive test such as a colonoscopy. A sigmoidoscopy is an endoscopic examination of the rectum and the lower portion of the colon where 60% of colorectal cancers occur. A sigmoidoscopy involves relatively little patient preparation, only requiring self-administration of a single enema. A colonoscopy is the most extensive screening test and involves an endoscopic examination of both the upper and lower colon, requiring extensive patient preparation 48 hours before the procedure and a specialized doctor to perform the exam. While it is both invasive and expensive, a colonoscopy is also the most sensitive diagnostic tool and is becoming the standard of care in the United States. All of these screening techniques have been found to be cost

effective ways of reducing the incidence of colorectal cancer by allowing physicians to remove polyps before they become cancerous and reducing mortality by diagnosing the cancer at an earlier, more treatable stage [153].

2.9.3 Colorectal Cancer Diagnosis and Staging

After colorectal cancer is detected by a colonoscopy, it is further characterized by a biopsy of the tumor as well as a CT scan to detect any metastatic sites [154]. The cancer is then staged according to three separate factors, known as the TNM classification system. The “T” or tumor factor, ranks the invasiveness of the primary tumor. The “N” or lymph node factor, ranks the number of regional lymph nodes that have been invaded. Finally, the “M” or metastasis factor, ranks the presence and number of distant metastases [154]. These three scores are combined to yield an overall stage, which can be used to provide the patient with a five year prognosis. For example, in Stage I where the primary tumor is adherent to the submucosa but there are no lymph node invasions or distant metastases, the five-year survival rate is over 97%. In contrast in late Stage III where many regional lymph nodes show metastatic disease, the five year survival rate is less than 30% [154]. These dramatic survival differences based on the stage of disease highlight both the importance of early detection and the great need for therapies to treat metastatic disease.

2.9.4 Colorectal Cancer Metastasis and Treatment

The most common site of colorectal cancer metastasis is the liver, with over 20% of patients presenting liver metastases at the time of diagnosis and 50% in the duration of

the disease [23]. In addition, liver metastases are responsible for two-thirds of all colorectal cancer deaths, indicating the grave need for novel treatments for this condition. Unlike early stage colorectal cancer where the tumor is confined to a small area and can be removed by surgery, hepatic metastases are much more difficult to remove and often require a combination of surgery and chemotherapy. After a patient is diagnosed with hepatic metastases, the size and location of the tumors are measured to determine resectability. Patients must be left with 20-40% of the initial liver volume in order to have a functioning liver after surgery [23]. If the metastatic tumors are small, the tumors can be resected immediately and followed by adjuvant chemotherapy to prevent recurrence. If the tumors are initially unresectable, patients are often given neoadjuvant chemotherapy to shrink the tumors, making them removable.

Several different chemotherapy drugs have been approved for the treatment of colorectal cancer hepatic metastases. 5-fluorouracil was first approved by the FDA in 1962 and has played an important role in the treatment of metastatic colorectal cancer. Originally used as a single agent and now combined with leucovorin to enhance activity, 5FU works by disrupting RNA synthesis and inhibiting the enzyme thymidylate synthase [155]. In 2001, Capecitabine, an oral prodrug of 5FU, was approved and has shown higher response rates than IV administered 5FU in patient groups with advanced disease [156]. Recently, combination therapies using 5FU/Leucovorin coupled either with Irinotecan, a topoisomerase inhibitor (FOLFIRI), or Oxaliplatin, a platinum-based cytotoxic agent (FOLFOX), have become the standard of care for advanced metastatic disease. While there is some debate on which treatment regimen is better, they both show significant increases in survival time compared to single agent therapy and are

often used together as first and second line treatments [155]. In addition, both of these treatment regimens have shown great potential for reducing tumor size in a neoadjuvant setting as well as preventing tumor recurrence when used after surgery. Depending on the patient, biological agents such as Cetuximab, an anti-VEGF therapy or Bevacizumab, an anti-EGFR antibody, can be added to the treatment regimens to improve response. Coupled with surgical resection, chemotherapy plays a key role in the treatment of colorectal cancer hepatic metastases and serves to extend patient life and reduce potential relapse.

2.10 SN38

7-Ethyl-10-hydroxy-camptothecin, or SN38, is the active metabolite of Irinotecan, a water-soluble analogue of camptothecin that is commonly used for treatment of metastatic colorectal cancer. Camptothecin, a naturally occurring alkaloid extract from the plant *Camptotheca acuminata*, was first discovered in the 1960's [21]. Camptothecin showed promising anti-tumor activity *in vitro* and appeared to strongly inhibit DNA and RNA synthesis. By the 1980's, topoisomerase I, an enzyme required for DNA coiling and uncoiling, was identified as the target of camptothecin. Since then, many different camptothecin analogues have been synthesized, including Irinotecan, and Topotecan which have been approved to treat colorectal and ovarian cancers, respectively, as well as many other analogues in clinical trials and preclinical development [21].

2.10.1 Mechanism of Action of Irinotecan and SN38

In order to cause anti-tumor activity, Irinotecan must be cleaved by carboxylesterase to release SN38 (Figure 2.10) [157]. Carboxylesterases are present in many sites of the body with the highest expression in the liver, where majority of free SN38 is released. After release, SN38 acts as a topoisomerase poison, effectively inhibiting the action of topoisomerase I, which is heavily involved in DNA and RNA synthesis. Importantly, the lactone ring on SN38 and CPT-11 is in dynamic equilibrium between the closed ring lactone form (active) and the open ring carboxylate form (inactive) (Figure 2.10). Interconversion of the lactone and carboxylate forms is pH dependent with the lactone form favored at low pH and in the presence of human serum albumin. Finally, SN38 metabolism occurs by glucuronidation by UDPGA and UDPGT, converting SN38 to SN38-glucuronide [157].

SN38 has significantly higher activity than the parent Irinotecan prodrug. In particular, SN38 has been shown to have greater topoisomerase I inhibition, more significant reduction in DNA and RNA synthesis and an increase in DNA strand breaks relative to Irinotecan at equivalent concentrations [158]. This highlights the importance of free SN38 release from the prodrug for anticancer activity. Designing a prodrug of SN38 with more efficient release properties would have the potential to create a drug that is more effective than Irinotecan.

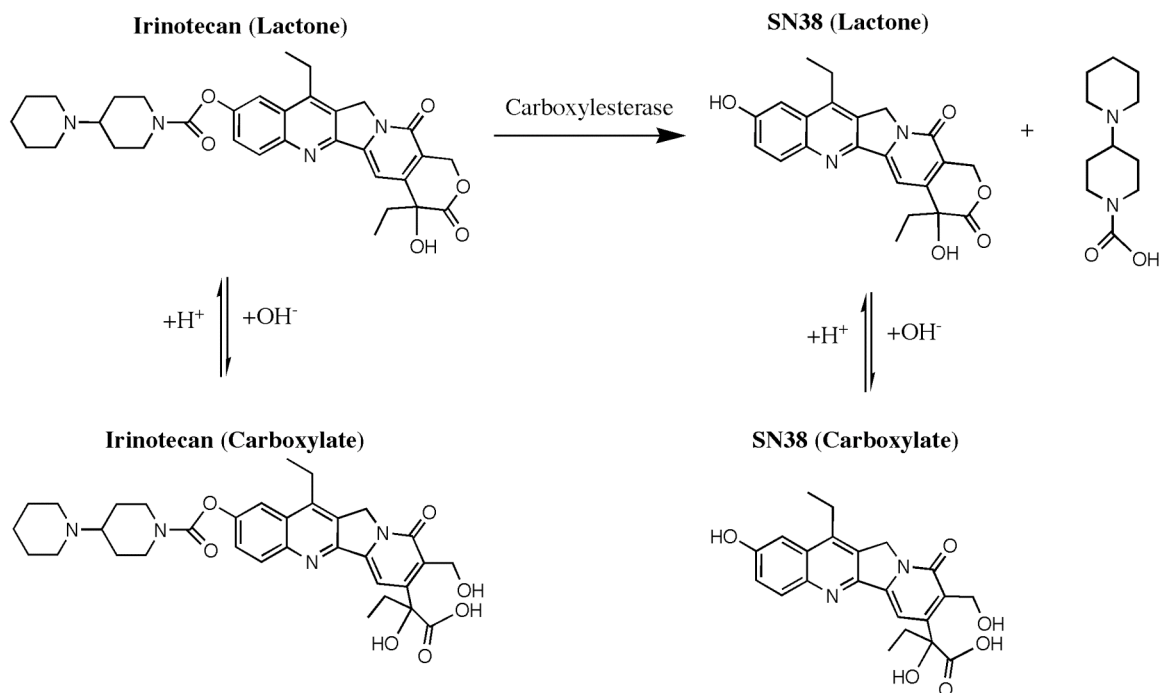


Figure 2.10. Conversion of Irinotecan to SN38 by Carboxylesterase and Equilibrium of Carboxylate and Lactone forms of SN38 and Irinotecan. The closed ring/ lactone form of SN38 is required for anticancer activity. (Adapted from [157].)

2.10.2 Current SN38 Drug Delivery Systems

While SN38 shows 100-1000 fold greater *in vitro* activity than Irinotecan, it has had limited success in the clinic due to poor water solubility and significant gastrointestinal side effects. Several drug delivery systems have been synthesized to overcome these limitations. Zhao and colleagues reported using a 4-arm-PEG system to improve the water solubility of SN38 [159]. Using several different amino acid spacers to alter stability, these SN38-PEG conjugates showed favorable release profiles under neutral pH conditions, high efficacy *in vitro* and *in vivo* in a mouse xenograft model. In addition, PEG conjugation at the 20-OH position on SN38 helped to stabilize the lactone ring until the point of release. The PEG-SN38 conjugate using a glycine spacer showed the most promising therapeutic profile and is currently in Phase I clinical trials (ENZ-2208) [44]. Meyer-Losic et al. reported a cationic peptide-linked SN38 prodrug designed to reduce the gastrointestinal toxicity and hepatic metabolism of Irinotecan. The peptide was linked to SN38 in the 10-hydroxyl position by an ester bond [160]. The conjugates were tested *in vitro* and *in vivo* in a human xenograft model in mice and dogs. In addition to showing promising *in vitro* toxicity against a variety of colon, lung and breast cell lines, the SN38-peptide conjugate showed higher activity than Irinotecan *in vivo* with fewer gastrointestinal side effects.

To date there have been two dendrimer-based drug delivery systems developed for SN38. As described in Section 2.8.5, Kolhatkar and co-workers reported the use of G4 dendrimers complexed with SN38 through non-covalent interactions as a potential oral drug delivery system [150]. The complexes enhanced the solubility, transepithelial transport and cellular uptake of SN38 relative to free drug. PAMAM-SN38 complexes

released 40% of the drug within 24 hours in PBS and 90% of the drug within 30 minutes at pH 5. Because of the instability in acidic conditions, these dendrimer-SN38 complexes would require enteric coating for use in oral administration. In addition, Vijayalakshmi et al. recently reported conjugation of SN38 via glycine and β -alanine spacers to carboxylic-acid terminated G3.5 PAMAM dendrimers at the 20-OH position [161]. These G3.5-SN38 conjugates showed promising *in vitro* activity against colorectal adenocarcinoma HCT-116 cells and produced nuclear fragmentation and cell cycle arrest in the G2/M phase similar to free drug. The conjugates were stable in PBS, and showed up to 20% release in cell culture media and rat plasma during a 72-hour incubation period. These initial studies established the potential of PAMAM dendrimers as drug delivery systems of SN38 for the treatment of colorectal cancer. Importantly, PAMAM dendrimers have the potential to not only improve the oral bioavailability of SN38, but they can also reduce its non-specific toxicity and enhance accumulation at the tumor site. Taken together, these studies illustrate the potential for improvement of the therapeutic efficacy of SN38 by using PAMAM dendrimers.

2.11 Unresolved Issues in Oral Delivery by Dendrimers

Despite the wealth of research on dendrimers as oral drug carriers, there are still many remaining questions that must be resolved for their successful use in oral drug delivery. While PAMAM dendrimers are thought to be transported by a combination of transcellular and paracellular pathways, the mechanism of tight junction opening and precise endocytosis and trafficking pathways are still unknown. In depth knowledge of transepithelial transport pathways of PAMAM dendrimers will help to better design these

constructs as oral drug carriers. In addition, while there is a significant body of work on the transepithelial transport of native dendrimers, there have been comparably few studies on dendrimer-drug conjugates. Detailed studies of the transport, cellular uptake and toxicity of PAMAM dendrimer-drug conjugates are necessary to further establish their utility in oral drug delivery. In addition, chemical linkers that promote stability of the dendrimer-drug conjugates in the gastrointestinal milieu while favoring release of drug in the presence of carboxylesterase must be developed to achieve a functional delivery system for the treatment of colorectal cancer hepatic metastases. Finally, the impact of surface chemistry and conjugation chemistry on the degree and mechanism of dendrimer transport need to be investigated.

Chapter 3 : Cellular Entry of G3.5 Poly (amido amine) Dendrimers by Clathrin- and Dynamin-Dependent Endocytosis Promotes Tight Junctional Opening in Intestinal Epithelia

3.1 Introduction

As discussed in Chapter 2, poly (amido amine) (PAMAM) dendrimers have shown promise as drug delivery carriers due to their unique physical properties including nanoscale size and near monodispersity [114]. With each increase in dendrimer generation, the diameter increases linearly while the number of surface groups increases exponentially, creating high density surface groups that can be conjugated to drugs, imaging agents and targeting moieties, making dendrimers versatile multifunctional nanocarriers [12, 24]. Reports from our laboratory [15, 16, 145, 146] and others [17, 19, 20, 162] have demonstrated that PAMAM dendrimers in a specified size and charge window can effectively cross the epithelial layer of the gut, showing potential as oral drug delivery carriers. Conjugation or complexation of therapeutics with poor solubility and low permeability to water-soluble dendrimers that can permeate the epithelial layer of the gut has the potential to render these drugs orally bioavailable [113, 150, 151]. Oral drug administration has many advantages including the convenience of at-home administration, reduction of direct and indirect costs, and a more flexible dosing regimen, resulting in higher patient compliance and a lower burden on hospitals and the healthcare system [8].

PAMAM dendrimers are known to cross the epithelial barrier by a combination of transcellular and paracellular mechanisms. As described in Chapter 2, transport of cationic dendrimers has been found to be energy-dependent and is reduced in the presence of endocytosis inhibitors, signifying the importance of endocytosis in dendrimer transport [148]. In addition, dendrimers were found to colocalize with clathrin and early endosome markers, suggesting the involvement of clathrin-mediated endocytosis in dendrimer internalization [18]. Dendrimers have also been reported to interact with tight junctions, transiently opening them to allow for paracellular transport [15]. While there has been significant progress in understanding the mechanisms by which dendrimers enter cells and are transported across the epithelial barrier, several important questions remain to be addressed. In particular, the contributions of different endocytosis pathways to dendrimer cellular uptake and transcytosis and the specific mechanisms by which dendrimers open tight junctions have yet to be elucidated. Additionally, the majority of mechanistic studies to date have focused on cationic dendrimers, which are promising due to their high transport rates, but are limited by their significant cytotoxicity. Anionic dendrimers show comparably low cytotoxicity but still appreciable transport rates, making them well suited for oral delivery [27, 144].

In this Chapter, the mechanisms of cellular uptake, transepithelial transport and tight junctional modulation of anionic G3.5 PAMAM dendrimers are investigated by examining the impact of endocytosis inhibitors on dendrimer interaction with Caco-2 cells and differentiated Caco-2 monolayers. In addition, we present the intracellular trafficking of dendrimers from endosomes to lysosomes over time. Knowledge of the

specific pathways of endocytosis, intracellular trafficking and transepithelial transport will aid in rational design of dendrimers for oral delivery.

3.2 Materials and Methods

3.2.1 Materials

G3.5 PAMAM dendrimers (reported molecular weight=12,931), lucifer yellow CH dipotassium salt (LY), oregon green carboxylic acid succinimidyl ester (OG), monodansyl cadaverine (MDC), phenylarsine oxide (PAO), filipin (FIL), genistein (GEN) and dynasore (DYN) were purchased from Sigma Aldrich (St. Louis, MO). Superose 12 HR 10/300 GL column was obtained from Amersham Pharmacia Biotech (Piscataway, NJ) and WST-1 cell proliferation reagent from Roche Applied Sciences (Indianapolis, IN). Caco-2 cells were obtained from American Type Cell Culture (Rockville, MD).

3.2.2 Synthesis of G3.5-OG

Purified G3.5 PAMAM dendrimers were first modified with pendant primary amine groups to facilitate OG labeling [144]. 50 mg dendrimer was dissolved in deionized (DI) water to a final concentration of 10 mg/ml and the pH was adjusted to 6.5. 1-Ethyl-3-(3-dimethylaminopropyl)-carbodiimide (EDC) was added at a 5:1 molar ratio to the dendrimer and stirred for 30 minutes at room temperature, after which ethylene diamine was added at a 5:1 molar ratio and stirred for 4 hours at room temperature. The sample volume was reduced to 1 ml by rotoevaporation of water and then run through a PD10 column followed by purification with an amicon centrifugal filter (MWCO 4000)

to remove the EDC and ethylene diamine. Size exclusion chromatography was used to confirm the absence of low molecular weight impurities. The number of amines per dendrimer was determined to be 2.5 by the ninhydrin assay. 10 mg of amine-modified dendrimer was dissolved in 25 ml of DI water and 1 equivalent of OG per dendrimer was added and stirred for 30 minutes. The water was removed by rotoevaporation and the product was redissolved in methanol and added dropwise to diethyl ether to precipitate the G3.5-OG conjugate. The solution was centrifuged, the ether decanted and then the precipitate was dried overnight under vacuum. The precipitate was then redissolved in 1 ml of water, and passed through a PD10 column to remove unreacted OG. Size exclusion chromatography was used to confirm the absence of free dye. OG content was determined by a fluorescence standard curve ($\lambda_{\text{excitation}} = 485 \text{ nm}$, $\lambda_{\text{emission}} = 535 \text{ nm}$) to be 0.75 molecules of OG per dendrimer on average.

3.2.3 Caco-2 Cell Culture

Caco-2 cells (passages 30–45) were grown at 37°C in an atmosphere of 95% relative humidity and 5% CO₂. Cells were maintained in T-75 flasks using Dulbecco's Modified Eagle's Medium (DMEM) supplemented with 10% fetal bovine serum (FBS), 1% non-essential amino acids, 10,000 units/mL penicillin, 10,000 µg/mL streptomycin and 25 µg/mL amphotericin B. Media was changed every other day and cells were passaged at 80–90% confluence using a 0.25% trypsin/ethylenediamine tetraacetic acid (EDTA) solution. Incubation buffer used in assays consisted of Hank's balanced salt solution (HBSS), supplemented with 1.0 mM N-(2-hydroxyethyl)piperazine-N'-179 (2 ethanesulfonic acid) hemisodium salt (HEPES) buffer (pH 7.4).

3.2.4 Cytotoxicity of Endocytosis Inhibitors

Potential short-term cytotoxicity of endocytosis inhibitors was assessed in Caco-2 cells to ensure cell viability during uptake and transport assays. Chemical inhibitors were prepared at a range of concentrations known to reduce clathrin-mediated endocytosis (phenylarsine oxide (1-20 μM), monodansyl cadaverine (100-300 μM)), caveolin-mediated endocytosis (filipin (1-4 μM), genistein (100-300 μM)) or dynamin-dependent endocytosis (dynasore (40-80 μM)) [163-165]. Cytotoxicity of the inhibitors was assessed by the water soluble tetrazolium salt (WST-1) assay. Caco-2 cells were seeded at 50,000 cells per well in 96 well cell culture plates (Corning, Corning, NY) and maintained at 37°C, 95% relative humidity and 5% CO₂ for 48 hours. Cells were washed with warm HBSS buffer and incubated for 2 hours with 100 μL of varying concentrations of endocytosis inhibitors. After 2 hours, the inhibitor solutions were removed and the cells were washed with warm HBSS buffer. 10 μL WST-1 cell proliferation reagent in 100 μL of HBSS buffer was added to each well and incubated for 4 hours at 37°C. Absorbance at 460 nm and background at 600 nm were measured using a SpectraMax 384 plate reader (Molecular Devices, Sunnyvale, CA). HBSS was used as a negative control for 100% cell viability. Cytotoxicity of inhibitor concentration was assessed in four replicates. Cell viability of greater than 85% was classified as acceptable for uptake and transport assays.

3.2.5 Cellular Uptake

Cellular uptake of G3.5-OG dendrimers was determined in the presence and absence of endocytosis inhibitors. Inhibitors were used at concentrations that showed a

minimum of 85% cell viability during the 2-hour assay period. Caco-2 cells were seeded at 300,000 cells per well in 12 well plates (Corning, Corning, NY) and maintained for 48 hours at 37°C, 95% relative humidity and 5% CO₂. Cells were washed with HBSS and pretreated with endocytosis inhibitors or HBSS for 1 hour at 37°C. Endocytosis inhibitors were removed and 25 µM G3.5-OG, 5 µM Transferrin-AF488 (Molecular Probes, Carlsbad, CA) or 5 µM Cholera Toxin B-AF488 (Molecular Probes, Carlsbad, CA) was added in the presence of endocytosis inhibitor solutions or HBSS for one hour at 37°C. Cells were washed once with cold HBSS, trypsinized for 5 minutes and then complete cell culture media was added to halt the trypsinization process. The cells were removed from plates, collected in microcentrifuge tubes and were centrifuged for 5 minutes at 1,000 rpm after which the supernatant was removed. The cells were washed with PBS and finally fixed in 1% paraformaldehyde in PBS at a final concentration of 500,000 cells/ml. Flow cytometry was used to assess cellular fluorescence using a BD LSR II flow cytometer (Becton Dickenson, Franklin Lakes, NJ) with a 530/30 bandpass filter. Twenty-five thousand to forty-five thousand events were collected per sample. Percent uptake was determined for two different cell populations by the shift in mean fluorescence in the presence of endocytosis inhibitors compared to HBSS control.

3.2.6 Colocalization and Intracellular Trafficking

Caco-2 cells were seeded at 40,000 cells/cm² on collagen-coated 8-chamber slides. Slides were used when cells were 90% confluent, typically 4-5 days after seeding. Cells were washed with DPBS and then incubated in DPBS for 30 minutes at 37°C. Cells were treated with G3.5-OG (1 µM) or Transferrin-AF488 (250 µg/ml) for 30 minutes at

4°C to allow for attachment but not internalization (pulse). Subsequently, the cells were washed three times with ice cold DPBS to remove unbound ligand and incubated with warm DPBS at 37°C for 5, 15, or 30 minutes (chase) after which they were fixed with 4% paraformaldehyde, 4% sucrose in DPBS for 20 minutes. All subsequent steps were carried out at room temperature. The cells were washed twice with 25 mM glycine and then once with DPBS, permeabilized with 0.2% Triton X-100 in blocking solution (3% Bovine Serum Albumin (BSA)/DPBS) and then incubated with blocking solution to prevent non-specific binding. Primary antibodies for early endosomes (rabbit polyclonal early endosome antigen-1 (EEA-1)) and lysosomes (rabbit polyclonal lysosome-associated membrane protein 1 (LAMP-1)) (Molecular Probes, Carlsbad, CA) were added to separate chambers and incubated for one hour. The antibodies were removed, cells were washed three times with blocking solution and Alexa Fluor-568 goat anti-rabbit IgG (Molecular Probes, Carlsbad, CA) was added at 1:400 in blocking solution for one hour. The cells were then washed three times with DPBS, and incubated with 300 nM 4',6-diamidino-2-phenylindole (DAPI) 10 minutes to stain the nuclei. The cells were then washed once with DPBS, once with DI water and the chambers were removed. The slides were mounted, covered with glass coverslips, allowed to dry for a minimum of 2 hours before sealing and stored at 4°C prior to visualization.

Images were acquired using a Nikon Eclipse TE2000 inverted confocal laser scanning microscope (Nikon Instruments, Melville, NY). Excitation and emission wavelengths for DAPI, OG/ AF488 and AF568 were 405/450, 488/515 and 543/605, respectively. Four Z-stacks were obtained for each treatment using the following microscope settings: 60x oil objective, 2x optical zoom, 60 µm pinhole and 512 x 512

image size. Z-stacks contained 41, 0.5 μm slices to encompass the entire cell layer.

Detector gains were set to be constant between samples to facilitate sample comparison.

Colocalization between G3.5-OG or Transferrin-AF488 with early endosomes and lysosomes was quantified using Volocity 3D Imaging software (Improvision, Lexington, MA). The extent of colocalization between the green and red channels (M_x) was calculated by the software using the following equation:

$$M_x = \frac{\sum_i x_{i,coloc}}{\sum_i x_i} \quad (\text{Eq. 3.1})$$

where $x_{i,coloc}$ is the value of voxel i of the overlapped red and green components and x_i is the value of the green component. M_x is reported for each treatment as an average of the four regions. Transferrin-AF488 was used as an endocytosis control ligand to establish the validity of the assay methods for monitoring intracellular trafficking over time.

3.2.7 Transepithelial Transport

Caco-2 cells were seeded at 80,000 cells/cm² onto polycarbonate 12-well Transwell[®] filters of 0.4 μm mean pore size with 1.0 cm² surface area (Corning, Corning, NY). Caco-2 cells were maintained under standard incubation conditions where media was changed every other day and cells were used for transport experiments 21-25 days post-seeding. Prior to experiments, the transepithelial electrical resistance (TEER) of each monolayer was measured with an epithelial voltohmmeter (World Precision Instruments, Sarasota, FL). Monolayers with TEER > 600 $\Omega \cdot \text{cm}^2$ were used for assays. Cell monolayers were washed with HBSS and then incubated in the presence of HBSS or endocytosis inhibitors for 1 hour at 37°C. Inhibitors were used at concentrations that

showed a minimum of 85% cell viability during the 2-hour assay period. The solutions were removed and G3.5-OG (10 μ M) was added to the apical compartment in the presence of HBSS or endocytosis inhibitor and the corresponding solution was added to the basolateral compartment. After incubating for one hour, samples were taken from the basolateral compartment. Transport was quantified by measuring fluorescence in the basolateral compartment using a SpectraMax Gemini XS spectrofluorometer (Molecular Devices, Sunnyvale, CA) with excitation and emission wavelengths of 485 and 535 nm, respectively. Percent transport is reported comparing dendrimer transport in the presence of inhibitors to dendrimer transport in HBSS alone. The standard deviation for each reported value is calculated using propagation of error for the quotient of two experimentally determined values.

LY permeability was also monitored in the presence of HBSS and endocytosis inhibitors to ensure the integrity of the monolayers. LY apparent permeability was less than 1×10^{-6} for all conditions tested, which is within the accepted range of LY permeability for differentiated monolayers [166]. There was not a significant difference between LY permeability in the presence of HBSS or inhibitors, confirming that endocytosis inhibitors do not affect tight junctional integrity (data not shown).

3.2.8 Caco-2 Monolayer Visualization and Occludin Staining

After acquisition of samples for transport assays, Caco-2 cell monolayers were prepared for visualization by confocal microscopy. In particular, Caco-2 cell monolayers treated with G3.5-OG or HBSS in buffer or in the presence of dynasore were analyzed for occludin accessibility. The monolayers were washed twice with ice cold PBS, fixed,

permeabilized and blocked by the same procedures used in the immunofluorescence studies (Section 3.2.6). Subsequently, monolayers were treated with mouse anti-occludin (2 $\mu\text{g}/\text{ml}$) overnight at 4°C. The next day, the monolayers were washed twice with blocking solution and incubated with the same solution for 30 minutes. Alexa Fluor 568 goat anti-mouse IgG (1:400) was added in blocking solution for one hour. The cells were then washed and stained with DAPI. The membranes were carefully excised from the Transwell[®] supports using a scalpel, mounted on glass slides, covered with a glass coverslip and then sealed with clear nail polish. Slides were stored at 4°C prior to visualization.

Images were acquired using a Nikon Eclipse TE2000 inverted microscope using the same settings as described in Section 3.2.6. To visualize the G3.5 dendrimer interaction with the cell monolayer, Z-stacks were obtained with 51 0.5 μm slices using red, green and blue channels. To quantify occludin staining, four z-stacks were obtained per region, and only the red channel was used. Images were processed using Volocity software. Red voxels, corresponding to occludin staining, were quantified by thresholding the intensity between 20% and 100%. The number of red voxels was quantified for four z-stacks for each treatment. Results are reported as mean \pm standard deviation and statistical significance was determined by a one-way analysis of variance with Bonferroni post-hoc correction.

3.3 Results

3.3.1 Cytotoxicity of Endocytosis Inhibitors

Five endocytosis inhibitors were chosen to examine the pathways of cellular uptake and transepithelial transport of G3.5 PAMAM dendrimers. Before initiating uptake and transport studies, Caco-2 cell viability during the 2-hour assay time was confirmed in the presence of these inhibitors, whose concentrations were chosen based on literature reported values [163-165]. Inhibitors included chemicals known to prevent clathrin-mediated endocytosis (phenylarsine oxide (1-20 μM); monodansyl cadaverine (100-300 μM)), caveolin-mediated endocytosis (filipin (1-4 μM); genistein (100-300 μM)) and dynamin-dependent endocytosis (dynasore (40-80 μM)). We have shown previously that G3.5 dendrimers do not cause a reduction in Caco-2 cell viability up to 100 μM . Since the maximal dendrimer concentration used in these experiments was 25 μM , toxicity due to the dendrimers was not a concern.

Short-term cytotoxicity of endocytosis inhibitors was assessed by the WST-1 cell viability assay at 5 different concentrations in the reported range of each inhibitor (Table 3.1). 85% cell viability was chosen as the minimum allowable for use in uptake and transport assays. Monodansyl cadaverine and filipin did not show appreciable toxicity at any concentration tested and were used at their maximum reported concentrations of 300 μM and 4 μM , respectively. Phenylarsine oxide and genistein showed significant toxicity and were used at their lowest effective concentrations. Dynasore showed increasing toxicity over the range of concentrations tested, with the most acceptable (i.e. >85% viability) toxicity profile at 50 μM (Table 3.1).

Table 3.1. Endocytosis Inhibitor Concentration and % Cell Viability in Caco-2 Cells.

Endocytosis Inhibitors		Concentration (μ M)	% Cell Viability
<i>Clathrin Inhibiting</i>	Phenylarsine Oxide (PAO)	1	90.0 \pm 5.7%
	Monodansyl Cadaverine (MDC)	300	92.7 \pm 3.4%
<i>Caveolin Inhibiting</i>	Filipin (FIL)	4	95.9 \pm 2.7%
	Genistein (GEN)	100	86.7 \pm 2.9%
<i>Dynamin Inhibiting</i>	Dynasore (DYN)	50	106.1 \pm 5.0%

Results are reported as mean +/- standard deviation (n=4).

3.3.2 Cellular Uptake of G3.5-OG Dendrimers in the Presence of Endocytosis Inhibitors

As chemical inhibitors have varied effectiveness in different cell lines and can be somewhat non-specific, we took a multi-pronged approach, selecting one inhibitor for the general process of dynamin-dependent endocytosis and two inhibitors for distinct clathrin- and caveolin-mediated processes. In addition, we monitored the cellular uptake of transferrin and cholera toxin B, control ligands for clathrin- and caveolin-mediated endocytosis, respectively, to determine the efficacy and specificity of the selected inhibitors. Dynasore was used to block vesicular endocytosis by selectively inhibiting dynamin 1 and dynamin 2 GTPases, which are responsible for vesicle scission during both clathrin- and caveolin-mediated endocytosis [164]. Monodansyl cadaverine and phenylarsine oxide were used to block clathrin-mediated endocytosis. Monodansyl cadaverine is known to stabilize clathrin coated pits on the cell membrane, thereby preventing internalization [167]. Phenylarsine oxide has also been shown to inhibit clathrin endocytosis at low micromolar concentrations, but its mechanism is unknown [168, 169]. Filipin and genistein were selected to inhibit caveolin-mediated endocytosis. Filipin binds cholesterol and has been shown to disrupt caveolae-mediated endocytic pathways [170]. Genistein inhibits protein tyrosine kinases and, amongst other effects, has been shown to block internalization by caveolae [171]. The percent uptake relative to buffer control was calculated for G3.5 and control ligands in the presence of five endocytosis inhibitors (Table 3.2).

Table 3.2. Percent Uptake of G3.5-OG Dendrimers and Control Ligands in Caco-2 Cells in the Presence of Endocytosis Inhibitors.

Endocytosis Inhibitors		Percent Uptake		
		G3.5	Transferrin	Cholera Toxin B
<i>Clathrin Inhibiting</i>	Phenylarsine Oxide (PAO)	84.4 ± 0.6%	112.3 ± 1.5%	100.5 ± 4.0%
	Monodansyl Cadaverine (MDC)	57.8 ± 2.1%	65.6 ± 2.5%	61.8 ± 5.1%
<i>Caveolin Inhibiting</i>	Filipin (FIL)	81.0 ± 0.2%	110.2 ± 0.1%	114.4 ± 3.4%
	Genistein (GEN)	22.4 ± 0.7%	69.8 ± 2.4%	20.4 ± 0.7%
<i>Dynamin Inhibiting</i>	Dynasore (DYN)	20.4 ± 3.5%	15.0 ± 2.7%	57.1 ± 19.6%

Results are reported as mean +/- standard deviation (n=2).

G3.5 PAMAM dendrimers show reduction in cellular uptake in the presence of all endocytosis inhibitors tested, suggesting the involvement of both clathrin- and caveolin-mediated endocytosis pathways in dendrimer cellular uptake. As expected, dendrimers showed the greatest reduction in uptake in the presence of dynasore, a selective chemical inhibitor of dynamin, a protein integral to the hallmark event of vesicle pinching from the plasma membrane during receptor-mediated endocytosis. The significant decrease in uptake of dendrimers and control ligands in the presence of dynasore confirms the endocytosis of G3.5 PAMAM dendrimers by dynamin-dependent pathways. Dendrimers showed decreased uptake in the presence of both clathrin inhibitors, with a greater decrease seen in the presence of monodansyl cadaverine. Transferrin uptake was not reduced in the presence of phenylarsine oxide, indicating that this is not an effective clathrin-endocytosis inhibitor in Caco-2 cells at the concentration used and the decrease in dendrimer uptake may be due to a non-specific effect. Alternatively, dendrimer trafficking may be more sensitive to phenylarsine oxide compared to transferrin, which is affected only at higher phenylarsine oxide concentrations. In contrast, transferrin shows reduced uptake in the presence of monodansyl cadaverine, illustrating the efficacy of monodansyl cadaverine in Caco-2 cells. Cholera toxin B also shows reduced uptake in the presence of monodansyl cadaverine, but this decrease in uptake was expected since cholera toxin B can be endocytosed by clathrin- and caveolin-mediated pathways in Caco-2 cells [172]. Dendrimers also showed reduced uptake in the presence of both caveolin inhibitors, markedly seen with genistein; however, filipin did not reduce uptake of cholera toxin B, and this may represent a cell-specific effect. While genistein reduces the uptake of transferrin, it reduces the uptake of cholera toxin B to a much larger extent,

making it an effective and relatively specific inhibitor of caveolin-mediated endocytosis. The most effective and specific inhibitors (monodansyl cadaverine, genistein and dynasore) were chosen for further investigation in transport assays.

3.3.3 Intracellular Trafficking

In addition to determining the mechanism of dendrimer uptake, we investigated the intracellular trafficking of G3.5 PAMAM dendrimers in Caco-2 cells. Dendrimers colocalized with early endosomes (EEA-1) and lysosomes (LAMP-1) over time (Figure 3.1). Transferrin trafficking (Figure 3.2), which has been well-characterized in this cell line, was used as a control for the study [18]. Sample confocal images from each treatment and time point are included in Appendix 1. Five minutes after incubation, dendrimers showed initial localization in the early endosomes and lysosomes. By 15 minutes, however, they showed increasing localization in the lysosomes, indicating quick trafficking to these cellular compartments. Interestingly, at 30 minutes, the level of accumulation in the lysosomes remained unchanged, while their presence in endosomes increased. This suggests that the trafficking pathway was saturated, causing dendrimer retention in early endosomes once lysosomes were occupied. In contrast, transferrin showed almost constant presence in the early endosomes with increasing presence in the lysosomes over time. This is typical of transferrin, a classical ligand for clathrin-mediated endocytosis known to accumulate in the early endosomes, confirming the validity of the assay methods.

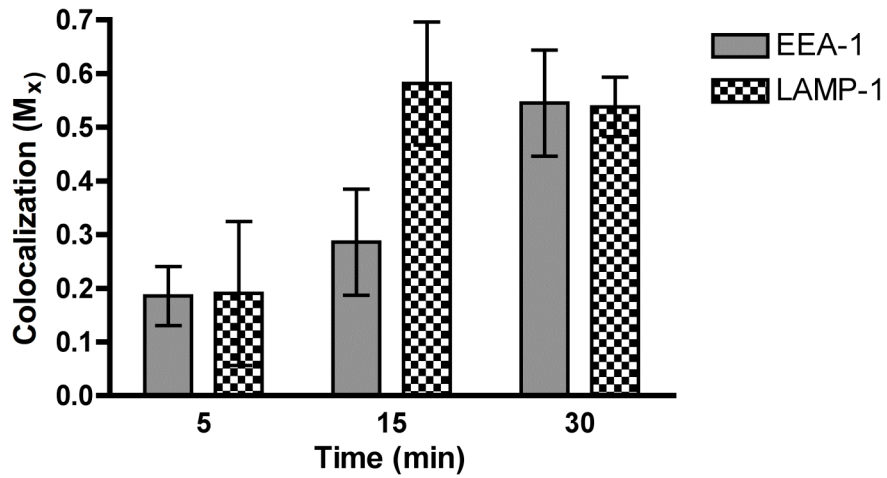


Figure 3.1. Intracellular Trafficking of G3.5-OG Dendrimers over Time in Caco-2 Cells. Colocalization (M_x) with early endosomes (EEA-1) and lysosomes (LAMP-1) is shown. Results are reported as mean \pm standard deviation (n=4).

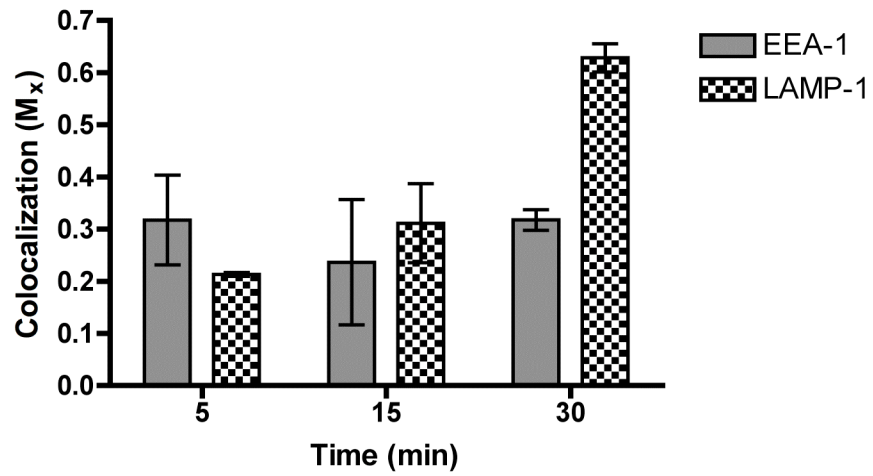


Figure 3.2. Intracellular Trafficking of Transferrin-AF488 over Time in Caco-2 Cells. Colocalization (M_x) with early endosomes (EEA-1) and lysosomes (LAMP-1) is shown. Results are reported as mean +/- standard deviation (n=4).

3.3.4 Transepithelial Transport of G3.5-OG Dendrimers in the Presence of Endocytosis Inhibitors

Transepithelial transport of G3.5-OG dendrimers was monitored in the presence of endocytosis inhibitors and at 4°C and compared to transport in buffer at 37°C (Figure 3.3). Transport of PAMAM G3.5 was significantly reduced at 4°C, illustrating strong energy dependence. Similar to Caco-2 uptake studies, transport was also reduced in the presence of dynasore and monodansyl cadaverine, indicating the importance of dynamin-dependent and clathrin-mediated endocytosis mechanisms in transepithelial transport. However, contrary to its effect on cellular uptake of dendrimers (Table 3.2), genistein does not significantly impact dendrimer transport across Caco-2 monolayers, suggesting that caveolin-mediated endocytosis may not play a significant role in this process. It has been suggested that fully differentiated Caco-2 cells lack caveolae [172], opening the possibility that, while caveolae play an important role in dendrimer endocytosis in undifferentiated Caco-2 cells, they are less important in dendrimer transepithelial transport because of their lower expression in differentiated enterocytes.

3.3.5 Visualization of G3.5-OG Dendrimer Interaction with Caco-2 Cell Monolayers

After cell monolayers were used for transport assays, they were fixed and stained for occludin and nuclear DNA. By excising the stained membranes from the Transwell[®] supports, we were able to visualize the dendrimer interacting with differentiated Caco-2 cell monolayers. Although there have been many studies documenting dendrimer interaction with Caco-2 cells grown on microscope slides [18], this is the first to show

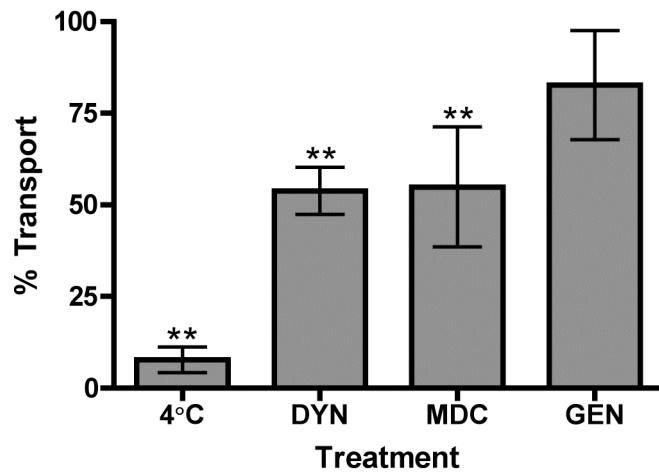


Figure 3.3. Percent Transport of G3.5-OG Dendrimers across Caco-2 Monolayers in the Presence of Endocytosis Inhibitors or at 4°C. Results are reported as mean +/- standard deviation (n=4). ** indicates a significant difference ($p < 0.01$) from 100% transport (buffer alone).

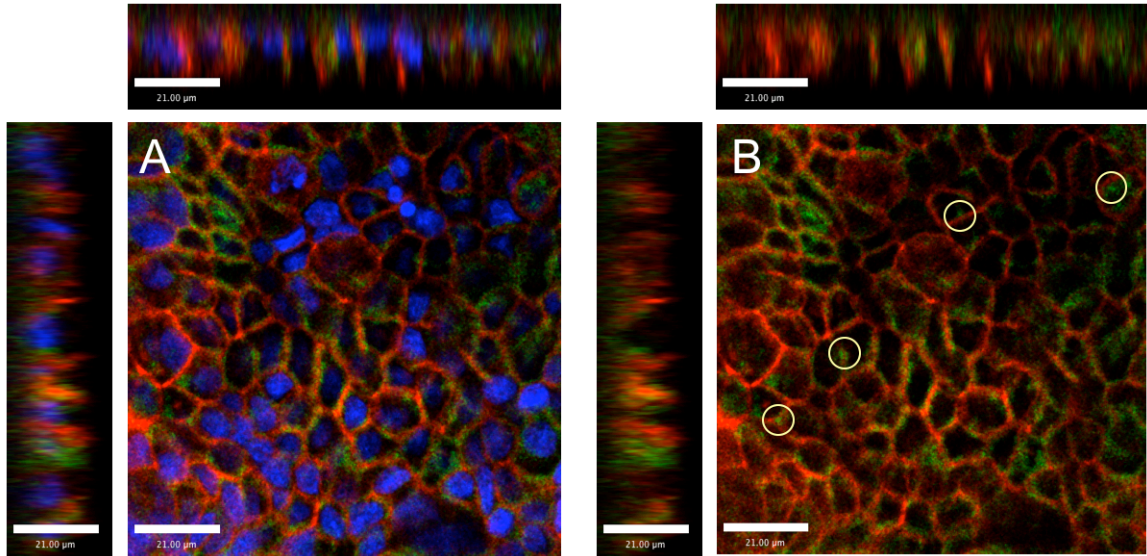


Figure 3.4. Visualization of G3.5-OG Dendrimer Interaction with Caco-2 Monolayers. Dendrimers are localized inside cell monolayers but avoid the nucleus (A) and small vesicles of G3.5 dendrimers (circled) can be seen interacting with cells (B). Scale bar = 21 μm .

interaction with fully differentiated and confluent monolayers. Figure 3.4 shows a representative image of the cell monolayer. The nuclear staining was omitted from Figure 3.4 B to allow for easier visualization of the dendrimer and tight junctions. In both figures, dendrimer staining is observed inside the confluent cells, confirming internalization. In addition, there are punctate regions strongly resembling vesicles (circled in Figure 3.4 B), which confirm the involvement of vesicular endocytosis in dendrimer transepithelial transport. Finally, dendrimers cannot be detected in the nuclear region of the cell, confirming their localization in the cell interior and without further trafficking into the cell nucleus. These images serve as complementary evidence of the importance of the transcellular pathway in dendrimer transport.

3.3.6 Occludin Staining in Presence of Dendrimers with and without Dynasore Treatment

Increased occludin staining is a well-established indicator for tight junctional opening in Caco-2 cell monolayers and has shown strong correlation with reduction in TEER and increase in paracellular marker permeability [173]. Previous studies have shown that monolayers treated with dendrimers showed increased occludin staining relative to cells treated with HBSS alone, indicating that dendrimers open tight junctions [15]. We examined occludin accessibility in Caco-2 cell monolayers treated with dendrimers or HBSS in the presence of dynasore or buffer alone (Figures 3.5 and 3.6). In cells treated with buffer, dendrimers significantly increased occludin staining relative to untreated cells, indicating tight junction opening (Figure 3.5 A,B). In contrast, in cells treated with dynasore, no difference could be detected in occludin staining between cells

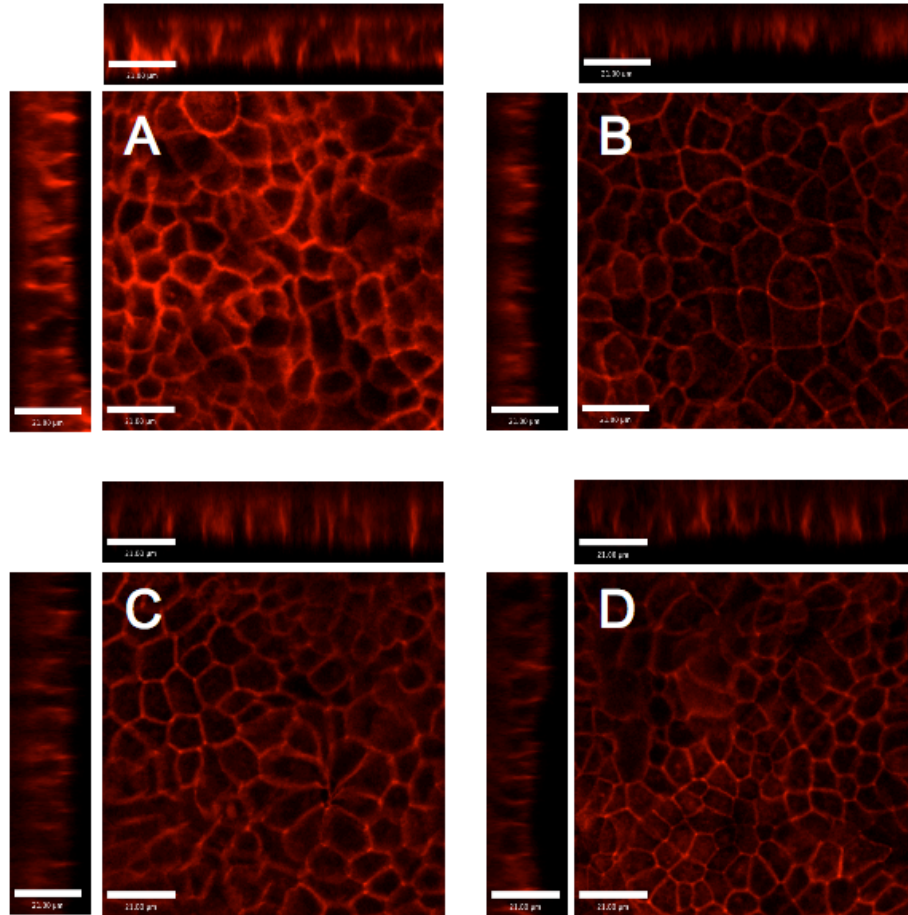


Figure 3.5. Occludin Staining in the Presence and Absence of G3.5-OG Dendrimers in Caco-2 Cells Treated with HBSS or Dynasore. A) G3.5/ HBSS, B) HBSS only C) G3.5/Dynasore and D) Dynasore only. Main panels illustrate the xy plane; horizontal bars illustrate the xz plane; vertical bars illustrate the yz plane. Scale bars equal 21 μm .

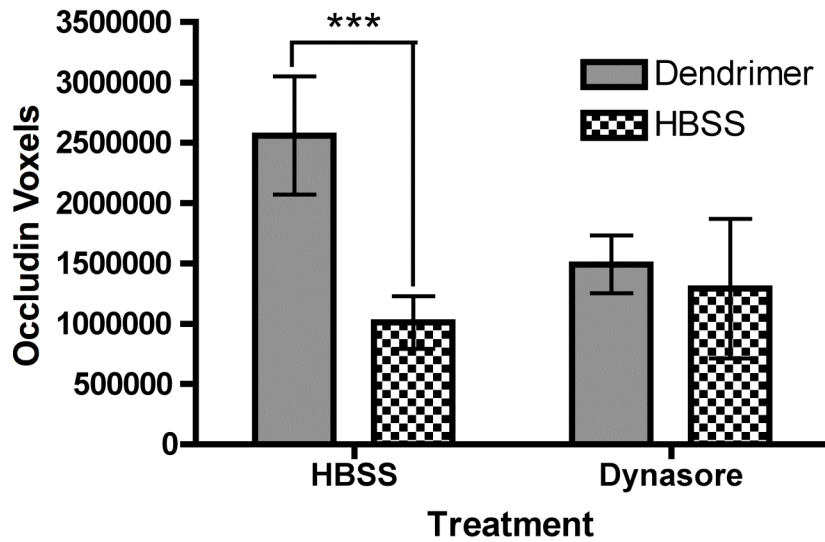


Figure 3.6. Quantification of Occludin Staining. Cells treated with G3.5-OG dendrimers in the presence of HBSS show a significant increase in occludin staining from untreated cells. (***) indicates $p < 0.001$. Cells treated with dendrimer in the presence of dynasore do not show a significant change in occludin staining relative to the control. Results are reported as mean \pm standard deviation ($n=4$).

treated with dendrimers or dynasore alone (Figure 3.5 C,D). This illustrates that dendrimers are unable to open tight junctions in cells where dynamin-dependent endocytosis is inhibited, suggesting that dendrimers must first be internalized to modulate cellular tight junctions.

Two major mechanisms have been established for opening tight junctions: depletion of divalent cations and disruption of intracellular tight junctional components. Disodium ethylenediaminetetraacetate, a calcium chelator, and polyoxyethylene, a surfactant, both lower extracellular calcium levels, causing dissociation of tight junctions [55]. Other compounds such as sodium caprate increase tight junctional opening by initiating a biochemical signaling cascade which results in the contraction of actin microfilaments, effectively dilating the intracellular tight junctions [55]. While it is possible that dendrimers interact with the tight junctions in multiple ways, it is clear that prevention of dendrimer endocytosis reduces both transcellular and paracellular transport, suggesting that dendrimer endocytosis is at least in part responsible for tight junction modulation. Dendrimers are most likely acting on intracellular cytoskeleton components to induce tight junction opening.

3.4 Discussion

PAMAM dendrimers have shown promise as oral drug delivery carriers due to their ability to translocate across the epithelial layer of the gut, taking poorly-bioavailable drug cargo in tow [150]. While many studies have suggested that dendrimers transiently open tight junctions and are transported through the intestinal barrier by transcellular and paracellular pathways [16, 19, 148], the details of these processes are poorly understood.

In order to design dendrimers as oral drug delivery carriers, it is critical to know the detailed mechanisms of their cellular entry, trafficking, transport and interaction with cellular tight junctions. In this Chapter, we have uncovered some of the details of anionic dendrimer transport, which can have significant implications for oral drug delivery.

Caco-2 cellular uptake of G3.5 dendrimers was found to occur primarily through dynamin-dependent endocytosis pathways, specifically clathrin- and caveolin-mediated endocytosis. Previous reports have suggested the involvement of clathrin in dendrimer endocytosis [18]. The present study confirms, for the first time, the involvement of caveolin-mediated endocytosis in dendrimer internalization. This suggests that dendrimers are not relegated to a single means of cellular entry, but instead take advantage of several specific endocytosis pathways. This has significant implications for drug delivery, as intracellular trafficking is largely dependent on initial pathway of cell entry. Therefore, it is to be expected that a portion of dendrimer dose applied to enterocytes will be trafficked to the lysosomes by the clathrin-mediated endocytosis pathway, while the dendrimers that enter via the caveolae may end up in the cell cytosol, allowing them to be targeted to either compartment depending on the desired effect.

Dendrimer transport across differentiated Caco-2 cell monolayers was found to be dependent on dynamin- and clathrin-mediated endocytosis, but independent of caveolin-mediated endocytosis. This result was expected since fully differentiated Caco-2 cells lack caveolae. The differences between dendrimer transport across differentiated epithelial cells and uptake in undifferentiated cells can be potentially exploited by drug delivery strategies that aim to specifically target cancer cells while simultaneously

avoiding intestinal cells by designing linkers that would be cleaved in caveolae-mediated transport pathways.

Intracellular trafficking studies shed further light on the environments that dendrimers encounter after cellular internalization. Kitchens and co-workers [18] examined G1.5 and G2 dendrimer colocalization with endosomal and lysosomal markers in Caco-2 cells and reported that dendrimers show constant presence in the early endosomes at 20 and 60 minutes, with time-dependent trafficking to the lysosomes. In this study G3.5 dendrimers were found to localize in the early endosomes and lysosomes after 5 minutes, displayed fast trafficking to the lysosomes after 15 minutes and increased endosomal and lysosomal accumulation at 30 minutes, likely due to pathway saturation. Often drugs are conjugated to dendrimers via pH-sensitive linkers that are cleaved in the acidic environment of mature endosomes or peptide linkers that are cleaved by lysosomal enzymes such as cathepsin B [174]. These intracellular trafficking studies corroborate the validity of such strategies, as dendrimers can be found in both environments following cellular internalization. Cleavage of pH-sensitive linkers in the endosomes may be promising as dendrimers are shown to accumulate in these compartments over time. Knowledge of the cellular uptake and intracellular trafficking pathways of dendrimers can have significant impact on designing them for use as drug delivery vehicles. In the context of oral drug delivery, knowledge of subcellular localization in intestinal cells can enable design of conjugates that are robust in these compartments and absorbed intact to the blood stream.

One of the most intriguing attributes of PAMAM dendrimers is that within a specified size and charge window, they have been shown to catalyze their own transport

via the paracellular pathway [16]. Previous reports have shown that dendrimers decrease TEER, increase paracellular marker flux (e.g. mannitol) and increase occludin accessibility in Caco-2 cells, confirming that they open tight junctions [16, 145, 146]. However the mechanism behind this phenomenon remained largely elusive. In this Chapter we examined the role of dendrimer cellular internalization on tight junction opening by monitoring the effects of dendrimers on confluent monolayers in buffer or in the presence of dynasore. While dendrimers were able to open tight junctions in the presence of buffer alone, they could not do so in the presence of dynasore, suggesting that dendrimer internalization is requisite for tight junction opening. This has significant implications for oral delivery using dendrimers because it shows that tight junction opening is at least in part modulated by dendrimers *within* the cells. Whether affecting tight junctional structures from the apical environment *outside* the cells by dendrimers also plays a role remains to be examined. Therefore, this mechanism (opening tight junction by internalization) results in temporary tight junction opening, which is consistent with our previous reports that TEER returns to pre-treatment values after 24 hours [149]. Taken together, these data establish that dendrimers can be used safely as oral drug carriers or penetration enhancers since depending on generation, concentration and incubation time their effects on tight junctions can be transient, not permanent. Figure 3.7 summarizes some of the possible G3.5 transport pathways across Caco-2 cell monolayers.

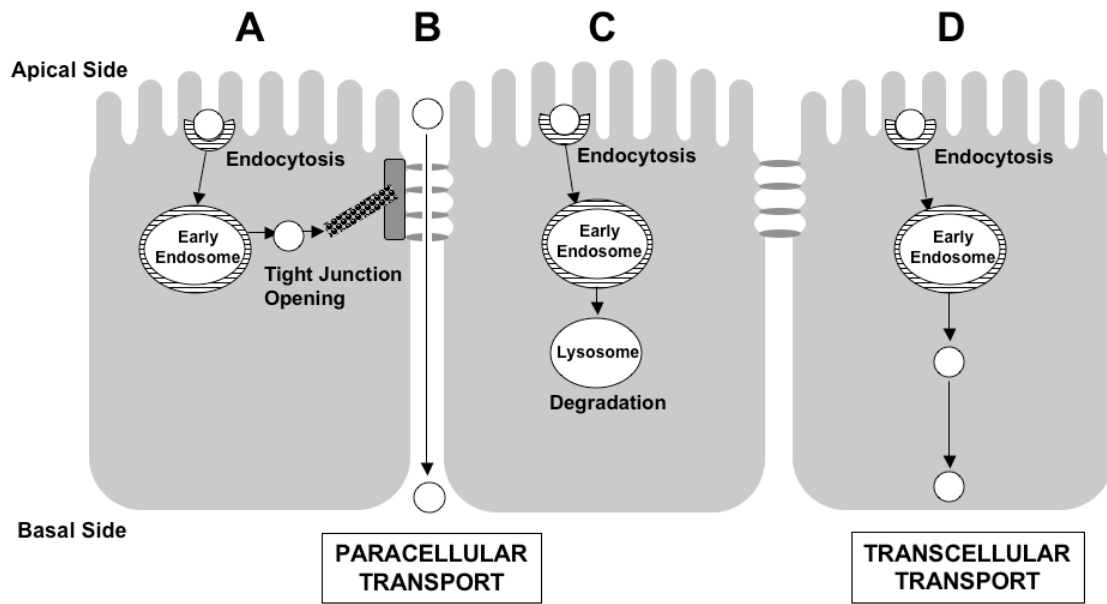


Figure 3.7. Mechanisms of Dendrimer Transport Across Caco-2 Cell Monolayers.

Once endocytosed, dendrimers can interact with tight junctions (A), allowing for paracellular transport (B), or they can be degraded by the lysosomes (C) or transcytosed (D).

3.5 Conclusion

In this Chapter we described the detailed mechanisms of cellular uptake, intracellular trafficking, transport and tight junction modulation of G3.5 PAMAM dendrimers in Caco-2 cells. We found that G3.5 PAMAM dendrimers enter undifferentiated Caco-2 cells by clathrin-, caveolin-, and dynamin-dependent pathways but that their transepithelial transport across confluent monolayers is governed by clathrin- and dynamin-dependent pathways only. Dendrimers were quickly trafficked to the lysosomes, but show increased endosomal accumulation once the lysosomal compartments become saturated. Finally, it was demonstrated that dendrimer endocytosis promotes tight junction opening, illustrating the interconnected nature of the transcellular and paracellular pathways in dendrimer transepithelial transport. Knowledge of detailed mechanisms of dendrimer cellular uptake, intracellular and transepithelial transport will assist in the design of PAMAM dendrimer-based oral drug delivery strategies by providing appropriate linker chemistry consistent with transepithelial transport and cellular trafficking pathways.

Chapter 4 : G3.5 PAMAM Dendrimers Enhance Transepithelial Transport of SN38 While Minimizing Gastrointestinal Toxicity

4.1 Introduction

Polymer-based drug delivery systems have shown promise due to their ability to improve the efficacy of traditional drugs [6]. Conjugation of small molecule therapeutics to a polymeric carrier can enhance the drug's solubility, increase accumulation at the target site and minimize non-specific toxicity. Because chemotherapy drugs are often plagued by poor water solubility and dose-limiting toxicities, they are promising candidates for polymeric drug delivery strategies. Attachment of chemotherapy drugs to water soluble polymers enhances solubility, allows for accumulation of the polymer-drug conjugate at the tumor site due to the enhanced permeability and retention effect, improves efficacy and reduces side effects [1]. Several polymer-drug conjugates using N-(2-hydroxypropyl)methacrylamide (HPMA) and poly (ethylene glycol) (PEG) as carriers are currently being evaluated in clinical trials [38, 44].

While conjugation of chemotherapy drugs to water-soluble polymers can improve their solubility and tumor uptake, the large size of these macromolecular constructs necessitates intravenous administration. Oral administration is typically limited to small, lipophilic drugs that can permeate the cell membrane, small, hydrophilic drugs that pass through the tight junctions or drugs that are substrates for intestinal transporters [175]. Studies have shown that compared to intravenous administration, oral chemotherapy is the preferred method of administration by cancer patients given similar efficacy for both

treatments [7]. Therefore, the combination of the distinct therapeutic advantages of polymer-drug conjugates with strong patient preference and lower costs of oral chemotherapy supports a significant need for orally bioavailable polymer therapeutics.

Because of its low water solubility and poor bioavailability, SN38 (7-ethyl-10-hydroxy-camptothecin), a potent topoisomerase-1 poison used to treat colorectal cancer and hepatic metastases, is an ideal candidate for polymeric delivery strategies [158]. While SN38 shows 100-1000-fold higher activity than CPT-11 *in vitro*, its use is limited by low water solubility and significant intestinal toxicity including diarrhea [176, 177]. Conjugation of SN38 to PAMAM dendrimers has the potential to allow for oral administration while also improving water solubility and minimizing gastrointestinal toxicity. Synthesis, characterization, and bioactivity of G3.5 PAMAM-SN38 conjugates against colorectal carcinoma cell lines has been previously established [161]. To successfully advance these systems for oral administration, their stability in the gastrointestinal tract and transport across the epithelial barrier of the gut must be determined. In this Chapter we examine G3.5 PAMAM-SN38 conjugates for their *in vitro* release profiles, cytotoxicity against Caco-2 and HT-29 colorectal cancer cells, cellular uptake, and transepithelial transport across Caco-2 monolayers as models of the intestinal epithelial barrier.

4.2 Materials and Methods

4.2.1 Materials

PAMAM G3.5 dendrimers (reported molecular weight=12,931), lucifer yellow CH dipotassium salt (LY), pepsin from porcine gastric mucosa, pancreatin from porcine

pancreas and carboxylesterase from rabbit liver were purchased from Sigma Aldrich (St. Louis, MO). Simulated Intestinal Fluid (SIF) and Simulated Gastric Fluid (SGF) were obtained from Ricca Chemical Company (Arlington, Texas). 7-ethyl-10-hydroxy camptothecin (SN38) was obtained from AK Scientific Company (Mountain View, CA). WST-1 cell proliferation reagent was purchased from Roche Applied Sciences (Indianapolis, IN). Caco-2 cells and HT-29 cells were obtained from American Type Cell Culture (Rockville, MD).

4.2.2 Synthesis and Characterization of G3.5-Gly-SN38 and G3.5-βAla-SN38 Conjugates

G3.5-Gly-SN38 and G3.5-βAla-SN38 were synthesized as previously described [161]. Briefly, SN38 was modified at the 20-OH position via an ester linker with glycine or β-alanine [178]. The modified SN38 molecules were then conjugated to carboxylic acid-terminated G3.5 dendrimers using EDC / NHS as a coupling agent. The products were dialyzed against distilled water using 3,500 MWCO membranes to remove low molecular weight impurities and further purified using preparative fast protein liquid chromatography (FPLC). ¹H NMR was used to quantify the number of SN38 molecules per dendrimer by comparing the area of the dendrimer protons between 2.1 and 3.8 ppm with the methyl protons of SN38 between 0.9-1.1 ppm. The drug loading per dendrimer was 2.9 and 4 for G3.5-Gly-SN38 and G3.5-βAla-SN38, respectively. Figure 4.1 illustrates the conjugation strategy used to synthesize G3.5-Gly-SN38 and G3.5-βAla-SN38.

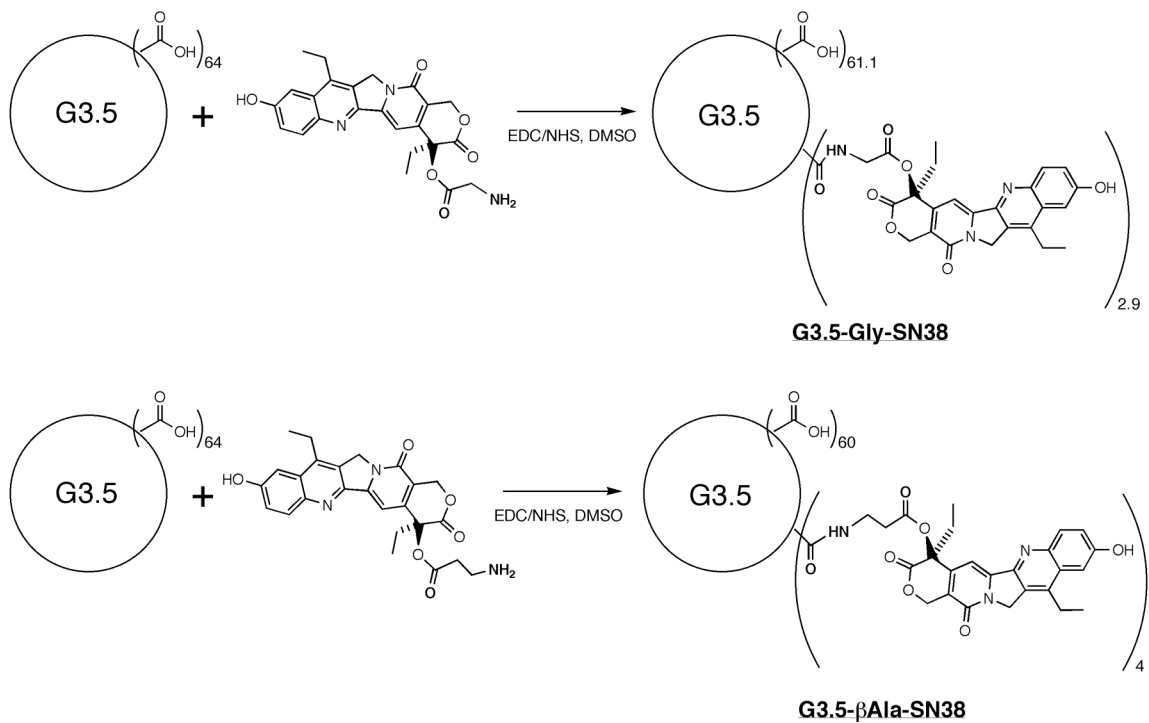


Figure 4.1. Conjugation of SN38 to G3.5 Dendrimers via Glycine and β-Alanine Linkers. (Adapted from [161]).

4.2.3 Stability Studies

G3.5-Gly-SN38 and G3.5- β Ala-SN38 conjugates were prepared at 0.15 and 0.10 mg/ml respectively in the release buffer of interest and incubated at 37°C with rotation in glass vials. Release buffers included SGF with and without 0.32% w/v pepsin [179], SIF with and without 1% w/v pancreatin [179] and PBS with and without carboxylesterase (17.3 IU/ml) [180]. Release in gastric conditions was monitored for up to 6 hours and in the intestinal conditions for up to 24 hours, mimicking the expected residence time in each of these compartments [49]. Enzyme activity was confirmed at each time point using bovine serum albumin [181], Z-Arg-AMC [182] and p-nitrophenol acetate [183] as model substrates for pepsin, pancreatin and carboxylesterase, respectively.

During the release experiment, 100 μ L of sample was taken at each time point and added to an additional 400 μ L of release buffer. Released SN38 was separated from G3.5-SN38 conjugate by passing the sample through a 3,000 MWCO Amicon Ultra 0.5 centrifugal concentrator (Millipore, Billerica, MA) by centrifuging at 14,000 x g for 30 minutes. Amicon concentrators were pre-treated with 5% v/v Triton X-100 to minimize non-specific binding as per the manufacturer's instructions. SN38 is known to exist in a pH-dependent equilibrium between a closed ring lactone form and an open ring carboxylate form, with the lactone form favored at low pH [157]. For SIF and PBS, 350 μ L of the filtrate was taken and acidified to pH 2 with the addition of an appropriate volume of 1 N HCl and subsequently incubated at 37°C for 1 hour to convert SN38 to the lactone form. This acidification step was omitted for SGF since it is at a pH of 1-2. Next, the acidified SN38 was extracted by adding 200 μ L of acetonitrile followed by 200 μ L of chloroform. The solution was vortexed and centrifuged at 250 x g for 2 minutes to

separate the layers. The organic layer was isolated, the chloroform addition was repeated two more times, and the organic extracts were pooled. The extracts were then dried under nitrogen gas, redissolved in 70 μ L of 50/50 DMSO/0.1N HCl and then measured by high pressure liquid chromatography (HPLC).

SN38 was quantified by HPLC using a system containing a Waters 1525 Binary Pump, Waters 717plus Autosampler and Waters 2487 dual wavelength UV detector (Waters Corporation, Milford, MA) set at 375 nm with a Phenomenex C18 column (250 x 4.6 mm, 5 μ m) (Phenomenex, Torrance, CA). A gradient method with methanol and water with 0.1% TFA was used with a total flow rate of 1 ml per minute and an injection volume of 20 μ L. A calibration curve using the peak area versus concentration was generated for each release buffer by extracting known concentrations of SN38. Detailed HPLC methods and standard curves are included in Appendix 2. Extraction efficiencies comparing extracted standards to direct injection of SN38 standards were found to be 86%, 91%, 75%, 80%, 70% and 83% in SGF, SGF/ pepsin, SIF, SIF/ pancreatin, PBS, and PBS/ carboxylesterase, respectively, and were time and concentration-independent.

4.2.4 Cell Culture

Caco-2 cells (passages 20-40) were cultured as described in Section 3.2.3. HT-29 cells (passages 130-140) were cultured under the same incubation conditions as Caco-2 cells using McCoy's 5A media supplemented with 10% fetal bovine serum (FBS), 1% non-essential amino acids, 10,000 units/mL penicillin, 10,000 μ g/mL streptomycin and 25 μ g/mL amphotericin B.

4.2.5 Potential Short-Term Cytotoxicity of G3.5-SN38 Conjugates

Potential short-term cytotoxicity of G3.5-SN38 conjugates was assessed in Caco-2 cells to ensure cell viability during uptake and transport assays. Unmodified G3.5 dendrimers, G3.5-Gly-SN38 and G3.5- β Ala-SN38 were prepared at 10 and 100 μ M in HBSS transport buffer. SN38 was prepared as a concentrated stock in DMSO at 40,000 μ M and used to make solutions in HBSS at 4, 40, and 400 μ M. Cytotoxicity was assessed by the water soluble tetrazolium salt (WST-1) assay as described in Section 3.2.4. HBSS was used as a negative control for 100% cell viability and 0.01% Triton X-100 was used as a positive control. UV absorbance of G3.5-SN38 conjugates alone was also assessed to confirm that SN38 absorbance did not interfere with the cell viability dye (data not shown).

4.2.6 Potential Delayed Cytotoxicity of G3.5-SN38 Conjugates

Potential delayed cytotoxicity of G3.5-SN38 conjugates was assessed in Caco-2 cells by measuring cell viability 24 hours post-exposure. Cell viability 24 hours after short-term exposure mimics the potential long-term effects of the conjugates on the intestinal cells that may not be apparent when cell viability is measured immediately post-treatment. Caco-2 cells were prepared and treated the same as in Section 4.2.5. After the 2-hour exposure, the cells were washed twice with HBSS and incubated with 100 μ L of cell culture media for an additional 24 hours. The WST-1 assay was used to assess the cell viability 24 hours later, with HBSS used as a negative control for 100% cell viability and 0.01% Triton X-100 as a positive control.

4.2.7 Transepithelial Transport

Caco-2 cell monolayers were grown as described in Section 3.2.7. Monolayers were washed with HBSS and then 0.5 ml of 10 or 100 μM G3.5-Gly-SN38, G3.5- βAla -SN38 or 4 μM SN38 was added to the apical compartment and 1.5 ml HBSS was added to the basolateral compartment. After a 2-hour incubation, samples were taken from the basolateral compartment. Transport was quantified by measuring fluorescence in the basolateral compartment using a SpectraMax Gemini XS spectrofluorometer (Molecular Devices, Sunnyvale, CA) with excitation and emission wavelengths of 375 and 550 nm, respectively, and compared to fluorescence standard curves for each conjugate and free SN38. Presence of free SN38 in the basolateral compartment of monolayers treated with G3.5-SN38 conjugates was determined by the extraction methods described in Section 4.2.3. Equivalent SN38 flux was calculated by multiplying the measured molar flux of the conjugates with the number of SN38 molecules per dendrimer. Apical to basolateral flux is reported as the average of four replicates. Statistical significance was determined by analysis of variance followed by Tukey's multiple comparison test. LY permeability was also monitored in the presence of HBSS to ensure the integrity of the monolayers. LY apparent permeability was less than 1×10^{-6} cm/s, which is within the accepted range of LY permeability for differentiated monolayers (data not shown).

4.2.8 Cellular Uptake

Cellular uptake of G3.5-SN38 conjugates and free SN38 was assessed in differentiated Caco-2 monolayers. After the transport assay, the cells were washed twice with HBSS. 300 μl of 0.1% Triton X-100 was added to the apical side of each well and

incubated for 2 hours at 37°C to solubilize the cells. The cells were then removed from the Transwell[®] by pipette and transferred to a microcentrifuge tube. The cell debris was removed by centrifugation at 1000 RPM for 5 minutes. 100 µl of the clear supernatant was taken and the uptake of G3.5-SN38 conjugates and SN38 was quantified by fluorescence with excitation at 375 nm and emission at 550 nm as described in Section 4.2.7. Presence of free SN38 in the cellular compartment was determined by the extraction methods described in Section 4.2.3. Uptake is reported as an average of four replicates and normalized to total protein as determined by the Bradford Protein Assay (Bio-Rad, Hercules, CA). Statistical significance was determined by analysis of variance followed by Tukey's multiple comparison test.

4.2.9 IC₅₀ in HT-29 Cells

The IC₅₀ values of G3.5-SN38 conjugates and free SN38 were determined in HT-29 cells to assess the efficacy of the conjugates in colorectal cancer cells compared to the free drug. HT-29 cells were seeded at 2,500 cells/ per well in 96 well cell culture plates and incubated at 37°C for 24 hours. After 24 hours, the cells were treated with different concentrations of SN38, G3.5-Gly-SN38 and G3.5-βAla-SN38 in media and incubated for an additional 48 hours. Cells were also treated with comparable concentrations of G3.5 dendrimer alone to ensure that the carrier did not cause any long-term cytotoxicity. After 48 hours, the media was aspirated by pipette, the cells were washed with HBSS buffer and the WST-1 assay was used to assess cell viability. Cell viability was determined by the % absorbance relative to the control cells, which were treated with

media alone. GraphPad Prism software (La Jolla, CA) was used to generate the IC₅₀ curves and values using the sigmoidal dose-response non-linear curve fitting routine.

4.3 Results

4.3.1 Stability of G3.5-SN38 Conjugates

Stability of G3.5-SN38 conjugates in simulated gastric, intestinal and liver carboxylesterase conditions was assessed to determine the suitability of these conjugates for oral delivery of SN38 for the treatment of colorectal cancer hepatic metastases. In particular, stability of the conjugates was monitored in the presence of SGF with and without pepsin (Figure 4.2), SIF with and without pancreatin (Figure 4.3) and PBS with and without carboxylesterase (Figure 4.4).

Both G3.5-Gly-SN38 and G3.5-βAla-SN38 showed little to no release of free SN38 in the gastric environment (Figure 4.2). G3.5-βAla-SN38 did not release more than 0.5% SN38 during 6 hours in SGF with or without pepsin. In contrast, G3.5-Gly-SN38 showed a burst release of SN38 after 1 hour in SGF with and without pepsin and ultimately released approximately 9% in SGF with pepsin and 6% in SGF without pepsin. This small amount of gastric release could be prevented by use of enteric coating. These studies illustrate that although G3.5-Gly-SN38 released more SN38 than G3.5-βAla-SN38 in the gastric environment, they were both relatively stable in acidic conditions and were not substrates for pepsin.

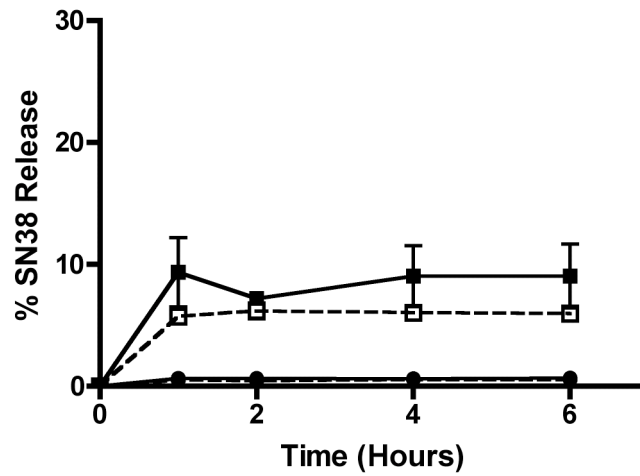


Figure 4.2. Stability of G3.5-Gly-SN38 and G3.5-βAla-SN38 Conjugates in Simulated Stomach Conditions for 6 hours. Results are reported as mean +/- standard deviation (n=2). G3.5-Gly-SN38 is represented by squares and G3.5-βAla-SN38 is represented by circles. Release in SGF with 0.32% w/v pepsin is depicted by solid lines with filled symbols, and release in SGF alone is depicted by dashed lines with open symbols.

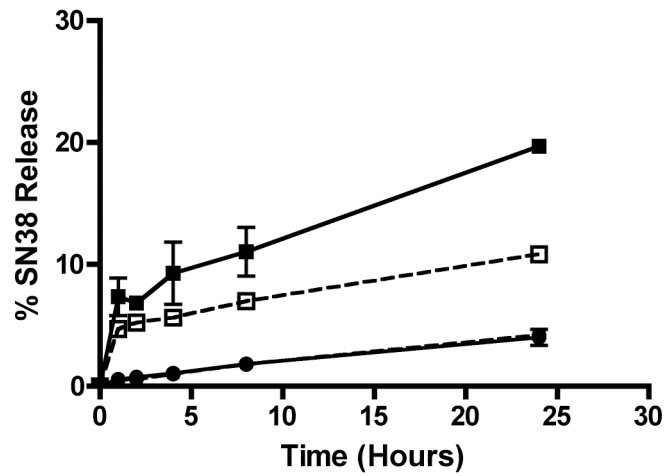


Figure 4.3. Stability of G3.5-Gly-SN38 and G3.5-βAla-SN38 Conjugates in Simulated Intestinal Conditions for 24 hours. Results are reported as mean +/- standard deviation (n=2). G3.5-Gly-SN38 is represented by squares and G3.5-βAla-SN38 is represented by circles. Release in SIF with 1% w/v pancreatin is depicted by solid lines with filled symbols, and release in SIF alone is depicted by dashed lines with open symbols.

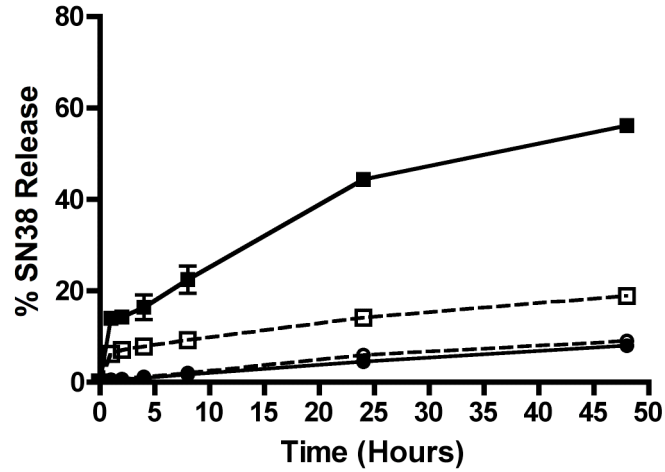


Figure 4.4. Stability of G3.5-Gly-SN38 and G3.5-βAla-SN38 Conjugates in Simulated Liver Conditions for 48 hours. Results are reported as mean +/- standard deviation (n=2). G3.5-Gly-SN38 is represented by squares and G3.5-βAla-SN38 is represented by circles. Release in PBS with carboxylesterase (17.3 IU/ml) is depicted by solid lines with filled symbols, and release in PBS alone is depicted by dashed lines with open symbols.

In comparison to SGF, G3.5-SN38 conjugates showed increased susceptibility for free drug release in the presence of SIF (Figure 4.3). G3.5- β Ala-SN38 showed up to 4% SN38 release in 24 hours in the presence of SIF, but the addition of pancreatin did not increase this release. In contrast, G3.5-Gly-SN38 released up to 10% SN38 in the presence of SIF and up to 20% with the addition of pancreatin. These results show that both conjugates are inherently more susceptible to hydrolysis in the basic pH of SIF compared to the acidic pH of SGF, which is common for ester linkages. In addition, while G3.5- β Ala-SN38 did not appear to be a substrate for pancreatin, G3.5-Gly-SN38 showed increased release in the presence of pancreatin compared to SIF alone. However, with a maximum of 20% release after 24 hours, both of these conjugates showed a low extent and slow rate of release in the intestinal environment.

Finally, we examined the stability profile of the conjugates in the presence of liver carboxylesterase and in PBS alone (Figure 4.4). Carboxylesterase is highly expressed in the liver environment and can be used to estimate the release in this milieu. Both conjugates showed similar release profiles in PBS and SIF up to 24 hours, and the linear release kinetics continued until 48 hours, suggesting similar rates of hydrolysis in SIF and PBS without enzymes. G3.5- β Ala-SN38 did not show any additional release in the presence of carboxylesterase, suggesting that it is not a substrate for this enzyme. In contrast, G3.5-Gly-SN38 showed a significant increase in SN38 release in the presence of carboxylesterase, achieving 56% release after 48 hours, illustrating that the ester bond in G3.5-Gly-SN38 can be cleaved by carboxylesterase to release free SN38 in the liver environment. Taken together, these stability studies show that G3.5- β Ala-SN38 is stable in all three environments and is not a substrate for pepsin, pancreatin or carboxylesterase,

while G3.5-Gly-SN38 shows less stability in the gastric and intestinal environments and the greatest release in the presence of carboxylesterase, making it a potential candidate for oral delivery of SN38 to colorectal hepatic metastases.

4.3.2 Short-Term Cytotoxicity

Short-term cytotoxicity of G3.5 dendrimers, G3.5-SN38 conjugates and SN38 was assessed in Caco-2 cells by the WST-1 cell viability assay. This assay is predictive of the short-term effects of the conjugates on the intestinal barrier and also serves to ensure that cell viability is not compromised during the 2-hour time needed for transport and uptake assays. Figure 4.5 shows the cell viability of Caco-2 cells treated for 2 hours with unmodified G3.5 dendrimers and G3.5-SN38 conjugates. SN38 is also tested at 4, 40 and 400 μM for comparison, corresponding to 1, 10 or 100% of the drug loading on the G3.5- βAla -SN38 conjugate.

G3.5 dendrimers and G3.5-SN38 conjugates did not cause a significant reduction in cell viability up to 100 μM . In contrast, despite the short treatment time, SN38 shows a significant reduction in cell viability at 40 and 400 μM , corresponding to approximately 10% and 100% of the drug loading on the conjugates. This suggests that conjugation of SN38 to G3.5 dendrimers is able to significantly reduce intestinal toxicity of SN38. In addition, it is observed that G3.5-Gly-SN38 and G3.5- βAla -SN38 can be used in transport and uptake assays up to 100 μM without compromising cell viability.

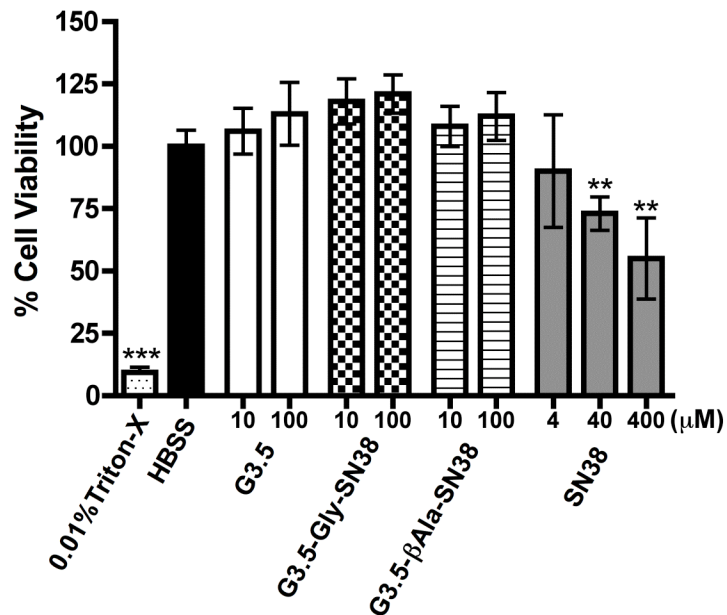


Figure 4.5. Caco-2 Cell Viability after Treatment for 2 hours with G3.5 Dendrimers, G3.5-SN38 Conjugates and SN38. Results are reported as mean +/- standard deviation (n=6). (**) and (***) indicate a statistically significant decrease in cell viability compared to HBSS control with $p < 0.01$ and $p < 0.001$, respectively. G3.5 dendrimers and G3.5-SN38 conjugates do not show a reduction in cell viability up to 100 μM while SN38 shows a significant cytotoxic effect at 40 and 400 μM .

4.3.3 Delayed Cytotoxicity

In order to assess the potential long-term effects of G3.5 dendrimers and G3.5-SN38 conjugates on the intestinal barrier, a delayed cytotoxicity assay was performed. In this assay, Caco-2 cells were treated for 2 hours, the treatment was removed and the cells were incubated for an additional 24 hours in cell culture media. This allows for the assessment of any potential delayed-onset responses of the cells to dendrimer treatment (e.g. apoptosis), which can be detected after 24 hours (Figure 4.6). Even after 24 hours, G3.5 dendrimers and G3.5-SN38 conjugates did not cause a statistically significant decrease in cell viability, with the exception of G3.5-Gly-SN38 at a 10 μM concentration, which displayed 85.4 % \pm 8.1% viability. While this is a statistically significant decrease from the HBSS control, 85% viability is still considered to be acceptable in such viability assays and 10 μM treatment with G3.5-Gly-SN38 does not show a significant difference from 100 μM treatment with the same conjugate. In contrast, SN38, which is known to cause apoptosis by inhibition of topoisomerase-1 [158], had a significant impact on cell viability 24 hours post treatment at 4, 40 and 400 μM concentrations. This illustrates that by conjugating SN38 to dendrimers, intestinal toxicity is minimized compared to the free drug and that G3.5-SN38 conjugates should be safe for oral administration.

4.3.4 Transepithelial Transport

Transepithelial transport of G3.5-SN38 conjugates and free SN38 was measured across differentiated Caco-2 monolayers in the apical to basolateral direction and expressed as the equivalent SN38 flux calculated at 2 hours (Figure 4.7). In this study

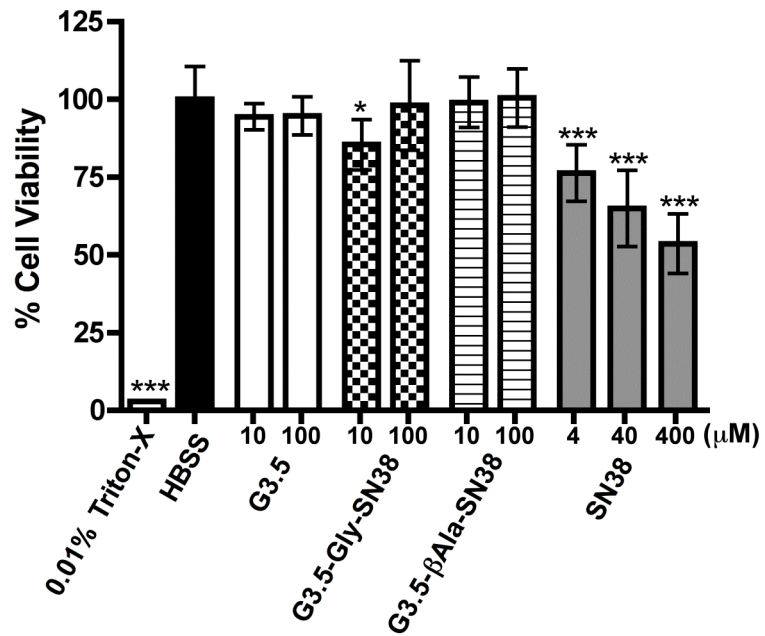


Figure 4.6. Caco-2 Cell Viability 24 hours after 2-hour Treatment with G3.5, G3.5-SN38 Conjugates and SN38. Results are reported as mean +/- standard deviation (n=6). (*) and (***) indicate a statistically significant decrease in cell viability relative to HBSS control with $p < 0.05$ and $p < 0.001$, respectively.

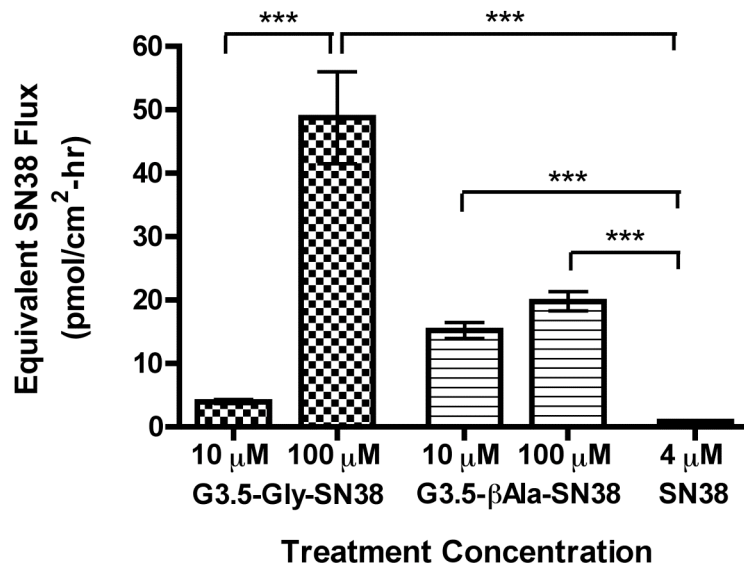


Figure 4.7. Equivalent SN38 Flux across Differentiated Caco-2 Monolayers Treated with G3.5-SN38 Conjugates and SN38. Treatment concentrations of conjugates were 10 and 100 μM , corresponding to 29, 290 and 40, 400 μM equivalents of SN38 for G3.5-Gly-SN38 and G3.5- βAla -SN38 conjugates, respectively. Equivalent SN38 flux was calculated by multiplying the measured molar flux of the conjugates with the number of SN38 molecules per dendrimer. Results are reported as mean \pm standard deviation (n=4). (***) indicates a significant difference with $p < 0.001$.

SN38 was tested at 4 μM concentration since significant cytotoxicity was observed in Caco-2 cells treated with SN38 at 40 and 400 μM . It has been shown that SN38 is transported across Caco-2 cell monolayers by an active transport pathway, and that increasing the concentration from 2.5 μM to 25 μM does not increase transepithelial flux [184]. This suggests that 4 μM SN38 should be beyond the saturation limit for transport and uptake, thus permitting direct comparison of SN38 flux to that of G3.5-SN38 conjugates despite the difference in total drug concentration.

Presence of free SN38 in the basolateral compartment was found to be less than 5% of the amount transported for G3.5-Gly-SN38 and G3.5- β Ala-SN38 conjugates (data not shown). Hence the measured flux is due almost entirely to transport of intact conjugate. G3.5-Gly-SN38 at 100 μM and G3.5- β Ala-SN38 at 10 μM and 100 μM showed a statistically significant increase in apical to basolateral SN38 flux relative to free drug ($p < 0.001$). Taking into account the drug loading on each conjugate (2.9 SN38 per dendrimer for G3.5-Gly-SN38 and 4.0 SN38 per dendrimer for G3.5- β Ala-SN38), the overall SN38 flux increase compared to free drug is 13, 159, 69 and 89-fold for G3.5-Gly-SN38 at 10 μM and 100 μM and G3.5- β Ala-SN38 at 10 μM and 100 μM , respectively. These significant increases in the amount of SN38 transported across the monolayer indicate that G3.5 dendrimers are effective oral drug delivery carriers and can increase the permeability of SN38.

Interestingly, the impact of concentration on transport is different for G3.5-Gly-SN38 and G3.5- β Ala-SN38 conjugates. G3.5-Gly-SN38 shows approximately a 10-fold increase in transport with a 10-fold increase in concentration, indicating that diffusion-driven processes (i.e. paracellular transport) are predominantly involved. In contrast, G3.5- β Ala-SN38, shows minimal increase in transport with a 10-fold increase in concentration, suggesting that its epithelial flux may be controlled by a saturable, energy-dependent mechanism with minimal paracellular transport. Dendrimers have been shown to cross epithelia both by transcellular and paracellular pathways and the relative importance of each has been shown to be charge and surface chemistry dependent [149]. Factors such as the number of conjugated surface groups as well as the ability of these groups to shield the dendrimer surface charge have been found to impact the ability of dendrimers to open tight junction and overall mechanism of transport. Therefore, both the number of SN38 molecules conjugated and the identity of the linker could potentially impact the ultimate transport pathway. These studies further confirm the importance of dendrimer surface chemistry and drug linker chemistry in the degree and mechanism of transport. More detailed mechanistic studies, however, are required to explain the differences in transepithelial transport profiles of the two conjugates.

4.3.5 Cellular Uptake

Cellular uptake studies shed light on the contribution of the transcellular pathway to overall transepithelial transport as well as the ability of the carrier to promote drug uptake. Cellular uptake of G3.5-SN38 conjugates and SN38 was measured in differentiated Caco-2 monolayers after a 2-hour incubation time (Figure 4.8).

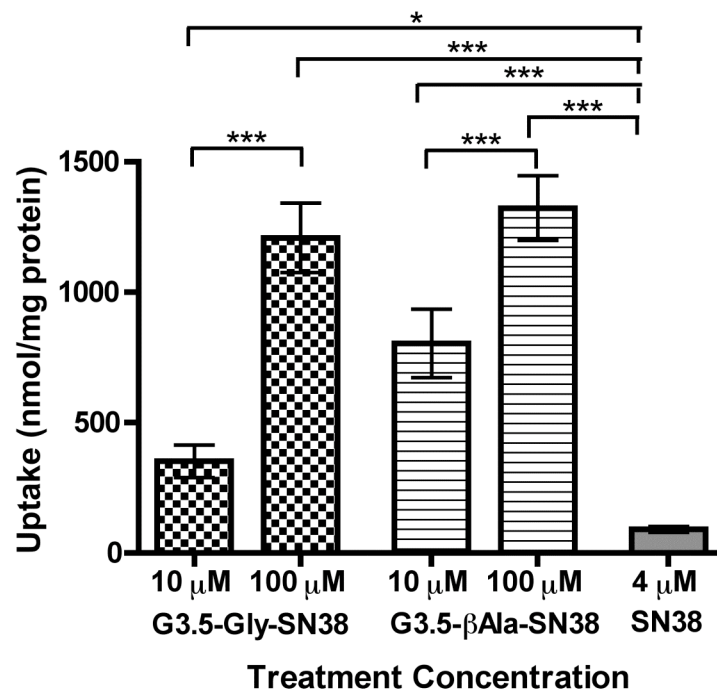


Figure 4.8. Cellular Uptake of G3.5-SN38 Conjugates and Free SN38 in Differentiated Caco-2 Monolayers after 2-hour Treatment on the Apical Side. Results are reported as mean +/- standard deviation (n=4). (*), (**), and (***) show statistical differences in uptake between groups with $p < 0.05$, 0.01 and 0.001, respectively. All conjugates show a statistically significant increase in uptake relative to SN38.

Similar to the transport studies, free SN38 in the cells after a 2-hour treatment was found to be less than 5% of conjugate uptake (data not shown). All conjugates tested showed a significant increase in uptake relative to free SN38. This illustrates that G3.5 dendrimers can enter cells more efficiently than SN38, and thus are suitable for cellular delivery. Both G3.5-Gly-SN38 and G3.5- β Ala-SN38 conjugates showed a significant increase in uptake ($p < 0.001$) with increase in concentration. However, for both conjugates the increase in uptake was less than the corresponding increase in concentration, suggesting the involvement of a saturable uptake mechanism, such as receptor-mediated endocytosis. Interestingly, both conjugates showed similar uptake for the 100 μ M treatment, suggesting that differences in overall transport may be due to differences in paracellular transport rather than transcellular transport at this concentration. These results confirm that cellular uptake of G3.5-SN38 conjugates by Caco-2 cells plays a significant role in G3.5-SN38 conjugate transport.

4.3.6 IC_{50} in HT-29 Cells

Toxicity of G3.5-SN38 conjugates and free SN38 was determined in HT-29 cells for 48 hours in order to compare the activity of the free drug and dendrimer-drug conjugates (Figure 4.9). HT-29 cells are derived from human colon adenocarcinoma, are well suited for IC_{50} studies of anti-cancer activity due to their uniform cell growth and morphology.

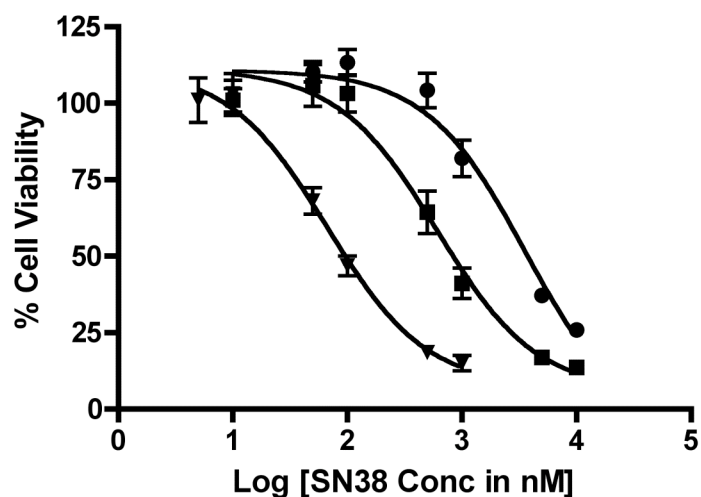


Figure 4.9. IC_{50} Curves of SN38, G3.5-Gly-SN38 and G3.5- β Ala-SN38 in HT-29 Cells. SN38 is represented by inverted triangles, G3.5-Gly-SN38 by squares and G3.5- β Ala-SN38 by circles. Results are reported as mean \pm standard deviation (n=6). IC_{50} values were determined from nonlinear sigmoidal dose response curve fitting by GraphPad Prism software and are 66.3 nM, 0.60 μ M and 3.59 μ M for SN38, G3.5-Gly-SN38 and G3.5- β Ala-SN38, respectively.

SN38 showed the highest activity against HT-29 cells with an IC_{50} value of 66.3 nM. In contrast, SN38 conjugated to G3.5 dendrimers showed much lower activity with IC_{50} values of 0.60 μ M and 3.59 μ M for G3.5-Gly-SN38 and G3.5- β Ala-SN38 conjugates, respectively, corresponding to approximately 10 and 60 times less potency than the free drug. Treatment with comparable G3.5 dendrimer concentrations did not cause any reduction in cell viability (data not shown), confirming that the carrier does not cause toxicity. Since cytotoxicity is dependent on free drug release from the dendrimer backbone, the lower IC_{50} value for G3.5-Gly-SN38 compared to G3.5- β Ala-SN38 is consistent with the higher release rate of SN38 from the G3.5-Gly-SN38 conjugate. Because the conjugates showed some release under acidic conditions and greater release at neutral pH, it is likely that the activity in HT-29 cells is due to a combination of extracellular release of SN38 in cell culture media and intracellular release. Further detailed studies are required to examine the relative contribution of extra- and intracellular drug release to cytotoxicity. Importantly, despite the loss in efficacy compared to the free drug, the IC_{50} values of the G3.5-SN38 conjugates are still in the nanomolar to micromolar range, which is acceptable for therapy.

4.4 Discussion

Dendrimers have shown promise as oral drug delivery carriers due to their ability to translocate across the epithelial layer of the gut. The impact of dendrimer properties such as generation, charge and concentration on transepithelial transport have been described in detail, but comparatively few reports have been published using dendrimers to translocate drugs across the intestinal barrier. Previously Kolhatkar and co-workers

reported the use of G4 dendrimers complexed with SN38 through non-covalent interactions as a potential oral drug delivery system [150]. While the conjugates increased the transepithelial transport and cellular uptake of SN38, they released 40% of the drug within 24 hours in PBS and 90% of the drug within 30 minutes at pH 5. Because of the instability in acidic conditions, these dendrimer-SN38 complexes would have significant limitations for oral administration. In addition, because of the high intrinsic toxicity of the G4 dendrimer carrier [16], these complexes could only be used up to a 10 μ M concentration, limiting the amount of drug transported across the intestinal barrier and into the bloodstream.

Vijayalakshmi and colleagues reported the preliminary synthesis and characterization of G3.5-SN38 conjugates with glycine and β -alanine linkers [161]. In this Chapter, we investigated the potential of these G3.5-SN38 conjugates for oral therapy of colorectal hepatic metastases. The G3.5-SN38 conjugates have several advantages compared to the previously reported G4-SN38 complexes. Because the drug is covalently conjugated to the dendrimer rather than complexed, the conjugates are relatively stable in the gastric and intestinal environments, minimizing premature drug release upon oral administration. In addition, the G3.5-Gly-SN38 conjugates release the drug in the presence of carboxylesterase, allowing for the targeted treatment of colorectal hepatic metastasis. These systems can be used at higher concentrations (100 μ M vs. 10 μ M) due to the low intrinsic toxicity of G3.5 dendrimers, allowing for greater drug transport across the gastrointestinal barrier and a higher dose at the site of action. Therefore, these conjugates show distinct advantages over previously published

dendrimer-SN38 complexes and are a significant step towards a functional dendrimer-based oral drug delivery system.

In order to determine their suitability for oral delivery, the stability of the conjugates in the gastrointestinal milieu as well as in the presence of liver carboxylesterase was investigated. G3.5- β Ala-SN38 conjugates were significantly more stable than G3.5-Gly-SN38 under the conditions studied, releasing a maximum of 1% drug in SGF after 6 hours, 4% in SIF after 24 hours and 8% in carboxylesterase after 48 hours. In addition, in each of the release buffers, the addition of an enzyme did not increase the release of SN38, illustrating that G3.5- β Ala-SN38 is not susceptible to enzymatic cleavage. In contrast, G3.5-Gly-SN38 showed much higher release in all of the conditions and showed increased rate and extent of release in the presence of pancreatin and carboxylesterase compared to buffer alone. Previous studies conjugating CPT to poly(l-lysine) dendrimers using glycine and β -alanine linkages at the 20-OH position showed similar results with the glycine linker indicating higher rates of hydrolysis than the stable β -alanine linker [185]. Although the β -alanine linker provides an extra methyl group as a spacer, this group appears to stabilize the bond against hydrolysis and enzymatic degradation.

The impact of linker chemistry on SN38 release shows a direct correlation with the IC_{50} values in which the G3.5-Gly-SN38 conjugates had six-fold greater efficacy than G3.5- β Ala-SN38 conjugates, illustrating the importance of SN38 release for anti-cancer activity. Since the conjugates were relatively stable at lower pH it is likely that only a small percentage of the drug was released in the intracellular acidic environment with the majority released in the extracellular media. Stability studies in PBS for 48 hours

showed a two-fold increase in SN38 release from G3.5-Gly-SN38 compared to G3.5-βAla-SN38, suggesting additional enzymatic mechanisms may play a role in enhancing G3.5-Gly-SN38 efficacy by 6-fold. Comparing the release profiles with and without enzymes, an increased release of SN38 from G3.5-Gly-SN38 in the presence of pancreatin and carboxylesterase was observed, but no such increase for G3.5-βAla-SN38 was seen, indicating the increased susceptibility of the glycine linker to enzymatic degradation.

In addition to differing release and toxicity profiles, G3.5-Gly-SN38 and G3.5-βAla-SN38 conjugates showed significant differences in transepithelial transport. Both conjugates showed increased flux of SN38 relative to free drug, which is critical for improving the oral bioavailability of SN38. In addition, neither conjugate showed short- or long-term effects on Caco-2 cells after a 2-hour treatment, illustrating that conjugation of SN38 to G3.5 dendrimers can minimize intestinal toxicity while maximizing transport. Interestingly, transport of G3.5-Gly-SN38 was highly concentration-dependent while G3.5-βAla-SN38 flux was unchanged between treatment with 10 and 100 μM concentrations. This suggests that G3.5-Gly-SN38 may be transported primarily by a concentration gradient-driven process, such as paracellular diffusion, whereas a saturable process, such as transcellular transport, governs G3.5-βAla-SN38 transport. This phenomenon, however, needs further examination. While the uptake data suggests comparable uptake of the conjugates at 100 μM this measurement could include surface bound dendrimer or dendrimer that would be degraded in the cell and not transcytosed. Therefore, reduction in G3.5-βAla-SN38 transport at 100 μm compared to G3.5-Gly-SN38 transport could be due to decreases in both transcellular and paracellular pathways.

In Chapter 5 we will show the impact of surface chemistry on the mechanism of transport and uptake of PAMAM dendrimers. Specifically, reduction of surface charge on G3.5 dendrimers by the addition of low molecular weight poly (ethylene glycol) is found to reduce tight junction opening, transepithelial transport and uptake in Caco-2 cells. Thus, it is possible that addition of a methyl group in the β -alanine linker as well as the increase of drug loading from 2.9 to 4.0 molecules of SN38 increased the hydrophobicity of the conjugates, hence reducing the degree to which G3.5- β Ala-SN38 conjugates opened the tight junctions, resulting in an overall transport mechanism dominated by the transcellular route. Importantly, these studies illustrate the choice of drug linker and the degree of drug loading not only impact drug release and ultimate efficacy but can also impact transport. Therefore, dendrimer-drug conjugates for oral delivery must be carefully designed to meet transport, release and efficacy demands.

4.5 Conclusion

In this Chapter we investigated G3.5-SN38 conjugates for oral delivery of SN38 by determining their *in vitro* release profiles in simulated gastric and intestinal conditions and in the presence of carboxylesterase, their toxicity against intestinal cells and target colorectal cancer cells, and their transepithelial transport and cellular uptake in Caco-2 monolayers. We demonstrated that conjugation of SN38 to G3.5 dendrimers increased the transepithelial transport while simultaneously reducing intestinal toxicity compared to free SN38, illustrating the potential for these conjugates in oral drug delivery. A significant impact of linker chemistry on drug release and efficacy in HT-29 cells was shown with G3.5-Gly-SN38 showing lower *in vitro* stability and higher efficacy than

G3.5- β Ala-SN38 conjugates. The drug linker chemistry and drug loading also impacted the transport pathway with G3.5-Gly-SN38 having a concentration-dependent transport profile and G3.5- β Ala-SN38 conjugates having a saturable transport profile. G3.5-Gly-SN38 shows promise for oral delivery of SN38 for the treatment of colorectal hepatic metastases. Treatment with 100 μ M G3.5-Gly-SN38 caused a 159-fold increase in SN38 transepithelial transport compared to free SN38 illustrating its potential to enhance SN38 bioavailability. In addition, G3.5-Gly-SN38 was relatively stable in gastric and intestinal milieu with increased release in the presence of liver carboxylesterase. Finally, G3.5-Gly-SN38 shows an IC_{50} of 0.60 μ M in HT-29 cells, which is acceptable for cancer therapy. Together these results show that PAMAM dendrimers have the potential to improve the oral bioavailability of potent anti-cancer therapeutics and that appropriate selection of drug linker is a critical step in designing dendrimers for oral drug delivery applications.

Chapter 5 : Transepithelial Transport of PEGylated Anionic Poly (amido amine) Dendrimers: Implications for Oral Drug Delivery

5.1 Introduction

As illustrated in Chapter 4, PAMAM dendrimers can effectively enhance transepithelial transport of SN38. Previous studies in our laboratory [15, 18, 24, 148, 149] and others [19, 144, 186, 187] indicate that dendrimers in a specified size and charge window can effectively translocate across the gastrointestinal epithelia. In addition, several studies have demonstrated that conjugation or complexation of drugs with PAMAM dendrimers can enhance the oral bioavailability of drugs normally limited to intravenous administration, supporting dendrimers as viable oral drug delivery carriers [20, 113, 150, 151]. Due to their intrinsically low cytotoxicity and appreciable transepithelial permeation characteristics across Caco-2 monolayers and everted rat intestinal sac models [15, 144], anionic dendrimers show distinct advantages as vehicles for oral drug delivery, with higher generation dendrimers showing the greatest potential because of their large number of modifiable surface groups. As demonstrated in Chapter 4, in addition to the surface charge, the drug linker can also play a significant role in transport and drug release. This Chapter aims to evaluate the potential of G3.5 and G4.5 dendrimers in facilitating the delivery of drugs across the gastrointestinal tract, specifically examining the effect of poly (ethylene glycol) (PEG) surface modification.

PEGylation of drug delivery systems and bioactive agents is known to reduce toxicity and immunogenicity, influence pharmacokinetics and biodistribution and

enhance water solubility [188]. Okuda and colleagues [189, 190] showed that PEGylation of dendritic systems produces desirable biodistribution effects upon intravenous administration; however, the impact of PEGylation on transepithelial transport of PAMAM dendrimers across intestinal cells is presently unknown. In the context of oral drug delivery, PEG can be used as a surface modifier to modulate the degree and mechanism of transport or it can act as drug linker, altering release properties from the polymer backbone. In this Chapter we describe the synthesis and characterization of differentially PEGylated G3.5 and G4.5 anionic PAMAM dendrimers and evaluate their cytotoxicity, cellular uptake and transport across Caco-2 cell monolayers. In addition, the effect of PEGylation on tight junction modulation was investigated. These studies provide the first evidence of the impact of PEG conjugation on dendrimer transepithelial transport.

5.2 Materials and Methods

5.2.1 Materials

PAMAM G3.5 (reported molecular weight=12,931) and PAMAM G4.5 (reported molecular weight 26,258), [¹⁴C]-mannitol (specific activity 50mCi/mmol), D₂O, and Hank's balanced salt solution (HBSS buffer) salts were purchased from Sigma Aldrich (St. Louis, MO). [³H]-Acetic anhydride was purchased from American Radiolabeled Chemicals (St. Louis, MO). Superose 12 HR 10/300 GL column was purchased from Amersham Pharmacia Biotech (Piscataway, NJ). Caco-2 cells were purchased from American Type Cell Culture (Rockville, MD). WST-1 cell proliferation reagent was

purchased from Roche Applied Science (Indianapolis, IN). The BD Biocoat Caco-2 Assay was purchased from BD Biosciences (San Jose, CA).

5.2.2 Conjugation of mPEG750 to PAMAM Dendrimers

PEGylation of PAMAM G3.5 and G4.5 was achieved by formation of ester bonds between surface carboxyl groups of the dendrimers and hydroxyl terminated PEG (Molecular Weight (M_w) 750) using benzotriazole-1-yl-oxy-tris-(dimethylamino)-phosphoniumhexafluorophosphate (BOP) as a coupling agent and methanol as a solvent (Figure 5.1). 1, 2 and 4 equivalents of methoxy polyethylene glycol (mPEG) were reacted with dendrimers to yield samples G3.5-P1, G3.5-P1.4 and G3.5-P2.3, G4.5-P.85, G4.5-P1.9 and G4.5-P2.8 respectively, where G represents the generation number and P represents the number of PEG chains conjugated. For each reaction, 75 mg of dendrimer and three equivalents of BOP per equivalent of mPEG were dissolved in anhydrous methanol. mPEG750 was dissolved in methanol to a concentration of 100 mg/mL and the appropriate molar equivalent was added to the mixture. The solution was stirred at room temperature for 72 hours, after which methanol was evaporated to leave the crude product. This product was dissolved in distilled water and purified by dialysis against distilled water using 3,500 molecular weight cut off (MWCO) membranes (Spectrum Laboratories, Rancho Dominguez, CA). Subsequently, the product was freeze dried and stored at 4°C.

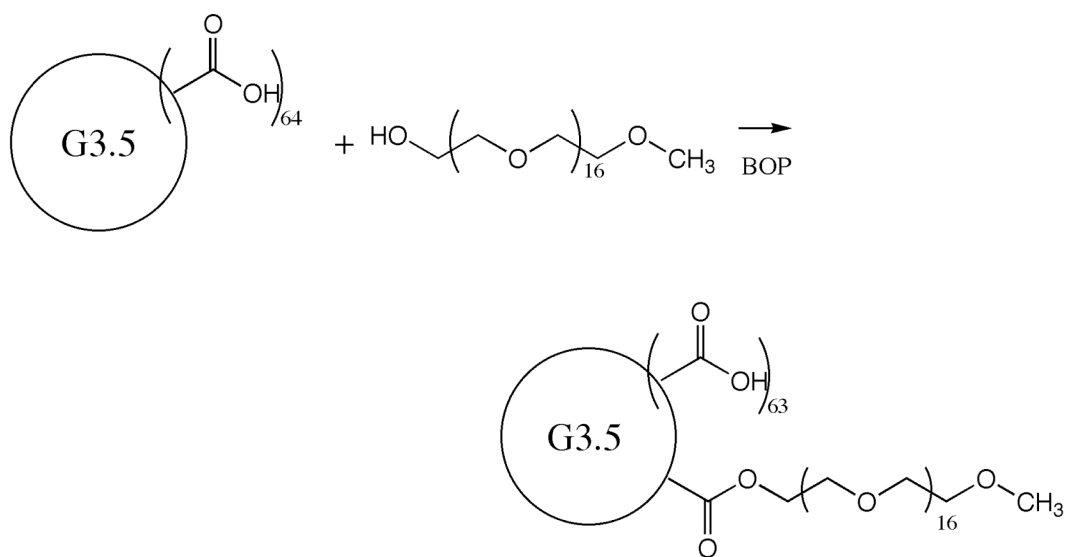


Figure 5.1. PEGylation of G3.5 Dendrimer with mPEG750.

5.2.3 Characterization of PEGylated G3.5 and G4.5 Dendrimers

Dendrimer-PEG conjugates were characterized by size exclusion chromatography (SEC) using an Acta FPLC system (Acta UPC 900, P-920, INV-907 from GE Healthcare) and phosphate buffered saline (PBS, pH 7.4) with 0.05% sodium azide as the eluent. Samples were injected onto the FPLC system at 5 mg/mL and simultaneously monitored for Ultra-Violet (UV), Refractive Index (RI), Multi-Angle Laser Light Scattering (MALLS) and Dynamic Light Scattering (DLS) detection. SEC was used to confirm the absence of low molecular weight impurities and to compare the elution volumes of modified and native dendrimers. In addition, the dendrimer peak was analyzed to determine the hydrodynamic radius using a Wyatt Quasi-Elastic Light Scattering Detector (QELS) and the calculations were performed using the Astra 5.3.4 software. All samples were run in duplicate. ^1H NMR was used to determine the number of PEG chains conjugated per dendrimer. ^1H NMR samples were prepared at approximately 8 mg/mL in D_2O with 0.05 wt % 3-(trimethylsilyl) propionic-2,2,3,3- d_4 acid (TSP- d_4). ^1H Nuclear Magnetic Resonance (NMR) spectra were obtained using Varian 500 MHz FT NMR and were processed using Spinworks software (Kirk Marat, University of Manitoba, Winnipeg, Canada, © 2008). The number of PEG chains per dendrimer was determined from ratios of integral values for peaks assigned to PEG (3.6-3.7 ppm) and dendrimer (2-3.6). Finally, the zeta potential of PEGylated dendrimers was obtained using the Malvern Nano-ZS system. Dendrimer solutions were prepared at 5 mg/mL in DI water and analyzed in triplicate.

5.2.4 Synthesis of Radiolabeled Dendrimers

Dendrimers and dendrimer-PEG conjugates were radiolabeled using [^3H]-acetic anhydride (American Radiolabeled Chemicals, St. Louis, MO) which reacts with internal amines known to be present in carboxyl terminated dendrimers due to defects formed during their synthesis [191]. Dendrimers and dendrimer-PEG conjugates were dissolved in methanol and reacted with three equivalents of [^3H]-acetic anhydride in the presence of excess triethylamine overnight. The methanol was dried under a stream of nitrogen and the product was redissolved in distilled water. Triethylamine and unreacted acetic anhydride were removed by Sephadex G-25 protein desalting (PD10) columns. Specific activities of the radiolabeled compounds were also calculated.

5.2.5 Caco-2 Cell Culture

Caco-2 cells (passages 20-40) were cultured as described in Section 3.2.3.

5.2.6 Cytotoxicity Assay

Cytotoxicity of unmodified and differentially PEGylated PAMAM dendrimers was assessed by the water soluble tetrazolium salt (WST-1) assay as described in Section 3.2.4.

5.2.7 Cellular Uptake Studies

The effect of PEGylation on cellular uptake of radiolabeled dendrimers was investigated. Caco-2 cells were seeded at 40,000 cells/ well in 24-well cell culture plates (Corning, Corning NY) and maintained at 37°C, 95% relative humidity and 5% CO₂ for

48 hours. Cells were washed with warm HBSS buffer and 300 μ L of 0.02 mM dendrimer solution in HBSS was added for 30 or 60 minutes. After the given incubation period, the cells were washed twice with ice cold HBSS to halt the uptake process. They were then lysed with NaOH and neutralized with HCl. Uptake was measured by quantifying the cell-associated radioactivity using a liquid scintillation counter (Beckman Coulter, Fullerton, CA) with Econosafe scintillation cocktail (Research Products International, Mount Prospect, IL). Uptake was normalized to total protein content using the Bicinchoninic acid (BCA) protein assay kit (Pierce, Evanston, IL). Statistical significance was determined by a two-way analysis of variance and Bonferroni post-hoc correction.

5.2.8 Transepithelial Permeability Assessment

The effect of differential PEGylation on transport of radiolabeled dendrimers across Caco-2 cell monolayers was assessed in the BD Biocoat HTS Caco-2 Assay System (BD Biosciences, San Jose, CA). The three-day assay protocol defined by the manufacturer was used to prepare the monolayers. Briefly, Caco-2 cells were grown past confluency to a density of $>250,000$ cells/cm² in T-25 flasks. Cells were seeded at 200,000 cells per well, in 24-well Transwell[®] plates with fibrillar collagen-coated cell culture inserts in basal cell seeding medium supplemented with MITO+ (mitogenic stimulating) serum extender and 10% FBS. After 24 hours, the medium was switched to entero-STIM, a fully defined media containing butyric acid, which induces differentiation of intestinal epithelial cells and form a competent monolayer [192]. After an additional 48 hours, the monolayers were used for experiments. Cells were washed twice with warm HBSS buffer. To test dendrimer permeability, 100 μ L of dendrimer solution (0.1 mM)

was added to the apical compartment and 600 μL of HBSS added to the basal compartment. After 2 hours, 400 μL from the basal compartment was taken for scintillation counting. Apparent permeability (P_{app}) was calculated by:

$$P_{app} = \frac{dQ}{A \cdot C_0 \cdot dt} \quad (\text{Eq. 5.1})$$

where dQ/dt is the change in the amount of solute over time (permeability rate), A is the surface area of the insert, and C_0 is the donor concentration. [^{14}C]-Mannitol was used to monitor monolayer integrity. The transepithelial flux of the paracellular marker [^{14}C]-mannitol was 2.6×10^{-6} cm/s, which demonstrates monolayer integrity as shown previously [193, 194]. Statistical significance was determined by Tukey's Multiple Comparison test.

5.2.9 Occludin Staining

Caco-2 cells were seeded at 20,000 cells/cm² on collagen-coated four chamber culture slides (BD Biosciences, Bedford MA), maintained under normal cell culture conditions for 5 days and used for experiments when the cells reached confluence. The cells were equilibrated in HBSS for 2 hours prior to the experiment. The cells were incubated with 300 μl of 0.1 mM dendrimer solutions for 2 hours at 37°C and then washed three times with ice cold PBS to remove the dendrimers. G3.5, G3.5-P1, G4.5 and G4.5-P.85 were used with HBSS as a control. The cells were then fixed with 300 μl of 4% paraformaldehyde solution for 20 minutes at room temperature, washed twice with 25 mM glycine and once with PBS and then permeabilized with 300 μl of 0.2% Triton X-100 in blocking solution made of 1% bovine serum albumin (BSA) in PBS for 20 minutes at room temperature. Cells were washed three times with PBS and then

incubated with blocking solution for 30 minutes. The blocking solution was removed and the cells were incubated with 300 μ l of 2 μ M mouse anti-occludin (Invitrogen (Zymed), Carlsbad, CA) and kept at 4°C overnight. Cells were washed three times with blocking solution and then incubated with the same solution for 30 minutes. After the blocking solution was removed, the cells were incubated with 300 μ l of 10 μ g/mL Alexa Fluor 568 goat anti-mouse IgG (H+L) (Invitrogen, Molecular Probes, Carlsbad, CA) for 1 hour. They were then washed three times with PBS and the chambers were removed. Gel mount was added to each region and allowed to dry for 2 hours at room temperature. The slides were then sealed with clear nail polish and kept at 4°C prior to visualization.

Slides were visualized using a Zeiss LSM510 META confocal laser scanning microscope (Carl Zeiss, Jena, Germany). Alexa Fluor 568 was visualized with excitation and emission wavelengths of 543 and 603 nm respectively. Z-stacks were obtained with the following microscope settings: 63x oil objective, 1 airy unit pinhole, 543 nm laser set to 20% power with 1000 gain, 0.1 amplifier offset and 1 amplifier gain. The scan speed was set to 8 in line mode with mean averaging set to 4. Z-stack sections were taken 0.5 μ m apart with 15 sections per region. Three z-stacks were acquired per treatment and analyzed using Volocity 3D imaging software. (Version 4.3.2; Improvision, Inc., Lexington, MA). Red voxels, corresponding to occludin staining, were quantified by thresholding the intensity between 25% and 100%. The number of red voxels was quantified for each region and normalized to the number of cells. Results are reported as mean \pm standard deviation and statistical significance was determined using a one-tailed Student's *t*-test.

5.3 Results

5.3.1 Synthesis and Characterization of PEGylated Anionic PAMAM Dendrimers

^1H NMR studies confirmed the formation of the conjugates with new peaks corresponding to the protons from PEG. ^1H NMR spectra are shown in Appendix 3. ^1H NMR quantification showed a concomitant increase in the number of PEG moieties conjugated with the number of equivalents of PEG, but this increase was less than the stoichiometric amount used (Table 5.1). This may be attributed to steric hindrance, which was more evident in lower generation dendrimers likely due to their lower number of available acid groups and smaller surface area.

Characterization by SEC showed the absence of free PEG and other small molecular weight impurities (data not shown). Elution volumes of native and PEGylated dendrimers are shown in Table 5.1. While there is a decrease in elution volume from G3.5 dendrimers to G4.5 dendrimers due to the larger size, native and modified dendrimers of the same generation do not show any significant differences in elution volume. This illustrates that PEGylation does not increase the hydrodynamic volume of the dendrimers, suggesting that PEG is preferentially wrapped around the dendrimer rather than protruding from the surface. Hydrodynamic radii of the conjugates measured by dynamic light scattering support this hypothesis (Table 5.1). Increasing the degree of PEGylation does not increase the hydrodynamic radii. In fact, the hydrodynamic radii are slightly decreased, indicating that PEG may shield the surface charge and decrease charge-charge repulsion of functional groups and therefore the size of the polymers in solution.

Table 5.1. Characteristics of PAMAM Dendrimer-PEG Conjugates

Dendrimer Sample	# mPEG Equivalents	# mPEG Conjugated*	Calculated Molecular Weight**	Specific Activity (mCi/mmol)	SEC Elution Volume (ml)	Hydrodynamic Radius (nm)
G3.5	-	-	12931	1.06	13.2	1.90 ± 0.00
G3.5-P1	1	1.01	13688	3.25	13.2	1.65 ± 0.07
G3.5-P1.4	2	1.36	13951	3.96	13.2	1.65 ± 0.07
G3.5-P4.5	4	2.32	14671	3.91	13.2	1.70 ± 0.00
G4.5	-	-	26258	2.64	12.8	2.35± 0.07
G4.5-P.85	1	0.85	26896	4.47	12.5	2.10 ± 0.00
G4.5-P1.9	2	1.86	27653	5.11	12.6	2.15 ± 0.07
G4.5-P2.8	4	2.80	28358	4.81	12.6	2.10 ± 0.00

*Calculated from NMR data

**Calculated based on NMR data and reported (Sigma) dendrimer molecular weights

Zeta potential measurements shed light on the impact of PEGylation on dendrimer surface charge. Figure 5.2 illustrates that zeta potential becomes less negative upon further PEGylation, with G3.5 and G4.5 dendrimers showing similar behavior, confirming that PEG shields surface charge. Shcharbin et al. [195] reported a zeta potential for G4.5 PAMAM dendrimers in deionized water as -56 ± 0.5 mV. Comparing this with our data shows that even one PEG is able to shield a significant amount of charge on the dendrimer surface.

5.3.2 Short-Term Cytotoxicity

While amine-terminated PAMAM dendrimers are known to be highly cytotoxic at higher generations, anionic dendrimers have been found to be much less toxic [16]. In this study we examined whether PEGylation of anionic dendrimers would influence their toxicity profile. G3.5 and G4.5 dendrimers and dendrimer-PEG conjugates were tested at concentrations up to 0.1 mM and did not show appreciable cytotoxicity (cell viability > 90%) over the entire range of concentrations tested (Figures 5.3, 5.4). This toxicity profile confirmed that treatment of Caco-2 cells with up to 0.1 mM of the dendrimer-PEG conjugates would not affect cell viability during uptake or transport experiments. In addition, dendrimer-PEG conjugates would be safe to use for oral drug delivery applications.

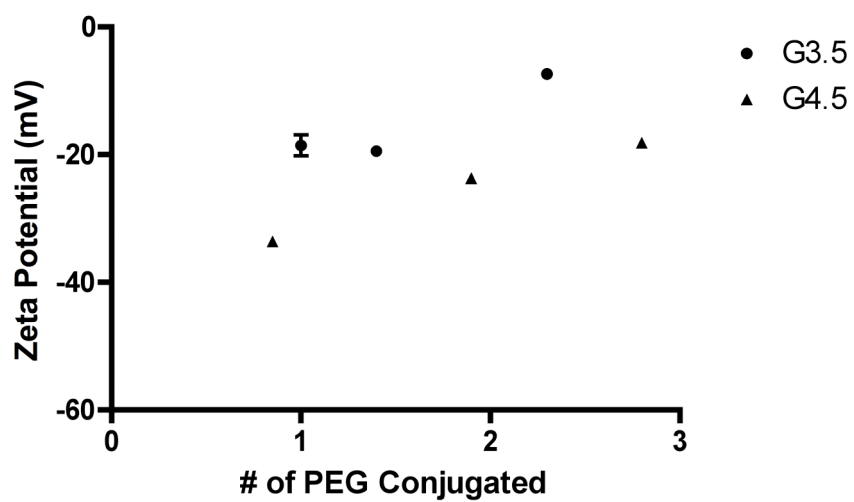


Figure 5.2. Zeta Potential of PEGylated G3.5 and G4.5 PAMAM Dendrimers. Zeta potential becomes less negative with addition of PEG to G3.5 and G4.5 dendrimers. Results are reported as mean +/- standard deviation (n=3).

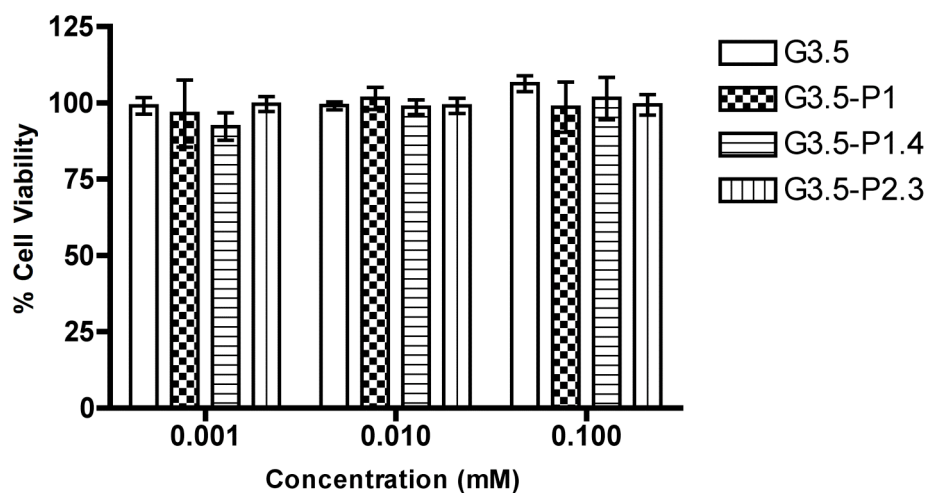


Figure 5.3. Caco-2 Cell Viability in the Presence of G3.5 Native and PEGylated Dendrimers after a 2-hour Incubation Time. Results are reported as mean +/- standard deviation (n=6). Treatment with up to 0.1 mM G3.5 of G3.5-PEG conjugates maintains cell viability.

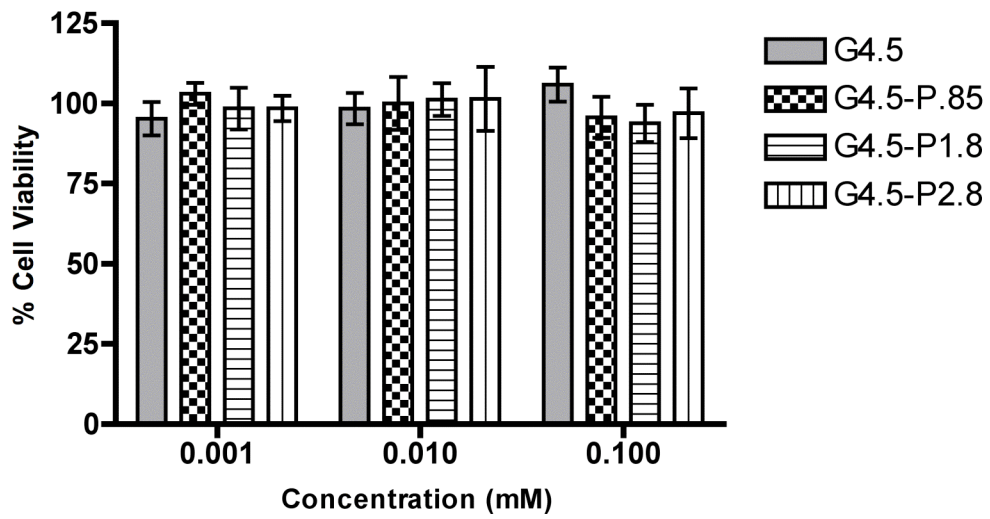


Figure 5.4. Caco-2 Cell Viability in the Presence of G4.5 Native and PEGylated Dendrimers after a 2-hour Incubation Time. Results are reported as mean +/- standard deviation (n=6). Treatment with up to 0.1 mM G4.5 and G4.5-PEG conjugates maintains cell viability.

5.3.3 Cellular Uptake

The impact of PEGylation on time-dependent cellular uptake of dendrimers was assessed in Caco-2 cells (Figures 5.5, 5.6). Uptake studies shed light on the degree to which the dendrimers are transported through transcellular pathways (passive diffusion and vesicular mechanisms) in the gastrointestinal epithelium and their eventual uptake in tumor cells at the site of action. In general, PEGylation decreased uptake of G3.5 dendrimers, but this effect is statistically significant only after 60 minutes. Notably, there is no significant impact of the degree of PEGylation on uptake, i.e. a single PEG chain can reduce dendrimer uptake by almost 50% after a 60-minute incubation period. In contrast, for G4.5 dendrimers, conjugation of 1 PEG chain appears to increase uptake, with further addition of PEG decreasing uptake from this point.

5.3.4 Transepithelial Transport

In order to assess the suitability of PEGylated dendrimers for oral drug delivery, their transport across Caco-2 cell monolayers was studied and compared to unmodified dendrimers. Transport experiments complement the uptake studies, giving an overall picture of transepithelial transport including both transcellular and paracellular pathways. PEGylation significantly decreased transport of both G3.5 and G4.5 dendrimers (Figures 5.7, 5.8), yielding apparent permeabilities approximately 60-70% lower than unmodified dendrimers. Despite this decrease in overall transport flux, PEGylated dendrimers still show appreciable transport compared to traditional linear polymers [196], indicating that the PEGylated dendrimers continue to enhance their own transport to some degree. Addition of more than one PEG per dendrimer did not further decrease transport.

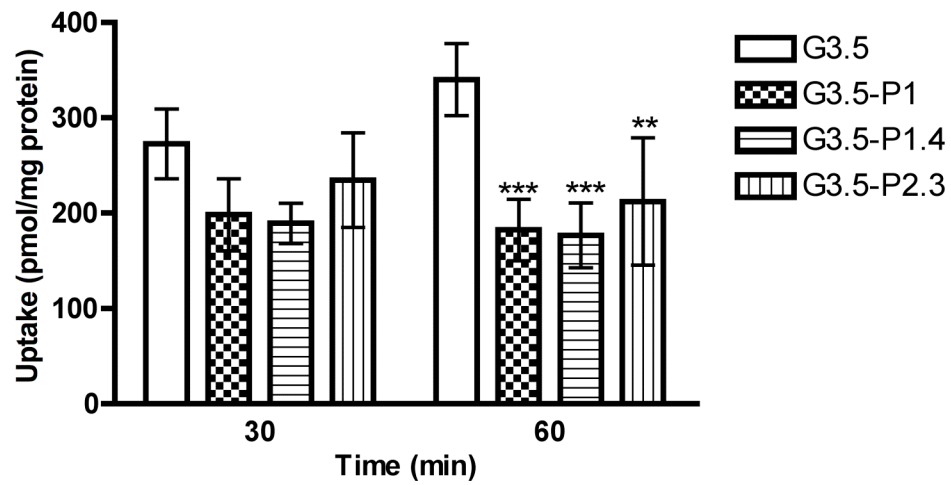


Figure 5.5. Uptake of G3.5 Native and Differentially PEGylated Dendrimers.

Caco-2 cells were treated at 0.02 mM for 30 and 60 minutes. Results are reported as mean +/- standard deviation (n=3). (**) and (***) denote significant differences from unmodified dendrimers with $p < 0.01$ and $p < 0.001$ respectively.

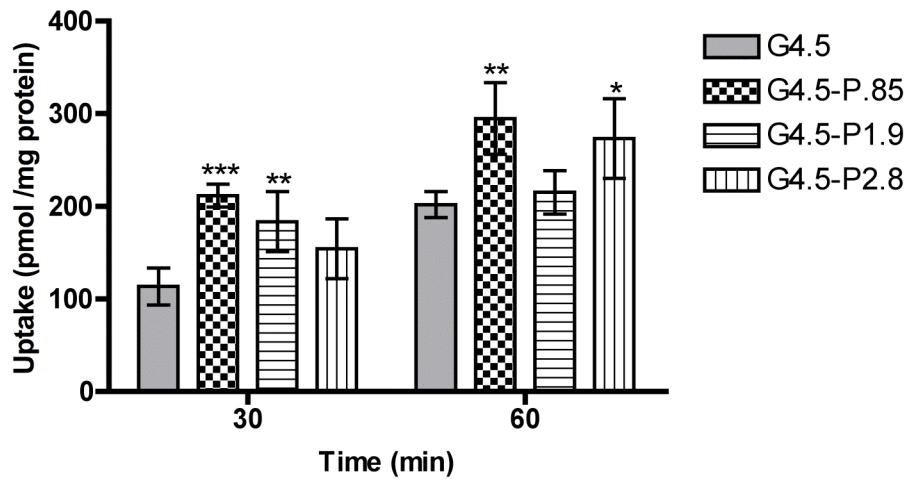


Figure 5.6. Uptake of G4.5 Native and Differentially PEGylated Dendrimers. Caco-2 cells were treated at 0.02 mM for 30 and 60 minutes. Results are reported as mean +/- standard deviation (n=3). (*),(**) and (***) denote significant differences from unmodified dendrimers with $p < 0.05$, $p < 0.01$ and $p < 0.001$ respectively.

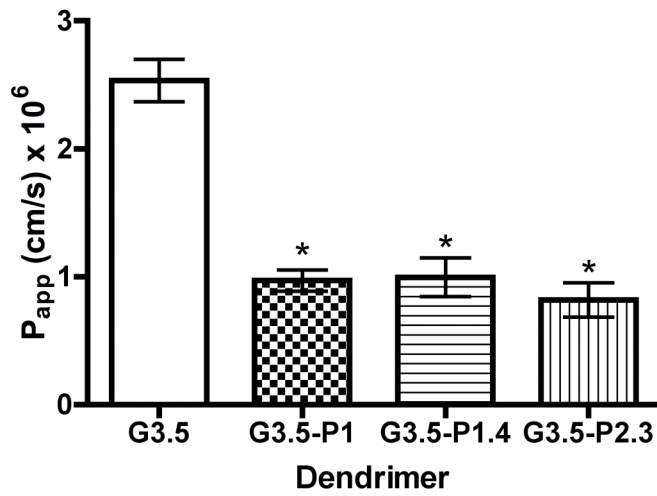


Figure 5.7. Apparent Permeability of G3.5 Native and Differentially PEGylated Dendrimers. Caco-2 cell monolayers were treated at 0.1 mM for a 2-hour incubation time. Results are reported as mean +/- standard deviation (n=3). (*) denotes a significant difference from unmodified dendrimers with $p < 0.001$.

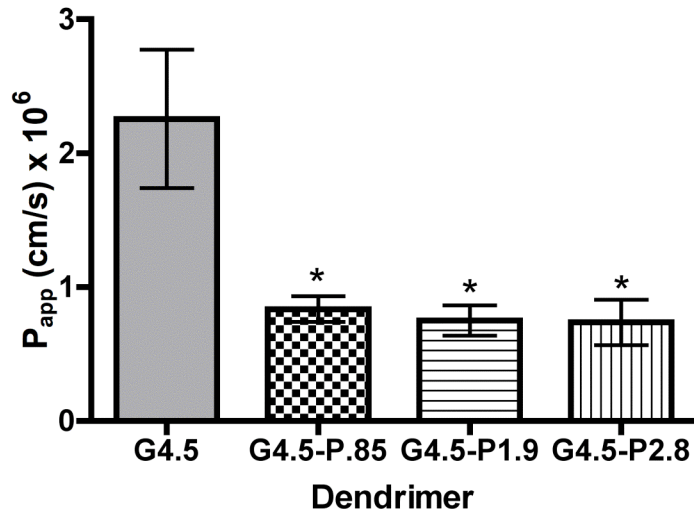


Figure 5.8. Apparent Permeability of G4.5 Native and Differentially PEGylated Dendrimers. Caco-2 cell monolayers were treated at 0.1 mM for a 2-hour incubation time. Results are reported as mean \pm standard deviation (n=3). (*) denotes a significant difference from unmodified dendrimers with $p < 0.001$.

5.3.5 Tight Junction Opening Monitored by Occludin Staining

To further assess the influence of dendrimer PEGylation on tight junctional modulation, Caco-2 cells were pretreated with native and PEGylated dendrimers and stained for occludin, a marker protein for tight junction integrity [15]. Previously, it was shown that Caco-2 cells treated with 1 mM G1.5, G2.5 and G3.5 dendrimers showed disrupted occludin staining patterns and increased occludin accessibility as compared to cells with no polymer treatment [15]. In this study, we used a ten-fold lower concentration (0.1 mM) in order to mimic the conditions used in the transport assay. Control cells treated with HBSS alone (Figure 5.9 E) show thin lines of red staining corresponding to occludin proteins linking cell membranes. In contrast, dendrimer-treated cells (Figure 5.9A-D) show brighter, wider bands of staining with increased intracellular staining, indicating accessibility of occludin protein to its antibody due to the opening of the tight junctions. In the case of G3.5 (Figure 5.9 A) confocal images show some amount of cell detachment, indicating tight junction opening. All dendrimers studied showed a statistically significant increase in occludin staining compared to the HBSS control ($p < 0.05$) (Figure 5.10), illustrating that native and PEGylated dendrimers open tight junctions to some degree, even at relatively low concentrations (0.1 mM).

5.4 Discussion

In this chapter, we investigated the impact of differential PEGylation of G3.5 and G4.5 dendrimers on uptake, transport and tight junction modulation in the context of oral delivery. Differential PEGylation of G3.5 and G4.5 dendrimers led to significant differences in cellular uptake, which can be attributed to charge-shielding properties of

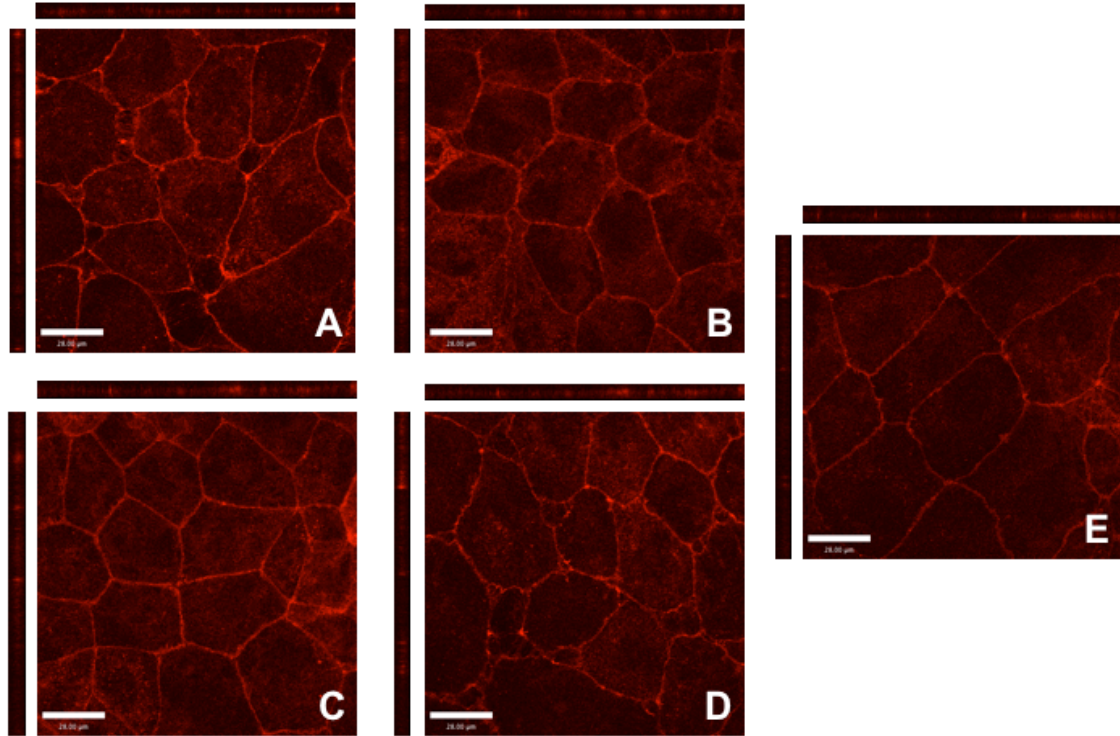


Figure 5.9. Staining of the Tight Junction Protein Occludin in the Presence and Absence of Dendrimers Visualized by Confocal Microscopy. Caco-2 cells incubated for 2 hours with 0.1 mM (A) G3.5, (B) G3.5-P1, (C) G4.5, (D) G4.5-P.85 and (E) with no polymer treatment. Main panels illustrate the xy plane; horizontal bars illustrate the xz plane; vertical bars illustrate the yz plane. Scale bars equal 28 μm .

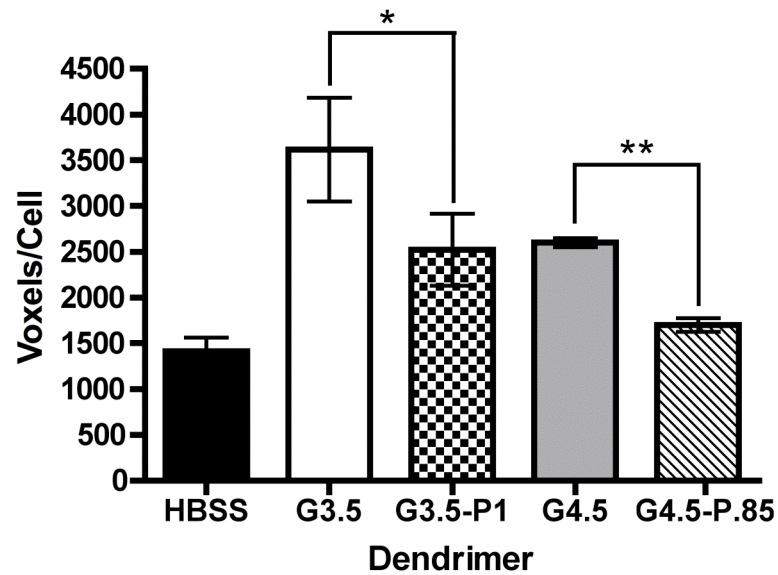


Figure 5.10. Quantification of Occludin Staining in the Presence and Absence of Dendrimers. Results reported are number of “red” voxels per region normalized to the number of cells in each region, mean +/- standard deviation (n=3). One-tailed Student’s *t*-tests were used to determine statistical significance. (*) and (**) denote significant differences from unmodified dendrimers with $p < 0.05$ and $p < 0.01$ respectively.

PEG. The flexible chain of PEG can wrap around the rigid, spherical dendrimer and shield some of the negative charge on the dendrimer surface. Methoxy-terminated 750 Da PEG contains 16 subunits, giving it an overall extended chain length of 5.7 nm based on calculated bond lengths and angles. In comparison, G3.5 dendrimers have a reported diameter of approximately 4 nm and G4.5 dendrimers approximately 5 nm [136]. This suggests that the PEG chain, due to its flexible random coil conformation, is of comparable size to the dendrimers. For the smaller G3.5 dendrimers, one PEG chain is enough to reduce the interactions with the cells, leading to decreased cellular uptake for all PEGylation ratios. This may be due to a stealth-like effect imposed by PEG, creating fewer interactions between the dendrimers and the cells. In contrast, for G4.5 dendrimers, addition of 1 PEG chain actually increases uptake as compared to unmodified G4.5. This may be explained by the charge density of the dendrimers, which can be calculated by dividing the number of charges (64, 128) by the surface area of the dendrimer, assuming a spherical conformation [197]. The higher charge density of G4.5 dendrimers (1.6 charges/nm²) compared to G3.5 dendrimers (1.3 charges/nm²) can presumably cause repulsion with the negatively charged cell membrane. Addition of 1 PEG chain reduces the charge on the surface, increasing the uptake to a point comparable to G3.5 dendrimers. However, addition of more PEG shields more of the negative charge, again, creating a stealth system and decreasing cellular uptake.

Correlating the uptake of the dendrimers with the zeta potential data shows that there may be an ideal zeta potential around -30 mV that promotes cellular uptake. In general, dendrimers with zeta potentials more negative than -30 mV had reduced cellular uptake (ie. G4.5) and dendrimers with zeta potentials greater than -30 mV (ie PEGylated

G3.5) also show lower uptake. Interestingly, incubation time-dependent behavior was observed between dendrimer generations. While there is no statistical difference between uptake of unmodified or PEGylated G3.5 at 30 and 60 minutes, there is a significant increase ($p < 0.01$) in uptake for the G4.5 dendrimers, suggesting that steady-state uptake of these larger dendrimers has not yet been achieved.

Dendrimers are known to be transported across Caco-2 cell monolayers by both transcellular and paracellular pathways [16, 18, 147, 148]. Uptake studies and tight junction modulation experiments in Caco-2 cells help to elucidate the relative contributions of these processes. Because PEGylation of G3.5 dendrimers decreases uptake, this surface modification may be of use in cases where it is desirable to transport the cargo across the cells while avoiding entrapment within the cells. Combining the uptake results with the occludin staining results allows us to understand the relative contributions of paracellular and transcellular transport of PEGylated dendrimers compared to unmodified dendrimers. In the case of G3.5 dendrimers, PEGylation causes a significant decrease in uptake and a moderate decrease in tight junction modulation, indicating that these dendrimers have less paracellular and less transcellular transport compared to unmodified dendrimers. By contrast, PEGylation of G4.5 dendrimers causes a modest increase in uptake and has only slightly more occludin accessibility than the control, suggesting that PEGylated G4.5 dendrimers have more transcellular transport and much less paracellular transport than unmodified G4.5 dendrimers. This sheds light on how PEGylation can impact transport mechanisms as well as overall transport rates. The strong correlation between the transport studies and the occludin staining studies

suggest that overall, anionic dendrimers are transported primarily through the paracellular route.

PAMAM dendrimers can be used for oral drug delivery to release drugs in the gastrointestinal tract and transport drugs into or across the intestinal barrier. PEGylation of PAMAM dendrimers can modulate toxicity, functionalize the surface for drug conjugation and facilitate drug release. While PEGylation decreases the transepithelial transport of anionic dendrimers, the conjugates still show appreciable transport, compared to traditional linear polymers [196], and have the potential for increased functionality. This work demonstrates that degree of PEGylation and dendrimer generation can modulate the mechanisms of transport, and can be custom tailored for different oral drug delivery applications.

5.5 Conclusion

In this Chapter we described the effect of PEGylation on cytotoxicity, uptake and transport of G3.5 and G4.5 anionic PAMAM dendrimers across Caco-2 cells. In the concentration range studied, PEGylation of these dendrimers maintained cell viability. PEGylation decreased uptake and transport for G3.5 dendrimers, whereas PEGylated G4.5 dendrimers demonstrated increased uptake with a concomitant decrease in overall dendrimer transport. Occludin staining of Caco-2 cell monolayers in the presence of conjugates showed that PEGylated dendrimers opened the tight junctions to a lesser extent than native dendrimers, indicating a reduction in paracellular transport. While PEGylated dendrimers showed decreased transport rates, they were still transported to an appreciable extent compared to traditional linear macromolecules [196] and offer

advantages of facilitated drug conjugation and release as well as potential for improved biodistribution. Together these studies demonstrate that in the design of PAMAM-PEG conjugates for oral drug delivery, the extent of transepithelial transport, uptake as well as the mechanism of transport can be controlled by a judicious choice of dendrimer generation and degree of PEGylation. These parameters can be custom-tailored to the specific needs of a desired drug delivery application.

Chapter 6 : Conclusions and Future Directions

6.1 Conclusions

Oral administration of polymer-drug conjugates for cancer treatment has the potential to improve the lives of cancer patients by reducing hospital visits and treatment costs while improving therapeutic efficacy of the drug by minimizing side effects and enhancing drug concentration at the tumor site. Due to the large number of emerging small molecule chemotherapy drugs with poor water solubility, low bioavailability and significant off-target toxicities, there is a significant need for orally administrable polymer therapeutics. As described in Chapter 2, it has been previously established that within a size and charge window, poly (amido amine) (PAMAM) dendrimers can permeate the epithelial layer of the gut. In this dissertation we evaluated anionic PAMAM dendrimers for their potential as oral drug delivery carriers and investigated the mechanisms by which they are transported across the epithelial barrier.

In Chapter 3 we demonstrated that G3.5 dendrimers are endocytosed by dynamin-dependent mechanisms, and that cellular internalization occurs by clathrin- and caveolin-mediated endocytosis while transcytosis is governed by clathrin-mediated pathways. We further confirmed the clathrin-endocytosis mechanism by monitoring G3.5 trafficking to the endosomes and lysosomes up to 30 minutes after cellular internalization. These studies illustrate that dendrimers take advantage of receptor-mediated mechanisms for cellular entry and can be found in the lysosomal and endosomal compartments after cellular uptake. This knowledge will aid in the design of PAMAM dendrimers for oral drug delivery in different potential applications. In the case of an oral therapy that is

locally targeted to the intestinal tissue for the treatment of diseases such as Crohn's, a pH-sensitive or lysosomal enzyme-cleavable linker could be used to promote drug release in the intestinal cells. Alternatively, in the case of a chemotherapy drug that must be targeted to a distant tumor site, the linker could be designed to avoid release in these compartments to minimize intestinal toxicity. Thus, knowledge of the cellular entry route and sub-cellular trafficking of the dendrimer carrier will aid in rational design of dendrimers for drug delivery applications. In Chapter 3, we monitored tight junction opening by dendrimers in the presence and absence of dynasore, a compound that inhibits dynamin-dependent endocytosis. Tight junction opening was found to be significantly decreased in the presence of dynasore suggesting that dendrimer cellular internalization may be a requisite step prior to opening of tight junctions by dendrimers. This implies that dendrimer modulation of tight junctions is not simply due to chelation of extracellular calcium, but may be a more complicated mechanism triggered by an intracellular signaling cascade that acts on the tight junction proteins. This illustrates the interconnectedness of the transcellular and paracellular routes. Importantly, this type of intracellular regulation is reversible, preventing permanent damage to the tight junctions and suggesting the safety of dendrimers as permeation enhancers.

In Chapter 4 we investigated G3.5-SN38 conjugates for oral delivery of the poorly-bioavailable chemotherapy drug SN38 in targeting colorectal hepatic metastases. In particular, we examined G3.5-Gly-SN38 and G3.5- β Ala-SN38 conjugates. These conjugates reduced the toxicity of SN38 towards intestinal cells and maintained Caco-2 cell viability with treatment concentrations of up to 100 μ M for 2 hours. This illustrates that the conjugates would be safe for oral administration and can minimize the known

gastrointestinal toxicities associated with SN38. In addition, both conjugates increased the transport of SN38 across Caco-2 cell monolayers, improving transport up to 160-fold compared to free drug, showing their potential in improving the oral bioavailability of SN38. Release profiles of the conjugates showed that G3.5- β Ala-SN38 was very stable, with only 1%, 4% and 8% release in SGF with pepsin, SIF with pancreatin and PBS with carboxylesterase at 6, 24 and 48 hours respectively. In contrast, G3.5-Gly-SN38 showed lower gastrointestinal stability with 10% and 20% released in the simulated gastric and intestinal environments with increased release in the presence of pancreatin compared to SIF alone. In addition, G3.5-Gly-SN38 released up to 56% of SN38 in the presence of liver carboxylesterase, suggesting the potential for controlled release in the liver environment. Finally, G3.5-Gly-SN38 and G3.5- β Ala-SN38 conjugates showed IC_{50} values of 0.60 and 3.59 μ M in HT-29 cells treated for 48 hours, suggesting their efficacy in the micromolar range in target colorectal cancer cells. These studies demonstrate that conjugation of SN38 to G3.5 dendrimers can reduce intestinal toxicity and improve oral bioavailability. Importantly, the linker chemistry (glycine vs. β -alanine) impacted the release profiles as well as the concentration-dependence in transport, illustrating the importance of choosing the appropriate linker for a given drug delivery application. G3.5-Gly-SN38 conjugates showed reasonable gastrointestinal stability with increased release in the presence of carboxylesterase, and an IC_{50} of 0.6 μ M in HT-29 cells suggesting their potential for oral therapy of colorectal hepatic metastases.

Finally, in Chapter 5 we investigated the impact of PEGylation on G3.5 and G4.5 dendrimers in the context of oral delivery. Conjugation of small PEG chains to dendrimers can improve biocompatibility, influence transport properties and serve as a

potential drug spacer. PEGylation decreased transport of G3.5 and G4.5 dendrimers and reduced tight junction opening, illustrating the importance of charge in tight junction modulation and transport. In addition, incremental PEGylation had differential effects on cellular uptake, with PEGylation decreasing G3.5 uptake while small amounts of PEGylation increased G4.5 uptake with additional PEGylation decreasing uptake. This suggests a balance between reducing charge-charge repulsion between anionic dendrimers and the negative cell membrane, enhancing cellular uptake, and creating a stealth system, reducing cellular uptake. These studies illustrate that even small changes in surface chemistry, particularly changes that cause reduction in dendrimer charge, can have significant impacts on cellular uptake, tight junction opening and overall transepithelial transport. Therefore, dendrimer-drug conjugates must be carefully designed in oral delivery applications to balance drug loading with permeability to create an effective drug delivery carrier. Taken together, these studies illustrate that anionic PAMAM dendrimers show potential in oral drug delivery and that with careful design they can be custom-tailored to a given application, enhancing intestinal permeability of the cargo while promoting specific release at the site of action.

6.2 Future Directions

While we have elucidated some details of the mechanism of transport and tight junction opening of G3.5 dendrimers, further studies should focus on identifying the signaling pathways involved in tight junction opening and the tight junction proteins that are affected. In particular, the impact of dendrimer treatment on claudin, ZO-1 and JAM should be investigated and the involvement of myosin light chain kinase in tight junction

opening should be determined. In addition, it is important to distinguish if tight junction modulation is due to reorganization of the tight junction proteins or if protein expression is being impacted. Comparison to permeation enhancers with known mechanisms of action such as EGTA and sodium caprate will also be useful to delineate the precise mechanism of dendrimer-mediated tight junction opening.

G3.5-Gly-SN38 shows promising *in vitro* results suggesting potential for oral therapy of colorectal hepatic metastases. Future studies should evaluate G3.5-Gly-SN38 *in vivo* activity including biodistribution after oral administration and efficacy studies in a colorectal hepatic metastasis mouse model. In addition, alternative linker chemistries should be investigated in order to optimize SN38 release in the presence of liver carboxylesterase. Since Gly-SN38 appears to be a substrate for carboxylesterase, peptide-Gly linkers or PEG-Gly linkers may enhance SN38 release by increasing accessibility of the ester bond to the active site of carboxylesterase. Computational modeling of the dendrimer-SN38 conjugate interaction with carboxylesterase may also be useful for linker selection. Strategies to improve drug loading on anionic dendrimers should also be investigated. Sub-optimal drug loading of SN38 was presumably due to low reactivity of the carboxylic acid terminal groups, low reactivity of the SN38 OH and steric hindrance. As an alternative strategy, the drug could be conjugated to amine-terminated dendrimers with subsequent modification of the remaining amine groups to carboxylic acid groups to complete the half-generation. Detailed studies should address the balance of drug loading with intestinal permeability.

Finally, while PEGylation decreased transport compared to unmodified dendrimers it still may be a useful surface modification or drug spacer for oral delivery

applications. Dendrimer-drug conjugates using PEG spacers should be synthesized to investigate if PEG can improve drug release in the presence of target enzymes without significantly decreasing permeability. In addition, higher generation dendrimers should be investigated for their greater potential of drug loading and enhanced EPR effect. In particular, it would be interesting to investigate the influence of polymer architecture as dendrimer generation increases on drug release and intestinal permeability. These proposed studies would serve to build upon the conclusions of this work and advance this research towards a fully realized oral dendrimer-drug delivery system.

Appendix 1: Visualization of Intracellular Trafficking of G3.5 Dendrimers and Transferrin in Caco-2 Cells

In Chapter 3, intracellular trafficking of Oregon Green-labeled G3.5 dendrimers and Alexa-Fluor-488-labeled transferrin (control) over time in Caco-2 cells was described. The presence of G3.5 and transferrin in the early endosomes and lysosomes at different time points was quantified by colocalization of green (dendrimer/ transferrin) and red (endosome/ lysosome) fluorescence by confocal microscopy. M_x , the colocalization coefficient, was reported as the average of four z-stacks for each treatment and time point. Colocalization of dendrimers with early endosomes and lysosomes provides further confirmation of clathrin-mediated endocytosis [18]. In addition, comparison of dendrimer trafficking patterns to transferrin, a classical clathrin RME ligand, allows for better understanding of the trafficking pathway and time course [198].

Figures A1.1 and A2.2 show sample images from each treatment and time point in the trafficking study. The early endosomes are present in the cells as punctate vesicles, often clustered toward the outside of the cell, away from the nucleus. In contrast, lysosomal proteins are found in close proximity to the nucleus and often overlap with the blue nuclear signal. These observations provide visual confirmation of the proper labeling of endosomal and lysosomal compartments. These images provide visual evidence of G3.5 dendrimer trafficking over time and are complementary to the colocalization quantification provided in Chapter 3.

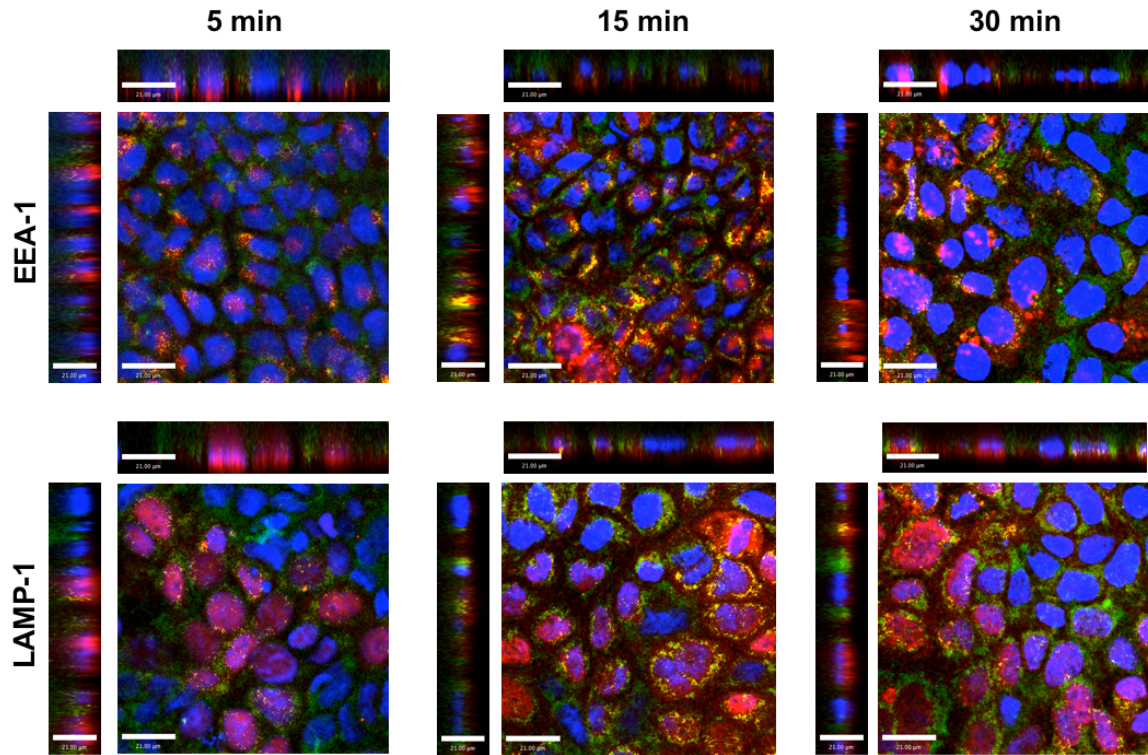


Figure A1.1. Visualization of G3.5 Dendrimer Trafficking over Time in Caco-2 Cells by Confocal Microscopy. G3.5 dendrimer is labeled with Oregon Green (green), early endosomes (EEA-1) and lysosomes are labeled with secondary antibody Alexa Fluor-568 goat anti-rabbit IgG (red) and the cell nuclei are labeled with DAPI (blue). Yellow regions indicate overlapping green and red signals (colocalization). Z-stacks are depicted as a main panel (xy plane), vertical panel (xz plane) and horizontal panel (yz plane).

Scale bar = 21 μm .

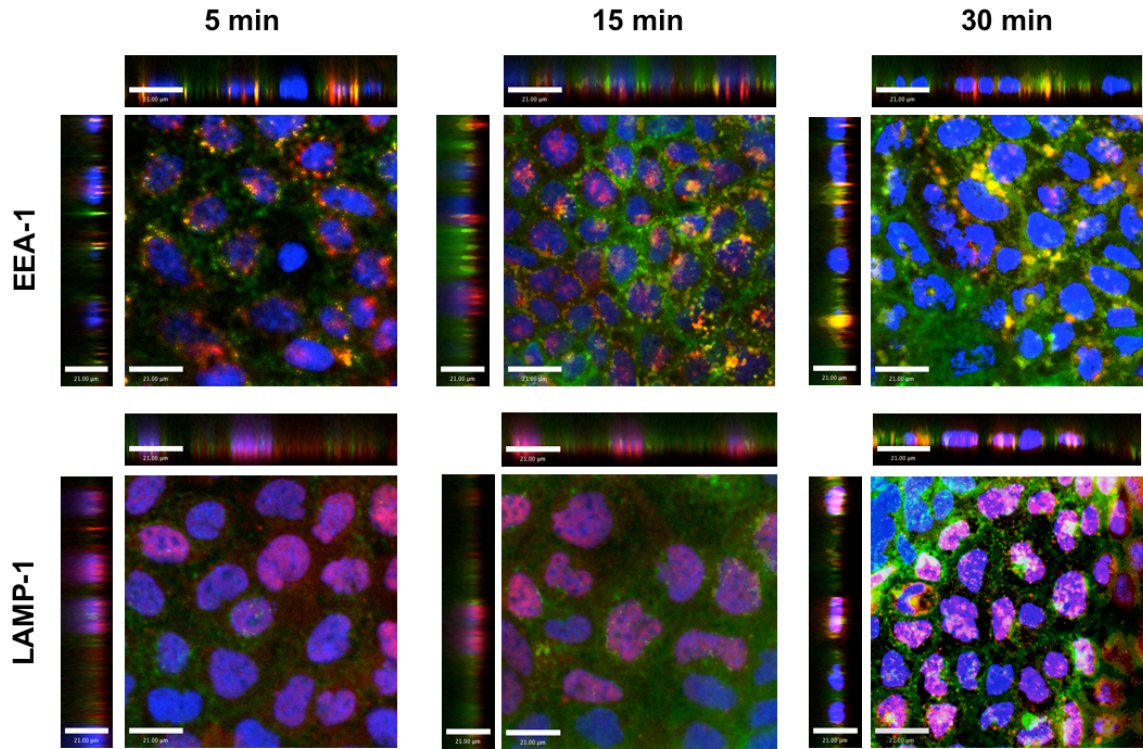


Figure A1.2. Visualization of Transferrin Trafficking over Time in Caco-2 Cells by Confocal Microscopy. Transferrin is labeled with Alexa Fluor-488 (green), early endosomes (EEA-1) and lysosomes are labeled with secondary antibody Alexa Fluor-568 goat anti-rabbit IgG (red) and the cell nuclei are labeled with DAPI (blue). Yellow regions indicate overlapping green and red signals (colocalization). Z-stacks are depicted as a main panel (xy plane), vertical panel (xz plane) and horizontal panel (yz plane). Scale bar = 21 μm .

Appendix 2: Quantification of SN38 by High Pressure Liquid Chromatography

In Chapter 4, stability studies of G3.5-SN38 conjugates were described where release of free SN38 over time was monitored by high pressure liquid chromatography (HPLC). Several HPLC methods to detect SN38 have been described in the literature [199, 200]. In this Appendix we will describe the detailed HPLC methods used to quantify SN38 release which have been adapted from Vijayalakshmi et al. [161].

As described in Chapter 4, release samples were dissolved in 50/50 DMSO/0.1 N HCl before HPLC analysis. This injection buffer was used to ensure that all SN38 is in the lactone, or closed ring form, which is favored at low pH. DMSO was used to solubilize the SN38 since SN38 has very low water solubility. A gradient method, with methanol and HPLC-grade water with 0.1% TFA as solvents, was used with a total flow rate of 1 ml per minute and an injection volume of 20 μ L. Table A2.1 shows the details of solvent flow during the 20-minute gradient method. Transitions between solvent compositions were accomplished by a linear gradient. The average retention time of SN38 was found to be 16.200 ± 0.014 min. A characteristic elution profile of SN38 is shown in Figure A2.1. Note that negative peaks were observed around 4-5 minutes due to DMSO present in the injection buffer.

Table A2.1. HPLC Gradient Method for SN38 Detection

Time (min)	% A (Water, 0.1% TFA)	% B (Methanol)	Total Flow Rate (ml/min)
0 (start)	90	10	1
14	20	80	1
16	0	100	1
16.1	90	10	1
20 (stop)	90	10	1

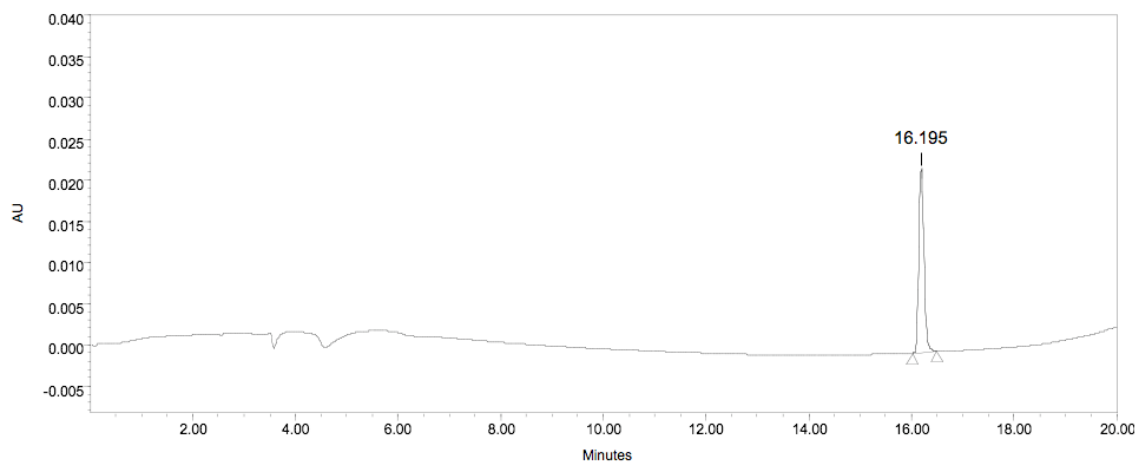


Figure A2.1. Typical HPLC Elution Profile of SN38. SN38 retention time was found to be 16.195 for this sample. Small negative peaks are typically seen around 4-5 minutes when DMSO is present in the sample injection buffer and are not due to SN38.

In order to quantify SN38 for release studies, a standard curve was developed for concentrations of SN38 from 0.05 $\mu\text{g/ml}$ to 12 $\mu\text{g/ml}$, corresponding to 0.5%-100% of drug content in G3.5-SN38 conjugates. Standard samples were prepared at 0.05, 0.1, 0.5, 1, 2, 4 and 12 $\mu\text{g/ml}$ with more focus on the lower concentrations as most of the release samples were found to occur in this concentration range. SN38 was prepared in a concentrated DMSO stock at 100 $\mu\text{g/ml}$ and used to make the direct injection standards in 50/50 DMSO/ 0.1 N HCl injection buffer. Standards were measured in triplicate and the concentration versus peak area was used to develop a linear correlation. Figure A2.2 shows the elution profiles of the 7 standard samples and Figure A2.3 shows the standard curve based on these direct injection standards. Finally, Figure A2.4 displays a single standard run in triplicate to illustrate the tight precision of the HPLC quantification.

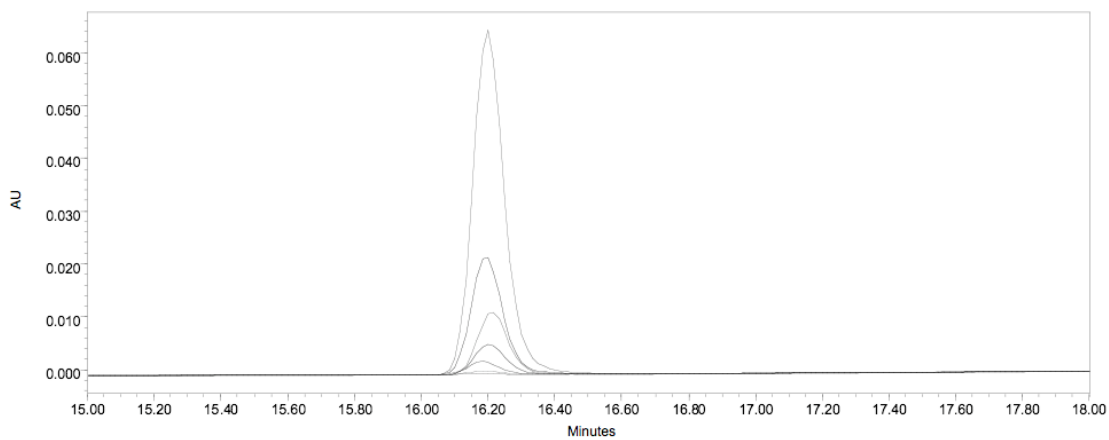


Figure A2.2. Standard Curve Elution Profiles. Samples are prepared at SN38 concentrations of 0.05, 0.1, 0.5, 1, 2, 4 and 12 $\mu\text{g/ml}$.

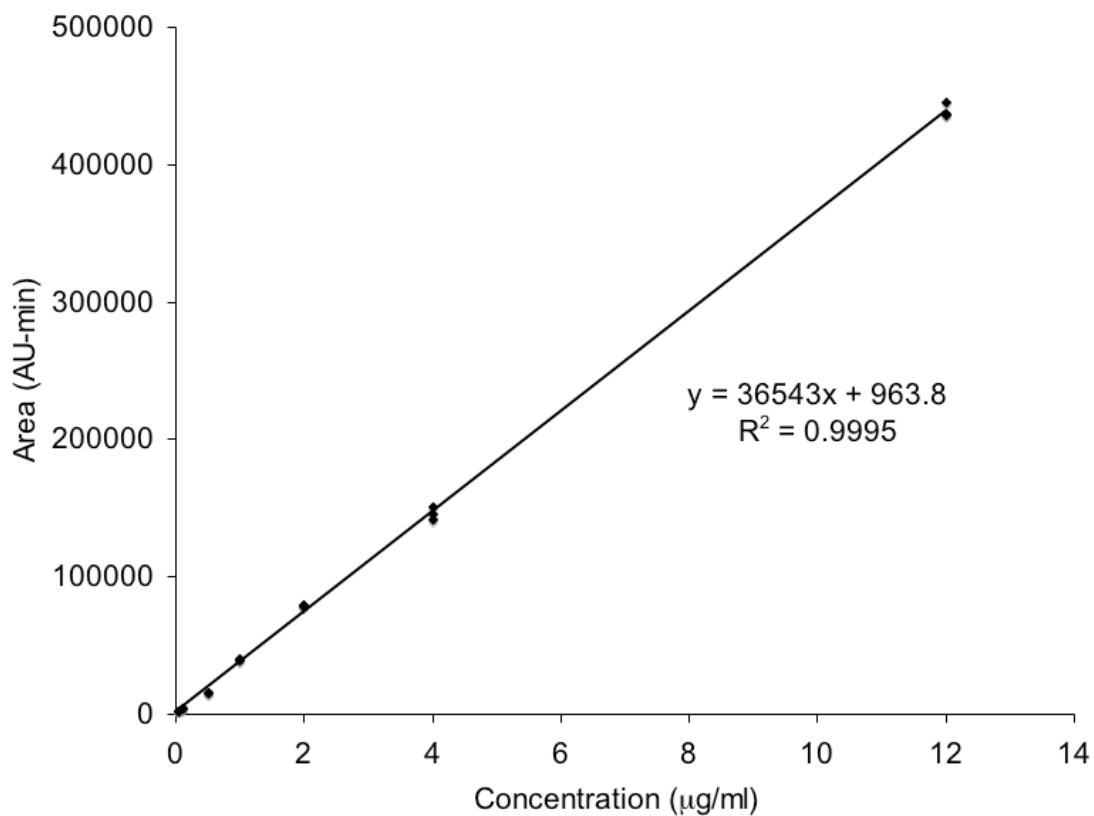


Figure A2.3. HPLC Standard Curve Comparing SN38 Concentration and Peak Area.

Samples are prepared at SN38 concentrations of 0.05, 0.1, 0.5, 1, 2, 4 and 12 µg/ml and analyzed in triplicate. R^2 of 0.9995 indicates a strong linear correlation.

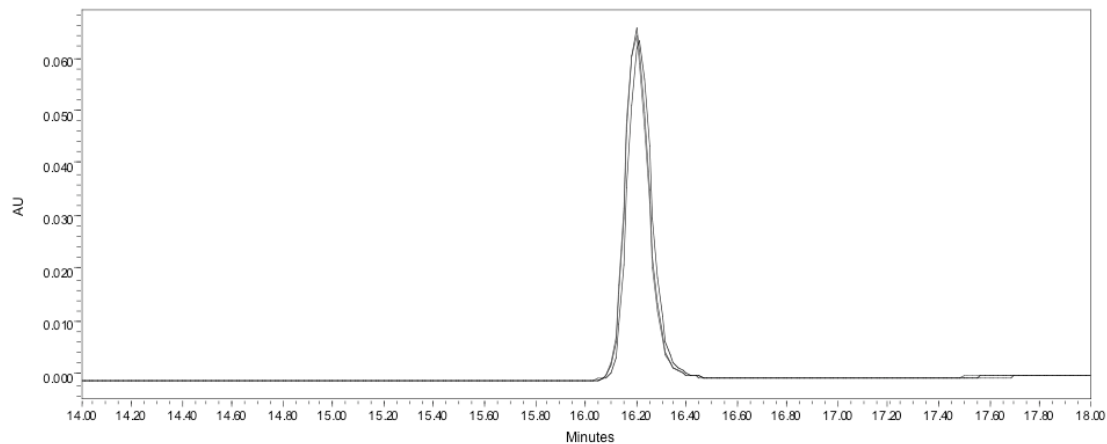


Figure A2.4. Precision of HPLC Detection. The HPLC chromatogram displays three separate injections of 12 $\mu\text{g/ml}$ SN38. Peak areas were 444,763, 436,916 and 435,529 AU-min, yielding a standard deviation of 4,979 or 1% of the average value. Retention times for the three peaks were 16.199, 16.201, 16.212, corresponding to an average value of 16.204 and a standard deviation of 0.0007 or 0.04% of the average.

Appendix 3: Quantification of PEG Content of PAMAM G3.5 and G4.5-PEG Conjugates by Proton Nuclear Magnetic Resonance

Nuclear Magnetic Resonance (NMR) has been applied to the characterization of dendrimers [201]. In particular, it is useful for monitoring conjugation reactions when the proton signals of the conjugated ligand are distinct from the proton signals of the dendrimer [149, 187]. As described in Chapter 5, ^1H NMR was used to quantify the number of PEG chains conjugated to G3.5 and G4.5 dendrimers by comparison of integration areas of dendrimer peaks (2.0-3.6 ppm) and PEG peaks (3.6-3.7 ppm). The general relationship comparing measured dendrimer and PEG areas with known numbers of protons is described by equation A3.1.

$$\frac{Area_{PEG}}{Area_{Dendrimer}} = \frac{\#PEG \times H_{PEG}}{H_{Dendrimer}} \quad (\text{Eqn. A3.1})$$

Solving for #PEG we obtain equation A3.2.

$$\#PEG = \frac{Area_{PEG}}{Area_{Dendrimer}} \times \frac{H_{Dendrimer}}{H_{PEG}} \quad (\text{Eqn A3.2})$$

Substituting known proton content for PEG750 (66), G3.5 (740) and G4.5 (1508) we derive equations A3.3 and A3.4 which can be used to calculate the number of PEG chains conjugated to G3.5 dendrimer and G4.5 dendrimers, respectively.

$$\#PEG / G3.5 = \frac{Area_{PEG}}{Area_{G3.5}} \times \frac{740}{66} \quad (\text{Eqn. A3.3})$$

$$\#PEG/G4.5 = \frac{Area_{PEG}}{Area_{G4.5}} \times \frac{1508}{66} \quad (\text{Eqn. A3.4})$$

Table A3.1 lists the dendrimer areas and PEG areas for each dendrimer-PEG conjugate along with the calculated number of PEGs per dendrimer. Figures A3.1 and A3.2 show the NMR scans of G3.5-1P, G3.5-1.4P, G3.5-2.3P, G4.5-.85P, G4.5-1.9P and G4.5-2.8P with the integration areas analyzed by Spinworks Software. These spectra illustrate that an incremental increase in the stoichiometric ratio of PEG used leads to an increase in the number of PEG chains conjugated to G3.5 and G4.5 dendrimers.

Table A3.1. Quantification of PEG Conjugation to G3.5 and G4.5 Dendrimers by ¹H NMR

Dendrimer Sample	Stoichiometric PEG Equivalents	PEG Area	Dendrimer Area	# PEG Conjugated
G3.5-P1	1	1.97	21.83	1.01
G3.5-P1.4	2	3.01	24.71	1.36
G3.5-P4.5	4	5.48	26.48	2.32
G4.5-P.85	1	0.49	12.99	0.85
G4.5-P1.9	2	0.85	10.46	1.86
G4.5-P2.8	4	3.11	25.39	2.80

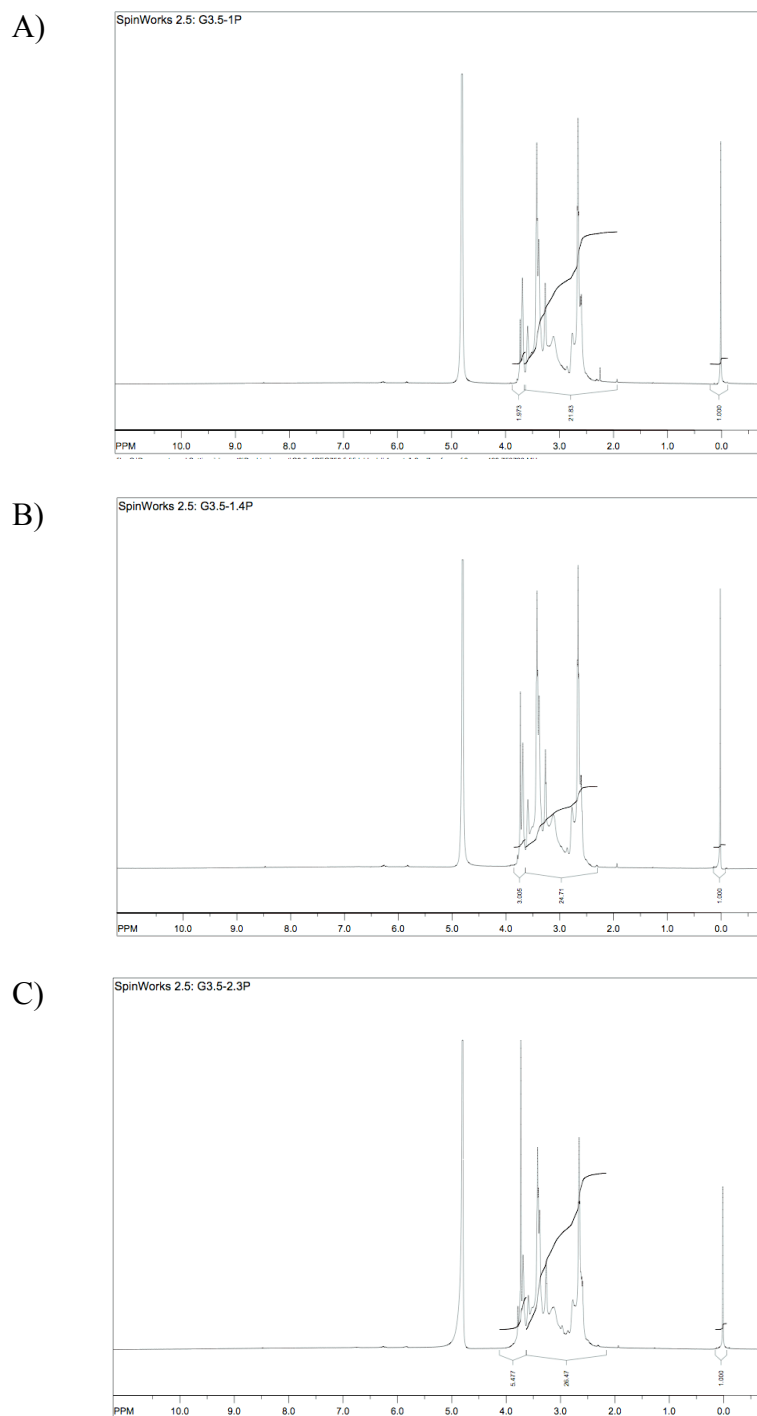


Figure A3.1. NMR Spectra of G3.5-PEG Conjugates. Feed molar ratios are 1 (A), 2 (B) and 4 (C) PEGs/ dendrimer. Dendrimer signals occur between 2.0 and 3.6 ppm and PEG signals occur between 3.6 and 3.7 ppm. TSP-d₄ standard is at 0 ppm.

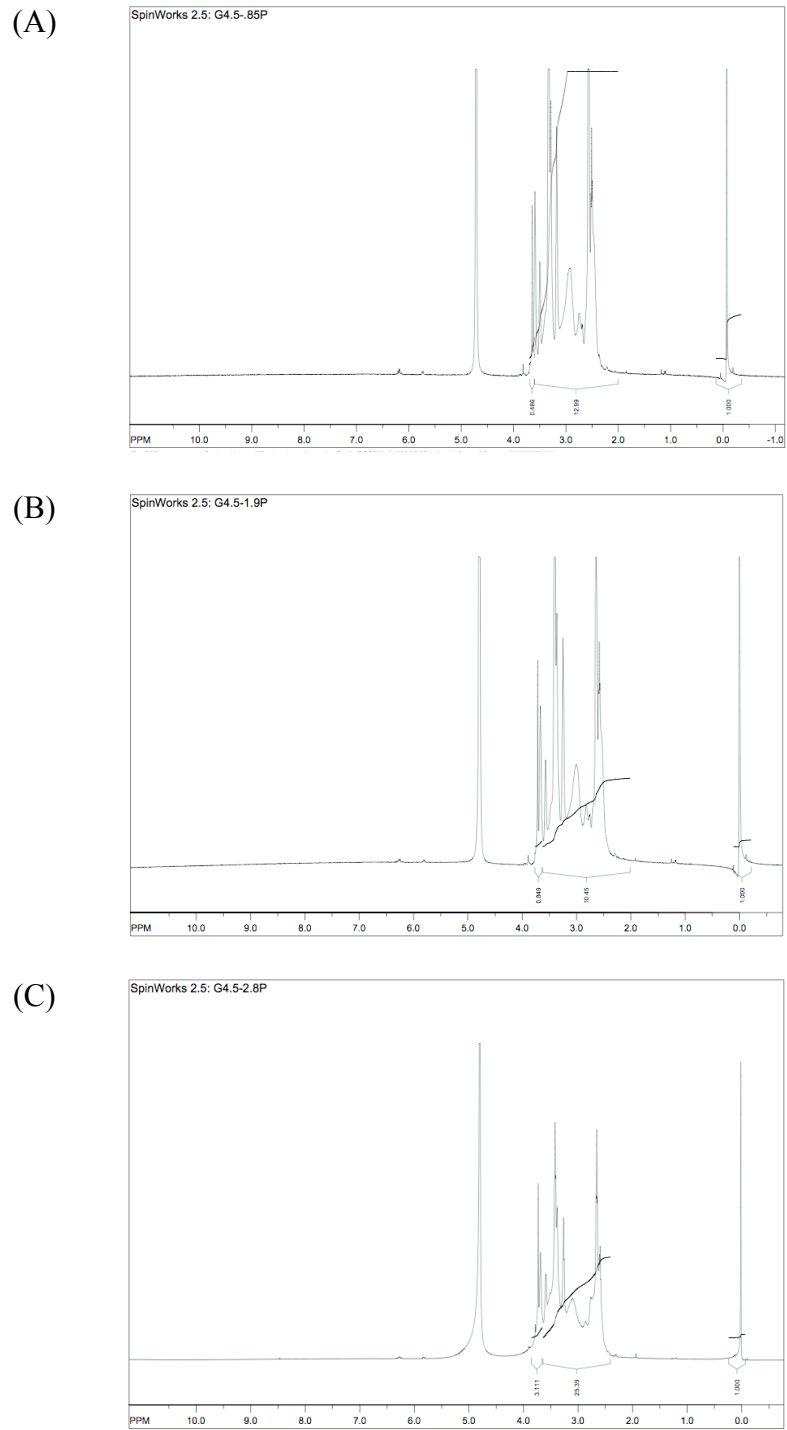


Figure A3.2. NMR spectra of G4.5-PEG Conjugates. Feed molar ratios are 1 (A), 2 (B) and 4 (C) PEGs/ dendrimer. Dendrimer signals occur between 2.0 and 3.6 ppm and PEG signals occur between 3.6 and 3.7 ppm. TSP-d₄ standard is at 0 ppm.

Bibliography

- [1] M.J. Vicent, R. Duncan, Polymer conjugates: nanosized medicines for treating cancer. *Trends Biotechnol.* 24(1) (2006) 39-47.
- [2] V. Torchilin, Multifunctional and stimuli-sensitive pharmaceutical nanocarriers. *Eur. J. Pharm. Biopharm.* 71(3) (2009) 431-444.
- [3] P. Debbage, Targeted drugs and nanomedicine: present and future. *Curr. Pharm. Des.* 15(2) (2009) 153-172.
- [4] H. Maeda, J. Wu, T. Sawa, Y. Matsumura, K. Hori, Tumor vascular permeability and the EPR effect in macromolecular therapeutics: a review. *J. Control. Release* 65(1-2) (2000) 271-284.
- [5] R. Duncan, Designing polymer conjugates as lysosomotropic nanomedicines. *Biochem. Soc. Trans.* 35(Pt 1) (2007) 56-60.
- [6] R. Duncan, The dawning era of polymer therapeutics. *Nat. Rev. Drug. Discov.* 2(5) (2003) 347-360.
- [7] M. Findlay, G. von Minckwitz, A. Wardley, Effective oral chemotherapy for breast cancer: pillars of strength. *Ann. Oncol.* 19(2) (2008) 212-222.
- [8] K. Le Lay, E. Myon, S. Hill, L. Riou-Franca, D. Scott, M. Sidhu, D. Dunlop, R. Launois, Comparative cost-minimisation of oral and intravenous chemotherapy for first-line treatment of non-small cell lung cancer in the UK NHS system. *Eur. J. Health Econ.* 8(2) (2007) 145-151.
- [9] S. Pashko, D.H. Johnson, Potential cost savings of oral versus intravenous etoposide in the treatment of small cell lung cancer. *Pharmacoeconomics* 1(4) (1992) 293-297.

- [10] M.D. Donovan, G.L. Flynn, G.L. Amidon, Absorption of polyethylene glycols 600 through 2000: the molecular weight dependence of gastrointestinal and nasal absorption. *Pharm. Res.* 7(8) (1990) 863-868.
- [11] G. Camenisch, J. Alsenz, H. van de Waterbeemd, G. Folkers, Estimation of permeability by passive diffusion through Caco-2 cell monolayers using the drugs' lipophilicity and molecular weight. *Eur. J. Pharm. Sci.* 6(4) (1998) 317-324.
- [12] D.A. Tomalia, L.A. Reyna, S. Svenson, Dendrimers as multi-purpose nanodevices for oncology drug delivery and diagnostic imaging. *Biochem. Soc. Trans.* 35(Pt 1) (2007) 61-67.
- [13] S. Svenson, D.A. Tomalia, Dendrimers in biomedical applications--reflections on the field. *Adv. Drug Delivery Rev.* 57(15) (2005) 2106-2129.
- [14] C.C. Lee, J.A. MacKay, J.M. Fréchet, F.C. Szoka, Designing dendrimers for biological applications. *Nat. Biotechnol.* 23(12) (2005) 1517-1526.
- [15] K.M. Kitchens, R.B. Kolhatkar, P.W. Swaan, N.D. Eddington, H. Ghandehari, Transport of poly (amido amine) dendrimers across Caco-2 cell monolayers: Influence of size, charge and fluorescent labeling. *Pharm. Res.* 23(12) (2006) 2818-2826.
- [16] K.M. Kitchens, M.E. El-Sayed, H. Ghandehari, Transepithelial and endothelial transport of poly (amido amine) dendrimers. *Adv. Drug Delivery Rev.* 57(15) (2005) 2163-2176.
- [17] R. Jevprasesphant, J. Penny, D. Attwood, N.B. McKeown, A. D'Emanuele, Engineering of dendrimer surfaces to enhance transepithelial transport and reduce cytotoxicity. *Pharm. Res.* 20(10) (2003) 1543-1550.

- [18] K. Kitchens, A. Foraker, R. Kolhatkar, P. Swaan, H. Ghandehari, Endocytosis and interaction of poly (amido amine) dendrimers with Caco-2 cells. *Pharm. Res.* 24(11) (2007) 2138-2145.
- [19] R. Jevprasesphant, J. Penny, D. Attwood, A. D'Emanuele, Transport of dendrimer nanocarriers through epithelial cells via the transcellular route. *J. Control. Release* 97 (2004) 259 – 267.
- [20] M. Najlah, S. Freeman, D. Attwood, A. D'Emanuele, In vitro evaluation of dendrimer prodrugs for oral drug delivery. *Int. J. Pharm.* 336(1) (2007) 183-190.
- [21] H. Ulukan, P.W. Swaan, Camptothecins: a review of their chemotherapeutic potential. *Drugs* 62(14) (2002) 2039-2057.
- [22] American Cancer Society. *Cancer Facts & Figures 2008*. Atlanta: American Cancer Society; 2008.
- [23] H. Shimada, K. Tanaka, I. Endou, Y. Ichikawa, Treatment for colorectal liver metastases: a review. *Langenbecks Arch. Surg.* 394(6) (2009) 973-983.
- [24] R. Kolhatkar, D. Sweet, H. Ghandehari, in: V. Torchilin (Ed.), *Multifunctional Pharmaceutical Nanocarriers*, Springer, New York, 2008, pp. 201-232.
- [25] D.S. Goldberg, H. Ghandehari, P.W. Swaan, Cellular entry of G3.5 poly (amido amine) dendrimers by clathrin- and dynamin-dependent endocytosis promotes tight junctional opening in intestinal epithelia. *Pharm. Res.* 27(8) (2010) 1547-1557.
- [26] D.S. Goldberg, N. Vijayalakshmi, P.W. Swaan, H. Ghandehari, G3.5 PAMAM dendrimers enhance transepithelial transport of SN38 while minimizing gastrointestinal toxicity. *J. Control. Release* (Submitted).

- [27] D. Sweet, R. Kolhatkar, A. Ray, P. Swaan, H. Ghandehari, Transepithelial transport of PEGylated anionic poly (amido amine) dendrimers: implications for oral drug delivery. *J. Control. Release* 138(1) (2009) 78-85.
- [28] A.M. Hillery, A.W. Lloyd, J. Swarbrick, *Drug Delivery and Targeting for Pharmacists and Pharmaceutical Scientists*, Taylor Francis, London, 2001.
- [29] S. Svenson, *Carrier-based Drug Delivery*, Oxford University Press, 2004.
- [30] V. Torchilin, *Nanoparticulates as Drug Carriers*, Imperial College Press, London, 2006.
- [31] G.S. Kwon, *Polymeric Drug Delivery Systems*, Taylor & Francis Group, Boca Raton, 2005.
- [32] T.A. Osswald, G. Menges, *Materials Science of Polymers for Engineers*, Carl Hanser, Munich, 2003.
- [33] H. Ringsdorf, Structure and properties of pharmacologically active polymers. *J. Polym. Sci. Symp.* 51 (1975) 135-153.
- [34] J.L. Richardson, G. Marks, A. Levine, The influence of symptoms of disease and side effects of treatment on compliance with cancer therapy. *J. Clin. Oncol.* 6(11) (1988) 1746-1752.
- [35] R. Duncan, Polymer conjugates as anticancer nanomedicines. *Nat. Rev. Cancer* 6(9) (2006) 688-701.
- [36] H. Maeda, G.Y. Bharate, J. Daruwalla, Polymeric drugs for efficient tumor-targeted drug delivery based on EPR-effect. *Eur. J. Pharm. Biopharm.* 71(3) (2009) 409-419.

- [37] T. Lammers, W.E. Hennink, G. Storm, Tumour-targeted nanomedicines: principles and practice. *Br. J. Cancer* 99(3) (2008) 392-397.
- [38] J. Kopecek, P. Kopeckova, HPMA copolymers: origins, early developments, present, and future. *Adv. Drug Delivery Rev.* 62(2) (2010) 122-149.
- [39] S.Q. Gao, Z.R. Lu, B. Petri, P. Kopeckova, J. Kopecek, Colon-specific 9-aminocamptothecin-HPMA copolymer conjugates containing a 1,6-elimination spacer. *J. Control. Release* 110(2) (2006) 323-331.
- [40] R. Duncan, M.J. Vicent, Do HPMA copolymer conjugates have a future as clinically useful nanomedicines? A critical overview of current status and future opportunities. *Adv. Drug Delivery Rev.* 62(2) (2010) 272-282.
- [41] L.W. Seymour, D.R. Ferry, D.J. Kerr, D. Rea, M. Whitlock, R. Poyner, C. Boivin, S. Hesslewood, C. Twelves, R. Blackie, A. Schatzlein, D. Jodrell, D. Bissett, H. Calvert, M. Lind, A. Robbins, S. Burtles, R. Duncan, J. Cassidy, Phase II studies of polymer-doxorubicin (PK1, FCE28068) in the treatment of breast, lung and colorectal cancer. *Int. J. Oncol.* 34(6) (2009) 1629-1636.
- [42] L.W. Seymour, D.R. Ferry, D. Anderson, S. Hesslewood, P.J. Julyan, R. Poyner, J. Doran, A.M. Young, S. Burtles, D.J. Kerr, Hepatic drug targeting: phase I evaluation of polymer-bound doxorubicin. *J. Clin. Oncol.* 20(6) (2002) 1668-1676.
- [43] D.P. Nowotnik, E. Cvitkovic, ProLindac (AP5346): a review of the development of an HPMA DACH platinum polymer therapeutic. *Adv. Drug Delivery Rev.* 61(13) (2009) 1214-1219.
- [44] G. Pasut, F.M. Veronese, PEG conjugates in clinical development or use as anticancer agents: an overview. *Adv. Drug Delivery Rev.* 61(13) (2009) 1177-1188.

- [45] C. Li, S. Wallace, Polymer-drug conjugates: recent development in clinical oncology. *Adv. Drug Delivery Rev.* 60(8) (2008) 886-898.
- [46] C. Li, D.F. Yu, R.A. Newman, F. Cabral, L.C. Stephens, N. Hunter, L. Milas, S. Wallace, Complete regression of well-established tumors using a novel water-soluble poly(L-glutamic acid)-paclitaxel conjugate. *Cancer Res.* 58(11) (1998) 2404-2409.
- [47] G. Mustata, S.M. Dinh, Approaches to oral drug delivery for challenging molecules. *Crit. Rev. Ther. Drug Carrier Syst.* 23(2) (2006) 111-135.
- [48] M.D. DeMario, M.J. Ratain, Oral chemotherapy: rationale and future directions. *J. Clin. Oncol.* 16(7) (1998) 2557-2567.
- [49] F. Gabor, C. Fillafer, L. Neusch, G. Ratzinger, M. Wirth, Improving oral delivery. *Handb. Exp. Pharmacol.*(197) (2010) 345-398.
- [50] S.K. Lai, Y.Y. Wang, J. Hanes, Mucus-penetrating nanoparticles for drug and gene delivery to mucosal tissues. *Adv. Drug Delivery Rev.* 61(2) (2009) 158-171.
- [51] L.R. Johson, *Physiology of the Gastrointestinal Tract*, Raven Press, New York, 1994.
- [52] A.M. Marchiando, W.V. Graham, J.R. Turner, Epithelial barriers in homeostasis and disease. *Annu. Rev. Pathol.* 5 (2010) 119-144.
- [53] J.R. Turner, Intestinal mucosal barrier function in health and disease. *Nat. Rev. Immunol.* 9(11) (2009) 799-809.
- [54] S.C. Corr, C.C. Gahan, C. Hill, M-cells: origin, morphology and role in mucosal immunity and microbial pathogenesis. *FEMS Immunol. Med. Microbiol.* 52(1) (2008) 2-12.

- [55] M. Kondoh, K. Yagi, Tight junction modulators: promising candidates for drug delivery. *Curr. Med. Chem.* 14(23) (2007) 2482-2488.
- [56] M. Furuse, T. Hirase, M. Itoh, A. Nagafuchi, S. Yonemura, S. Tsukita, Occludin: a novel integral membrane protein localizing at tight junctions. *J. Cell Biol.* 123(6 Pt 2) (1993) 1777-1788.
- [57] M.S. Balda, K. Matter, Transmembrane proteins of tight junctions. *Semin. Cell Dev. Biol.* 11(4) (2000) 281-289.
- [58] M. Furuse, H. Sasaki, K. Fujimoto, S. Tsukita, A single gene product, claudin-1 or -2, reconstitutes tight junction strands and recruits occludin in fibroblasts. *J. Cell Biol.* 143(2) (1998) 391-401.
- [59] M. Furuse, K. Fujita, T. Hiiragi, K. Fujimoto, S. Tsukita, Claudin-1 and -2: novel integral membrane proteins localizing at tight junctions with no sequence similarity to occludin. *J. Cell Biol.* 141(7) (1998) 1539-1550.
- [60] I. Martin-Padura, S. Lostaglio, M. Schneemann, L. Williams, M. Romano, P. Fruscella, C. Panzeri, A. Stoppacciaro, L. Ruco, A. Villa, D. Simmons, E. Dejana, Junctional adhesion molecule, a novel member of the immunoglobulin superfamily that distributes at intercellular junctions and modulates monocyte transmigration. *J. Cell Biol.* 142(1) (1998) 117-127.
- [61] J. Ikenouchi, M. Furuse, K. Furuse, H. Sasaki, S. Tsukita, Tricellulin constitutes a novel barrier at tricellular contacts of epithelial cells. *J. Cell Biol.* 171(6) (2005) 939-945.
- [62] M.A. Deli, Potential use of tight junction modulators to reversibly open membranous barriers and improve drug delivery. *Biochim. Biophys. Acta.* 1788(4) (2009) 892-910.

- [63] J.L. Madara, J.R. Pappenheimer, Structural basis for physiological regulation of paracellular pathways in intestinal epithelia. *J. Membr. Biol.* 100(2) (1987) 149-164.
- [64] T.Y. Ma, D. Tran, N. Hoa, D. Nguyen, M. Merryfield, A. Tarnawski, Mechanism of extracellular calcium regulation of intestinal epithelial tight junction permeability: role of cytoskeletal involvement. *Microsc. Res. Tech.* 51(2) (2000) 156-168.
- [65] C.J. Watson, M. Rowland, G. Warhurst, Functional modeling of tight junctions in intestinal cell monolayers using polyethylene glycol oligomers. *Am. J. Physiol. Cell Physiol.* 281(2) (2001) C388-397.
- [66] G.T. Knipp, N.F. Ho, C.L. Barsuhn, R.T. Borchardt, Paracellular diffusion in Caco-2 cell monolayers: effect of perturbation on the transport of hydrophilic compounds that vary in charge and size. *J. Pharm. Sci.* 86(10) (1997) 1105-1110.
- [67] S.J. Fisher, P.W. Swaan, N.D. Eddington, The ethanol metabolite acetaldehyde increases paracellular drug permeability in vitro and oral bioavailability in vivo. *J. Pharmacol. Exp. Ther.* 332(1) (2010) 326-333.
- [68] H. Inokuchi, T. Takei, K. Aikawa, M. Shimizu, The effect of hyperosmosis on paracellular permeability in Caco-2 cell monolayers. *Biosci. Biotechnol. Biochem.* 73(2) (2009) 328-334.
- [69] S.M. Krug, S. Amasheh, J.F. Richter, S. Milatz, D. Günzel, J.K. Westphal, O. Huber, J.D. Schulzke, M. Fromm, Tricellulin forms a barrier to macromolecules in tricellular tight junctions without affecting ion permeability. *Mol. Biol. Cell* 20(16) (2009) 3713-3724.
- [70] V.H.L. Lee, Membrane Transporters. *Eur. J. Pharm. Sci.* 11(Suppl 2) (2000) S41-S50.

- [71] P.W. Swaan, Recent advances in intestinal macromolecular drug delivery via receptor-mediated transport pathways. *Pharm. Res.* 15(6) (1998) 826-834.
- [72] L. Bareford, P. Swaan, Endocytic mechanisms for targeted drug delivery. *Adv. Drug Delivery Rev.* 59 (2007) 748-758.
- [73] P. Lajoie, I.R. Nabi, Lipid rafts, caveolae, and their endocytosis. *Int. Rev. Cell Mol. Biol.* 282 (2010) 135-163.
- [74] C.A. Lipinski, F. Lombardo, B.W. Dominy, P.J. Feeney, Experimental and computational approaches to estimate solubility and permeability in drug discovery and development settings. *Adv. Drug Delivery Rev.* 46(1-3) (2001) 3-26.
- [75] K. Beaumont, R. Webster, I. Gardner, K. Dack, Design of ester prodrugs to enhance oral absorption of poorly permeable compounds: challenges to the discovery scientist. *Curr. Drug Metab.* 4(6) (2003) 461-485.
- [76] G.L. Amidon, H. Lenernas, V.P. Shah, J.R. Crison, A theoretical basis for a biopharmaceutic drug classification: the correlation of in vitro drug product dissolution and in vivo bioavailability. *Pharm. Res.* 12(3) (1995) 413-420.
- [77] A. Dahan, J.M. Miller, G.L. Amidon, Prediction of solubility and permeability class membership: provisional BCS classification of the world's top oral drugs. *The AAPS Journal* 11(4) (2009) 740-746.
- [78] T. Hou, Y. Li, W. Zhang, J. Wang, Recent developments of in silico predictions of intestinal absorption and oral bioavailability. *Comb. Chem. High Throughput Screen.* 12(5) (2009) 497-506.

- [79] T. Hou, J. Wang, W. Zhang, X. Xu, ADME evaluation in drug discovery. 7. Prediction of oral absorption by correlation and classification. *J. Chem. Inf. Model.* 47(1) (2007) 208-218.
- [80] T. Hou, J. Wang, W. Zhang, X. Xu, ADME evaluation in drug discovery. 6. Can oral bioavailability in humans be effectively predicted by simple molecular property-based rules? *J. Chem. Inf. Model.* 47(2) (2007) 460-463.
- [81] M. Kansy, F. Senner, K. Gubernator, Physicochemical high throughput screening: parallel artificial membrane permeation assay in the description of passive absorption processes. *J. Med. Chem.* 41(7) (1998) 1007-1010.
- [82] B. Faller, Artificial membrane assays to assess permeability. *Curr. Drug Metab.* 9(9) (2008) 886-892.
- [83] I.J. Hidalgo, T.J. Raub, R.T. Borchardt, Characterization of the human colon carcinoma cell line (Caco-2) as a model system for intestinal epithelial permeability. *Gastroenterology* 96(3) (1989) 736-749.
- [84] S. Skolnik, X. Lin, J. Wang, X.H. Chen, T. He, B. Zhang, Towards prediction of in vivo intestinal absorption using a 96-well Caco-2 assay. *J. Pharm. Sci.* 99(7) (2010) 3246-3265.
- [85] V. Meunier, M. Bourrie, Y. Berger, G. Fabre, The human intestinal epithelial cell line Caco-2; pharmacological and pharmacokinetic applications. *Cell Biol. Toxicol.* 11(3-4) (1995) 187-194.
- [86] D.A. Volpe, Variability in Caco-2 and MDCK cell-based intestinal permeability assays. *J. Pharm. Sci.* 97(2) (2008) 712-725.

- [87] H. Bohets, P. Annaert, G. Mannens, L. Van Beijsterveldt, K. Anciaux, P. Verboven, W. Meuldermans, K. Lavrijssen, Strategies for absorption screening in drug discovery and development. *Curr. Top. Med. Chem.* 1(5) (2001) 367-383.
- [88] S. Yee, In vitro permeability across Caco-2 cells (colonic) can predict in vivo (small intestinal) absorption in man--fact or myth. *Pharm. Res.* 14(6) (1997) 763-766.
- [89] H. Yu, T.J. Cook, P.J. Sinko, Evidence for diminished functional expression of intestinal transporters in Caco-2 cell monolayers at high passages. *Pharm. Res.* 14(6) (1997) 757-762.
- [90] S. Yamashita, K. Konishi, Y. Yamazaki, Y. Taki, New and better protocols for a short-term Caco-2 cell culture system. *J. Pharm. Sci.* 91(3) (2002) 669-679.
- [91] J.D. Irvine, L. Takahashi, K. Lockhart, J. Cheong, J.W. Tolan, H.E. Selick, J.R. Grove, MDCK (Madin-Darby Canine Kidney) cells: A tool for membrane permeability screening. *J. Pharm. Sci.* 88(1) (1999) 28-33.
- [92] M.C. Gres, B. Julian, M. Bourrie, V. Meunier, C. Roques, M. Berger, X. Boulenc, Y. Berger, G. Fabre, Correlation between oral drug absorption in humans, and apparent drug permeability in TC-7 cells, a human epithelial intestinal cell line: comparison with the parental Caco-2 cell line. *Pharm. Res.* 15(5) (1998) 726-733.
- [93] C. Hilgendorf, H. Spahn-Langguth, C.G. Regardh, E. Lipka, G.L. Amidon, P. Langguth, Caco-2 versus Caco-2/HT29-MTX co-cultured cell lines: permeabilities via diffusion, inside- and outside-directed carrier-mediated transport. *J. Pharm. Sci.* 89(1) (2000) 63-75.

- [94] T.H. Wilson, G. Wiseman, The use of sacs of everted small intestine for the study of the transference of substances from the mucosal to the serosal surface. *J. Physiol.* 123(1) (1954) 116-125.
- [95] H. Levi, H.H. Ussing, Resting potential and ion movements in the frog skin. *Nature* 164(4178) (1949) 928-929.
- [96] G.M. Grass, S.A. Sweetana, In vitro measurement of gastrointestinal tissue permeability using a new diffusion cell. *Pharm. Res.* 5(6) (1988) 372-376.
- [97] V.J. Stella, in: V. J. Stella (Ed.), *Prodrugs: Challenges and Rewards*, Springer, 2007, pp. 3-36.
- [98] T. Heimbach, D. Fleisher, A. Kaddoumi, in: V. J. Stella (Ed.), *Prodrugs: Challenges and Rewards*, Springer, 2007, pp. 157-215.
- [99] A. Mantyla, J. Rautio, T. Nevalainen, P. Keski-Rahkonen, J. Vepsalainen, T. Jarvinen, Design, synthesis and in vitro evaluation of novel water-soluble prodrugs of buparvaquone. *Eur. J. Pharm. Sci.* 23(2) (2004) 151-158.
- [100] V.J. Stella, K.W. Nti-Addae, Prodrug strategies to overcome poor water solubility. *Adv. Drug Delivery Rev.* 59(7) (2007) 677-694.
- [101] V.J. Stella, in: V. J. Stella (Ed.), *Prodrugs: Challenges and Rewards*, Springer, 2007, pp. 37-82.
- [102] I.E. Kuppens, P. Breedveld, J.H. Beijnen, J.H. Schellens, Modulation of oral drug bioavailability: from preclinical mechanism to therapeutic application. *Cancer Invest.* 23(5) (2005) 443-464.

- [103] C.M. Kruijtzer, J.H. Beijnen, J.H. Schellens, Improvement of oral drug treatment by temporary inhibition of drug transporters and/or cytochrome P450 in the gastrointestinal tract and liver: an overview. *Oncologist* 7(6) (2002) 516-530.
- [104] D.F. Kehrer, R.H. Mathijssen, J. Verweij, P. de Bruijn, A. Sparreboom, Modulation of irinotecan metabolism by ketoconazole. *J. Clin. Oncol.* 20(14) (2002) 3122-3129.
- [105] D.J. Kempf, K.C. Marsh, G. Kumar, A.D. Rodrigues, J.F. Denissen, E. McDonald, M.J. Kukulka, A. Hsu, G.R. Granneman, P.A. Baroldi, E. Sun, D. Pizzuti, J.J. Plattner, D.W. Norbeck, J.M. Leonard, Pharmacokinetic enhancement of inhibitors of the human immunodeficiency virus protease by coadministration with ritonavir. *Antimicrob. Agents Chemother.* 41(3) (1997) 654-660.
- [106] M. Tomita, M. Hayashi, S. Awazu, Absorption-enhancing mechanism of EDTA, caprate, and decanoylcarnitine in Caco-2 cells. *J. Pharm. Sci.* 85(6) (1996) 608-611.
- [107] M.J. Cano-Cebrian, T. Zornoza, L. Granero, A. Polache, Intestinal absorption enhancement via the paracellular route by fatty acids, chitosans and others: a target for drug delivery. *Curr. Drug Deliv.* 2(1) (2005) 9-22.
- [108] A. Bernkop-Schnurch, in: A. Bernkop-Schnurch (Ed.), *Oral Delivery of Macromolecular Drugs: Barriers, Strategies and Future Trends*, Springer, New York, 2009, pp. 85-101.
- [109] A. Fasano, S. Uzzau, Modulation of intestinal tight junctions by Zonula occludens toxin permits enteral administration of insulin and other macromolecules in an animal model. *J. Clin. Invest.* 99(6) (1997) 1158-1164.

- [110] H.E. Junginger, in: A. Bernkop-Schunurch (Ed.), Oral Delivery of Macromolecular Drugs: Barriers, Strategies and Future Trends, Springer, New York, 2009, pp. 103-122.
- [111] R.C. Lindenschmidt, L.C. Stone, J.L. Seymour, R.L. Anderson, P.A. Forshey, M.J. Winrow, Effects of oral administration of a high-molecular-weight crosslinked polyacrylate in rats. *Fundam. Appl. Toxicol.* 17(1) (1991) 128-135.
- [112] N.G. Schipper, K.M. Varum, P. Artursson, Chitosans as absorption enhancers for poorly absorbable drugs. 1: Influence of molecular weight and degree of acetylation on drug transport across human intestinal epithelial (Caco-2) cells. *Pharm. Res.* 13(11) (1996) 1686-1692.
- [113] A. D'Emanuele, R. Jevprasesphant, J. Penny, D. Attwood, The use of a dendrimer-propranolol prodrug to bypass efflux transporters and enhance oral bioavailability. *J. Control. Release* 95(3) (2004) 447-453.
- [114] D.A. Tomalia, Birth of a new macromolecular architecture: dendrimers as quantized building blocks for nanoscale synthetic polymer chemistry. *Prog. Polym. Sci.* 30 (2005) 294-324.
- [115] D.A. Tomalia, J.M. Frechet, *Dendrimers and Other Dendritic Polymers*, John Wiley & Sons, West Sussex, 2001.
- [116] T.D. McCarthy, P. Karellas, S.A. Henderson, M. Giannis, D.F. O'Keefe, G. Heery, J.R. Paull, B.R. Matthews, G. Holan, Dendrimers as drugs: discovery and preclinical and clinical development of dendrimer-based microbicides for HIV and STI prevention. *Mol. Pharm.* 2(4) (2005) 312-318.

- [117] H.L. Crampton, E.E. Simanek, Dendrimers as drug delivery vehicles: non-covalent interactions of bioactive compounds with dendrimers. *Polym. Int.* 56 (2007) 489-496.
- [118] P. Couck, R. Claeys, E. Vanderstraeten, F.K. Gorus, Evaluation of the Stratus CS fluorometer for the determination of plasma myoglobin. *Acta Clin. Belg.* 60(2) (2005) 75-78.
- [119] A. D'Emanuele, D. Attwood, Dendrimer-drug interactions. *Adv. Drug Delivery Rev.* 57(15) (2005) 2147-2162.
- [120] M. Na, C. Yiyun, X. Tongwen, D. Yang, W. Xiaomin, L. Zhenwei, C. Zhichao, H. Guanyi, S. Yunyu, W. Longping, Dendrimers as potential drug carriers. Part II. Prolonged delivery of ketoprofen by in vitro and in vivo studies. *Eur. J. Med. Chem.* 41(5) (2006) 670-674.
- [121] U. Gupta, H.B. Agashe, A. Asthana, N.K. Jain, A review of in vitro-in vivo investigations on dendrimers: the novel nanoscopic drug carriers. *Nanomedicine* 2(2) (2006) 66-73.
- [122] R. Wiwattanapatapee, L. Lomlim, K. Saramunee, Dendrimers conjugates for colonic delivery of 5-aminosalicylic acid. *J. Control. Release* 88(1) (2003) 1-9.
- [123] C. Yiyun, X. Tongwen, Dendrimers as potential drug carriers. Part I. Solubilization of non-steroidal anti-inflammatory drugs in the presence of polyamidoamine dendrimers. *Eur. J. Med. Chem.* 40(11) (2005) 1188-1192.
- [124] A.S. Chauhan, N.K. Jain, P.V. Diwan, A.J. Khopade, Solubility enhancement of indomethacin with poly(amidoamine) dendrimers and targeting to inflammatory regions of arthritic rats. *J. Drug Target.* 12(9-10) (2004) 575-583.

- [125] A. Quintana, E. Raczka, L. Piehler, I. Lee, A. Myc, I. Majoros, A.K. Patri, T. Thomas, J. Mule, J.R. Baker, Jr., Design and function of a dendrimer-based therapeutic nanodevice targeted to tumor cells through the folate receptor. *Pharm. Res.* 19(9) (2002) 1310-1316.
- [126] G. Wu, R.F. Barth, W. Yang, S. Kawabata, L. Zhang, K. Green-Church, Targeted delivery of methotrexate to epidermal growth factor receptor-positive brain tumors by means of cetuximab (IMC-C225) dendrimer bioconjugates. *Mol. Cancer Ther.* 5(1) (2006) 52-59.
- [127] S.D. Konda, M. Aref, S. Wang, M. Brechbiel, E.C. Wiener, Specific targeting of folate-dendrimer MRI contrast agents to the high affinity folate receptor expressed in ovarian tumor xenografts. *Magn. Reson. Mater. Phys., Biol. Med* 12(2-3) (2001) 104-113.
- [128] A. Florence, Dendrimers: a versatile targeting platform. *Adv. Drug Delivery Rev.* 57(15) (2005) 2101-2286.
- [129] Y. Koyama, V.S. Talanov, M. Bernardo, Y. Hama, C.A. Regino, M.W. Brechbiel, P.L. Choyke, H. Kobayashi, A dendrimer-based nanosized contrast agent dual-labeled for magnetic resonance and optical fluorescence imaging to localize the sentinel lymph node in mice. *J. Magn. Reson. Imaging* 25(4) (2007) 866-871.
- [130] H. Kobayashi, S. Kawamoto, R.A. Star, T.A. Waldmann, Y. Tagaya, M.W. Brechbiel, Micro-magnetic resonance lymphangiography in mice using a novel dendrimer-based magnetic resonance imaging contrast agent. *Cancer Res.* 63(2) (2003) 271-276.

- [131] S. Langereis, Q.G. de Lussanet, M.H. van Genderen, E.W. Meijer, R.G. Beets-Tan, A.W. Griffioen, J.M. van Engelshoven, W.H. Backes, Evaluation of Gd(III)DTPA-terminated poly(propylene imine) dendrimers as contrast agents for MR imaging. *NMR Biomed.* 19(1) (2006) 133-141.
- [132] Y. Choi, T. Thomas, A. Kotlyar, M.T. Islam, J.R. Baker, Synthesis and functional evaluation of DNA-assembled polyamidoamine dendrimer clusters for cancer cell-specific targeting. *Chem. Biol.* 12(1) (2005) 35-43.
- [133] M. Mamede, T. Saga, T. Ishimori, T. Higashi, N. Sato, H. Kobayashi, M.W. Brechbiel, J. Konishi, Hepatocyte targeting of ¹¹¹In-labeled oligo-DNA with avidin or avidin-dendrimer complex. *J. Control. Release* 95(1) (2004) 133-141.
- [134] C.J. Hawker, J.M. Frechet, Preparation of polymers with controlled molecular architecture. A new convergent approach to dendritic macromolecules. *J. Am. Chem. Soc.* 112 (1990) 7638-7647.
- [135] F. Vogtle, M. Gorka, R. Hesse, P. Ceroni, M. Maestri, V. Balzani, Photochemical and photophysical properties of poly(propylene amine) dendrimers with peripheral naphthalene and azobenzene groups. *Photochem. Photobiol. Sci.* 1(1) (2002) 45-51.
- [136] R. Esfand, D.A. Tomalia, Poly (amidoamine)(PAMAM) dendrimers: from biomimicry to drug delivery and biomedical applications. *Drug Discov. Today* 6(8) (2001) 427-426.
- [137] V.K. Yellepeddi, A. Kumar, S. Palakurthi, Surface modified poly (amido amine) dendrimers as diverse nanomolecules for biomedical applications. *Expert Opin. Drug Deliv.* 6(8) (2009) 835-850.

- [138] V.J. Venditto, C.A. Regino, M.W. Brechbiel, PAMAM dendrimer based macromolecules as improved contrast agents. *Mol. Pharm.* 2(4) (2005) 302-311.
- [139] R. Duncan, L. Izzo, Dendrimer biocompatibility and toxicity. *Adv. Drug Delivery Rev.* 57(15) (2005) 2215-2237.
- [140] N. Malik, R. Wiwattanapatapee, R. Klopsch, K. Lorenz, H. Frey, J.W. Weener, E.W. Meijer, W. Paulus, R. Duncan, Dendrimers: relationship between structure and biocompatibility in vitro, and preliminary studies on the biodistribution of 125I-labelled polyamidoamine dendrimers in vivo. *J. Control. Release* 65(1-2) (2000) 133-148.
- [141] N. Malik, E.G. Evagorou, R. Duncan, Dendrimer-platinate: a novel approach to cancer chemotherapy. *Anticancer Drugs* 10(8) (1999) 767-776.
- [142] S. Kannan, P. Kolhe, V. Raykova, M. Glibatec, R.M. Kannan, M. Lieh-Lai, D. Bassett, Dynamics of cellular entry and drug delivery by dendritic polymers into human lung epithelial carcinoma cells. *J. Biomater. Sci. Polym. Ed.* 15(3) (2004) 311-330.
- [143] I.J. Majoros, A. Myc, T. Thomas, C.B. Mehta, J.R. Baker, PAMAM dendrimer-based multifunctional conjugate for cancer therapy: synthesis, characterization, and functionality. *Biomacromolecules* 7(2) (2006) 572-579.
- [144] R. Wiwattanapatapee, B. Carreño-Gómez, N. Malik, R. Duncan, Anionic PAMAM dendrimers rapidly cross adult rat intestine in vitro: a potential oral delivery system? *Pharm. Res.* 17(8) (2000) 991-998.
- [145] M. El-Sayed, M. Ginski, C. Rhodes, H. Ghandehari, Transepithelial transport of poly(amido amine) dendrimers across Caco-2 cell monolayers. *J. Control. Release* 81(3) (2002) 355-365.

- [146] M. El-Sayed, M. Ginski, C. Rhodes, H. Ghandehari, Influence of surface chemistry of poly (amido amine) dendrimers on Caco-2 cell monolayers. *J. Bioact. Compat. Polym.* 18(1) (2003) 7-22.
- [147] M. El-Sayed, C.A. Rhodes, M. Ginski, H. Ghandehari, Transport mechanism(s) of poly (amido amine) dendrimers across Caco-2 cell monolayers. *Int. J. Pharm.* 265(1-2) (2003) 151-157.
- [148] K.M. Kitchens, R.B. Kolhatkar, P.W. Swaan, H. Ghandehari, Endocytosis inhibitors prevent poly (amido amine) dendrimer internalization and permeability across Caco-2 cells. *Mol. Pharm.* 5(2) (2008) 364-369.
- [149] R.B. Kolhatkar, K.M. Kitchens, P.W. Swaan, H. Ghandehari, Surface acetylation of poly (amido amine) (PAMAM) dendrimers decreases cytotoxicity while maintaining membrane permeability. *Bioconjug. Chem.* 18(6) (2007) 2054–2060
- [150] R.B. Kolhatkar, P.W. Swaan, H. Ghandehari, Potential oral delivery of 7-ethyl-10-hydroxy-camptothecin (SN-38) using poly (amido amine) dendrimers. *Pharm. Res.* 25(7) (2008) 1723-1729.
- [151] W. Ke, Y. Zhao, R. Huang, C. Jiang, Y. Pei, Enhanced oral bioavailability of doxorubicin in a dendrimer drug delivery system. *J. Pharm. Sci.* 97(6) (2008) 2208-2216.
- [152] American Cancer Society, *Cancer Facts & Figures 2010*. Atlanta: American Cancer Society; 2010.
- [153] Z.F. Gellad, D. Provenzale, Colorectal cancer: national and international perspective on the burden of disease and public health impact. *Gastroenterology* 138(6) 2177-2190.

- [154] D. Cunningham, W. Atkin, H.J. Lenz, H.T. Lynch, B. Minsky, B. Nordlinger, N. Starling, Colorectal cancer. *Lancet* 375(9719) 1030-1047.
- [155] C. Kurkjian, S. Kummar, Advances in the treatment of metastatic colorectal cancer. *Am. J. Ther.* 16(5) (2009) 412-420.
- [156] P. Comella, A review of the role of capecitabine in the treatment of colorectal cancer. *Ther. Clin. Risk Manag.* 3(3) (2007) 421-431.
- [157] C.F. Stewart, W.C. Zamboni, W.R. Crom, P.J. Houghton, Disposition of irinotecan and SN-38 following oral and intravenous irinotecan dosing in mice. *Cancer Chemother. Pharmacol.* 40(3) (1997) 259-265.
- [158] Y. Kawato, M. Aonuma, Y. Hirota, H. Kuga, K. Sato, Intracellular roles of SN-38, a metabolite of the camptothecin derivative CPT-11, in the antitumor effect of CPT-11. *Cancer Res.* 51(16) (1991) 4187-4191.
- [159] H. Zhao, B. Rubio, P. Sapra, D. Wu, P. Reddy, P. Sai, A. Martinez, Y. Gao, Y. Lozanguiez, C. Longley, L.M. Greenberger, I.D. Horak, Novel prodrugs of SN38 using multiarm poly(ethylene glycol) linkers. *Bioconjug. Chem.* 19(4) (2008) 849-859.
- [160] F. Meyer-Losic, C. Nicolazzi, J. Quinonero, F. Ribes, M. Michel, V. Dubois, C. de Coupade, M. Boukaissi, A.-S. Chéné, I. Tranchant, V. Arranz, I. Zoubaa, J.-S. Fruchart, D. Ravel, J. Kearsey, DTS-108, a novel peptidic prodrug of SN38: in vivo efficacy and toxicokinetic studies. *Clin. Cancer Res.* 14(7) (2008) 2145-2153.
- [161] N. Vijayalakshmi, A. Ray, A. Malugin, H. Ghandehari, Carboxyl terminated PAMAM-SN38 conjugates: synthesis, characterization, and in vitro evaluation. *Bioconjug. Chem.* 21(10) (2010) 1804-1810.

- [162] R. Jevprasesphant, J. Penny, R. Jalal, D. Attwood, N.B. McKeown, A. D'Emanuele, The influence of surface modification on the cytotoxicity of PAMAM dendrimers. *Int. J. Pharm.* 252(1-2) (2003) 263-266.
- [163] A. Ivanov, *Exocytosis and Endocytosis*, Humana Press, 2008, pp. 15-33.
- [164] E. Macia, M. Ehrlich, R. Massol, E. Boucrot, C. Brunner, T. Kirchhausen, Dynasore, a cell-permeable inhibitor of dynamin. *Dev. Cell* 10(6) (2006) 839-850.
- [165] T. Lühmann, M. Rimann, A.G. Bittermann, H. Hall, Cellular uptake and intracellular pathways of PLL-g-PEG-DNA nanoparticles. *Bioconjug. Chem.* 19(9) (2008) 1907-1916.
- [166] H. Inokuchi, T. Takei, K. Aikawa, M. Shimizu, The effect of hyperosmosis on paracellular permeability in Caco-2 cell monolayers. *Biosci. Biotechnol. Biochem.* 73(2) (2009) 328-334.
- [167] Y. Phonphok, K.S. Rosenthal, Stabilization of clathrin coated vesicles by amantadine, tromantadine and other hydrophobic amines. *FEBS Lett.* 281(1-2) (1991) 188-190.
- [168] K. Sato, J. Nagai, N. Mitsui, Y. Ryoko, M. Takano, Effects of endocytosis inhibitors on internalization of human IgG by Caco-2 human intestinal epithelial cells. *Life Sci.* 85(23-26) (2009) 800-807.
- [169] A.E. Gibson, R.J. Noel, J.T. Herlihy, W.F. Ward, Phenylarsine oxide inhibition of endocytosis: effects on asialofetuin internalization. *Am. J. Physiol. Cell Physiol.* 257(2) (1989) C182-C184.

- [170] Z. Ma, L.-Y. Lim, Uptake of chitosan and associated insulin in Caco-2 cell monolayers: a comparison between chitosan molecules and chitosan nanoparticles. *Pharm. Res.* 20(11) (2003) 1812-1819.
- [171] E. Van Hamme, H.L. Dewerchin, E. Cornelissen, B. Verhasselt, H.J. Nauwynck, Clathrin- and caveolae-independent entry of feline infectious peritonitis virus in monocytes depends on dynamin. *J. Gen. Virol.* 89(Pt 9) (2008) 2147-2156.
- [172] M.L. Torgersen, G. Skretting, B. van Deurs, K. Sandvig, Internalization of cholera toxin by different endocytic mechanisms. *J. Cell Sci.* 114(Pt 20) (2001) 3737-3747.
- [173] E. Roger, F. Lagarce, E. Garcion, J.-P. Benoit, Lipid nanocarriers improve paclitaxel transport throughout human intestinal epithelial cells by using vesicle-mediated transcytosis. *J. Control. Release* 140(2) (2009) 174-181.
- [174] Y. Kurtoglu, M. Mishra, S. Kannan, R. Kannan, Drug release characteristics of PAMAM dendrimer-drug conjugates with different linkers. *Int. J. Pharm.* 384(1-2) (2010) 189-194.
- [175] C.A. Lipinski, Drug-like properties and the causes of poor solubility and poor permeability. *J. Pharmacol. Toxicol. Methods* 44(1) (2000) 235-249.
- [176] G. Xu, W. Zhang, M.K. Ma, H.L. McLeod, Human carboxylesterase 2 is commonly expressed in tumor tissue and is correlated with activation of irinotecan. *Clin. Cancer Res.* 8(8) (2002) 2605-2611.
- [177] M.L. Rothenberg, Irinotecan (CPT-11): recent developments and future directions-colorectal cancer and beyond. *Oncologist* 6(1) (2001) 66-80.

- [178] H. Zhao, B. Rubio, P. Sapra, D. Wu, P. Reddy, P. Sai, A. Martinez, Y. Gao, Y. Lozanguiez, C. Longley, L.M. Greenberger, I.D. Horak, Novel prodrugs of SN38 using multiarm poly(ethylene glycol) linkers. *Bioconjug. Chem.* 19(4) (2008) 849-859.
- [179] E. Roger, F. Lagarce, J.-P. Benoit, The gastrointestinal stability of lipid nanocapsules. *Int. J. Pharm.* 379(2) (2009) 260-265.
- [180] M. Ahlmark, J. Vepsäläinen, H. Taipale, R. Niemi, T. Järvinen, Bisphosphonate prodrugs: synthesis and in vitro evaluation of novel clodronic acid dianhydrides as bioreversible prodrugs of clodronate. *J. Med. Chem.* 42(8) (1999) 1473-1476.
- [181] R. Kimsey, E. Harding, A spectrophotometric assay optimizing conditions for pepsin activity. *Amer. Biol. Teach.* 60(3) (1998) 200-201.
- [182] M. Mullally, D. OCallaghan, R. FitzGerald, W. Donnelly, J. Dalton, Proteolytic and peptidolytic activities in commercial pancreatic protease preparations and their relationship to some ehey protein hydrolysate characteristics *J. Agric. Food Chem.* 42 (1994) 2973-2961.
- [183] C.E. Wheelock, T.F. Severson, B.D. Hammock, Synthesis of new carboxylesterase inhibitors and evaluation of potency and water solubility. *Chem. Res. Toxicol.* 14(12) (2001) 1563-1572.
- [184] W. Yamamoto, J. Verweij, P. de Bruijn, M.J. de Jonge, H. Takano, M. Nishiyama, M. Kurihara, A. Sparreboom, Active transepithelial transport of irinotecan (CPT-11) and its metabolites by human intestinal Caco-2 cells. *Anticancer Drugs* 12(5) (2001) 419-432.

- [185] M.E. Fox, S. Guillaudeu, J.M. Frechet, K. Jerger, N. Macaraeg, F.C. Szoka, Synthesis and in vivo antitumor efficacy of PEGylated poly(l-lysine) dendrimer-camptothecin conjugates. *Mol. Pharm.* 6(5) (2009) 1562-1572.
- [186] T. Sakthivel, I. Toth, A.T. Florence, Distribution of a lipidic 2.5 nm diameter dendrimer carrier after oral administration. *Int. J. Pharm.* 183(1) (1999) 51-55.
- [187] D. Pisal, V. Yellepeddi, A. Kumar, R. Kaushik, M. Hildreth, X. Guan, S. Palakurthi, Permeability of surface-modified poly (amido amine) (PAMAM) dendrimers across Caco-2 cell monolayers. *Int. J. Pharm.* 350(1-2) (2008) 113-121.
- [188] S. Parveen, S.K. Sahoo, Nanomedicine: clinical applications of polyethylene glycol conjugated proteins and drugs. *Clin. Pharmacokinet.* 45(10) (2006) 965-988.
- [189] T. Okuda, S. Kawakami, T. Maeie, T. Niidome, F. Yamashita, M. Hashida, Biodistribution characteristics of amino acid dendrimers and their PEGylated derivatives after intravenous administration *J. Control. Release* 114 (2006) 69-77.
- [190] T. Okuda, S. Kawakami, N. Akimoto, T. Niidome, F. Yamashita, M. Hashida, PEGylated lysine dendrimers for tumor-selective targeting after intravenous injection in tumor-bearing mice *J. Control. Release* 116 (2006) 320-336.
- [191] H. Yang, W.J. Kao, Dendrimers for pharmaceutical and biomedical applications. *J. Biomater. Sci., Polym. Ed.* 17(1-2) (2006) 3-19.
- [192] S. Chong, S.A. Dando, R.A. Morrison, Evaluation of biocoat intestinal epithelium differentiation environment (3-day cultured Caco-2 cells) as an absorption screening model with improved productivity. *Pharm. Res.* 14(12) (1997) 1835-1837.

- [193] A.B. Foraker, R.J. Walczak, M.H. Cohen, T.A. Boiarski, C.F. Grove, P.W. Swaan, Microfabricated porous silicon particles enhance paracellular delivery of insulin across intestinal Caco-2 cell monolayers. *Pharm. Res.* 20(1) (2003) 110-116.
- [194] P.W. Swaan, K.M. Hillgren, F.C. Szoka, Jr., S. Oie, Enhanced transepithelial transport of peptides by conjugation to cholic acid. *Bioconjugate Chem.* 8(4) (1997) 520-525.
- [195] D. Shcharbin, J. Mazur, M. Szwedzka, M. Wasiak, B. Palecz, M. Przybyszewska, M. Zaborski, M. Bryszewska, Interaction between PAMAM 4.5 dendrimer, cadmium and bovine serum albumin: a study using equilibrium dialysis, isothermal titration calorimetry, zeta-potential and fluorescence. *Colloids Surf. B Biointerfaces* 58(2) (2007) 286-289.
- [196] H. Ghandehari, P.L. Smith, H. Ellens, P.Y. Yeh, J. Kopecek, Size-dependent permeability of hydrophilic probes across rabbit colonic epithelium. *J. Pharmacol. Exp. Ther.* 280(2) (1997) 747-753.
- [197] P.M. Paulo, J.N. Lopes, S.M. Costa, Molecular dynamics simulations of charged dendrimers: low-to-intermediate half-generation PAMAMs. *J. Phys. Chem. B* 111(36) (2007) 10651-10664.
- [198] M. Moriya, M.C. Linder, Vesicular transport and apotransferrin in intestinal iron absorption, as shown in the Caco-2 cell model. *Am. J. Physiol. Gastrointest. Liver. Physiol.* 290(2) (2006) G301-309.
- [199] T. Xuan, J.A. Zhang, I. Ahmad, HPLC method for determination of SN-38 content and SN-38 entrapment efficiency in a novel liposome-based formulation, LE-SN38. *J. Pharm. Biomed. Anal.* 41(2) (2006) 582-588.

[200] M. Ramesh, P. Ahlawat, N.R. Srinivas, Irinotecan and its active metabolite, SN-38: review of bioanalytical methods and recent update from clinical pharmacology perspectives. *Biomed. Chromatogr.* 24(1) (2010) 104-123.

[201] J. Peterson, V. Allikmaa, J. Subbi, T. Pehk, M. Lopp, Structural deviations in poly (amido amine) dendrimers: a MALDI-TOF MS analysis. *Eur. Polym. J.* 39 (2003) 33-42.

Curriculum Vitae

I. PERSONAL DATA

Address: 6219 Sutton Court
Elkridge, MD 21201

Telephone: 301-325-690

Education

2010 Completion of Ph.D. in Bioengineering with emphasis on polymeric drug delivery, University of Maryland, College Park, MD

2006 Bachelors of Science, Chemical Engineering, University of Maryland, College Park, MD, *Summa Cum Laude*

II. PROFESSIONAL EXPERIENCE

2006-2010 Graduate Research Assistant, Fischell Department of Bioengineering, University of Maryland, College Park, MD and Department of Pharmaceutical Sciences, University of Maryland, Baltimore, MD.

2009 Summer Intern, Department of Formulation Sciences, MedImmune LLC, Gaithersburg, MD

2007-2008 Graduate Teaching Assistant, Fischell Department of Bioengineering, University of Maryland, College Park, MD.

III. PUBLICATIONS IN REFEREED JOURNALS

1. **D. Goldberg**, N. Vijayalakshmi, P. Swaan and H. Ghandehari. G3.5 PAMAM Dendrimer-SN38 Conjugates Enhance Transepithelial Transport of SN38 while minimizing Gastrointestinal Toxicity and Release. *J Control Release*, Submitted.
2. **D. Goldberg**, S. Bishop, A. Shah and H. Sathish, Formulation Development of Therapeutic Monoclonal Antibodies using High-throughput Fluorescence and Static Light Scattering Techniques: Role of Conformational and Colloidal Stability, *J Pharm Sci*, Epub ahead of print, Oct 19, 2010.
3. **D. Goldberg**, H. Ghandehari and P. Swaan, Cellular Entry of G3.5 PAMAM Dendrimers by Clathrin- and Dynamin-dependent Endocytosis is Required for Tight Junctional Opening in Intestinal Epithelia, *Pharm Res*, 27(8) (2010) 1547-57.
4. **D. Sweet**, R. Kolhatkar, A. Ray, P. Swaan, and H. Ghandehari, Transepithelial Transport of PEGylated Anionic Poly (Amido Amine) Dendrimers: Implications for Oral Drug Delivery. *J Control Release* 138(1) (2009) 78-85.
5. M. Al-Sheikhly, **D. Sweet**, L. Salamanca-Riba, B. Varughese, J. Silverman, A. Christou, and W. Bentley, Radiation-induced Failure Mechanisms of GaAs-based Biochips, *IEEE, Device and Materials Reliability*, 4, (2004) 192-197.

IV. BOOK CHAPTER

1. R. Kolhatkar, **D. Sweet**, and H. Ghandehari, Functionalized Dendrimers as Nanoscale Drug Carriers, in Multifunctional Pharmaceutical Nanocarriers, Springer 201-232, 2008.

V. ABSTRACTS FOR NATIONAL AND INTERNATIONAL CONFERENCES

1. **D. Goldberg**, N. Vijayalakshmi, P. Swaan and H. Ghandehari. G3.5 PAMAM Dendrimer-SN38 Conjugates Enhance Transepithelial Transport of the Drug while minimizing Gastrointestinal Toxicity, 8th Meeting of the Globalization of Pharmaceutics Education Network, Chapel Hill, NC, November 10-12, 2010. (Podium Presentation)
2. B. Avaritt, **D. Goldberg**, H. Ghandehari and P. Swaan, PAMAM Dendrimers as Potent Tight Junctional Modulators, 8th Meeting of the Globalization of Pharmaceutics Education Network, Chapel Hill, NC, November 10-12, 2010. (Poster)
3. **D. Goldberg**, N. Vijayalakshmi, P. Swaan and H. Ghandehari, G3.5 PAMAM Dendrimer-SN38 Conjugates Enhance Transepithelial Transport of the Drug while Minimizing Gastrointestinal Toxicity and Release, 8th International Nanomedicine and Drug Delivery Symposium (NanoDDS' 10), Omaha, NE, October 3-5, 2010. (Poster)
4. **D. Goldberg**, P. Swaan and H. Ghandehari, Mechanisms of PAMAM Dendrimer Transepithelial Transport and Tight Junction Modulation, 37th Annual Meeting and Exposition of the Controlled Release Society, Portland, OR, July 10-14, 2010. (Podium Presentation)
5. **D. Goldberg**, P. Swaan and H. Ghandehari, Mechanisms of PAMAM Dendrimer Transepithelial Transport and Tight Junction Modulation, The 26th Southern Biomedical Engineering Conference, College Park, MD, April 30- May 2, 2010. (Podium Presentation)

6. **D. Sweet**, R. Kolhatkar, P. Swaan, and H. Ghandehari, Mechanisms of Transport of PEGylated Anionic PAMAM Dendrimers Across Caco-2 Cell Monolayers, 14th International Symposium on Recent Advances in Drug Delivery Systems, Salt Lake City, UT, February 15-18, 2009. (Poster)
7. **D. Sweet**, R. Kolhatkar, and H. Ghandehari, PEGylation of Anionic PAMAM Dendrimers: Implications for Oral Delivery, 35th Annual Meeting and Exposition of the Controlled Release Society, New York, NY, July 12-16, 2008. (Poster).
8. R.B. Kolhatkar, **D. Sweet**, and H. Ghandehari, PAMAM Dendrimers: Surface Modification and Potential in Oral Delivery of SN-38, 3rd Annual Mountain West Biomedical Engineering Conference, Salt Lake City, Utah, September 14-15, 2007.
9. H. Ghandehari, R. Kolhatkar, A. Nan, S.B. Lee, and **D. Sweet**, Transcellular Transport and Toxicity of Dendritic and Silica-Based Nanoconstructs, The 5th International Nanomedicine and Drug Delivery Symposium (NanoDDS'07), Boston, MA, November 1-2, 2007.

VI. HONORS AND AWARDS

- | | |
|------|---|
| 2010 | Southern Biomedical Engineering Conference Graduate Student Paper Award |
| 2009 | Best Graduate Student Poster, MedImmune Intern Poster Competition |
| 2009 | Fischell Fellowship in Bioengineering: Awarded for “DendriPharm Systems” business plan detailing commercialization opportunity of graduate research |

- 2006-2009 National Science Foundation Graduate Research Fellowship
- 2006 A. James Clark School of Engineering Deans' Award
- 2006 Chemical Engineering Outstanding Senior Award
- 2005-2006 Barry M. Goldwater Scholarship (National Scholarship)

VII. LEADERSHIP ACTIVITIES

- 2008-2010 National Science Foundation Graduate Research Fellowship Contact
- 2007 High School Summer Student Mentor

VIII. PROFESSIONAL MEMBERSHIPS

1. Controlled Release Society
2. Tau Beta Pi Engineering Honors Society